

HYDROLOGICAL CONNECTIVITY IN SELECTED PRISTINE CATCHMENTS IN THE KRUGER NATIONAL PARK

By

D Fundisi

Submitted in fulfilment of the academic requirements for the degree of

Master of Science in the

Centre for Water Resources Research,

School of Agriculture, Earth and Environmental Sciences,

University of KwaZulu-Natal, Pietermaritzburg

APRIL 2014

ABSTRACT

The understanding of interactions between hydrological processes is essential, especially in water limited ecosystems in semi-arid environments. It is through this understanding that informed planning and management decisions for ecosystem conservation are developed. Assessment of groundwater- surface water connectivity at catchment scale provides a holistic view of the abiotic template that sustains life systems within the catchment. Spatial differences in hydrological responses are thus understood since these are characterised by nonlinearities emanating from catchment heterogeneity across spatial and temporal scales.

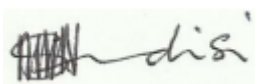
This study involved an assessment of groundwater-surface water interaction across incremental contributing areas which were based on stream orders. The study areas, Southern Granites and Southern Basalts, are located on the two dominant geologies in the Kruger National Park (KNP). At Southern Granites the 1st order, 2nd order and 3rd order contributing catchments have an area of 0.3km², 0.9km² and 1.5km² respectively. At the Southern Basalts site the areas for similar incremental catchments were 15.4km², 31.6km² and 47.8km² respectively. Both study sites had streamflow levelloggers installed at each outlet the 1st to 3rd order contributing areas. The assessment was done through a combination of hydrometric techniques, Electrical Resistivity Tomography (ERT) and tracer analysis methods. Monitoring of water levels and sampling in the stream, riparian boreholes and piezometers was conducted from September 2012 to May 2013. The monitoring network consisted of 28 piezometers and 19 boreholes at Southern Granites while 6 piezometers and 4 boreholes were installed at the Southern Basalts sites. Streambed hydraulic conductivities were determined using slug tests. Hydraulic gradients between the stream, piezometers and groundwater boreholes were calculated and used to determine direction of fluxes. Connectivity mechanisms were determined and contributions of different water sources to streamflow were quantified using two and three component tracer based hydrograph separations. Results showed that rainfall intensity was the major control to connectivity between surface and groundwater resources in these catchments. Contribution of event water to streamflow was estimated between 60% and 86% across the nested spatial scales for two monitored rainfall events (19 January and 20 February 2013) at Southern Granites study site. Although event water emerged as the dominant source at all scales, higher pre-event contributions were noted for lower order subcatchments at this site. A 2nd order stream channel, previously

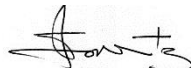
conceptualised as gaining was demonstrated through hydrometry and tracers to be increasingly losing subsequently behaving as an indirect recharge point at Southern Granites site. The study, therefore, revealed that lower order reaches on the granitic geology are important water sources that sustain baseflow at higher order perennial streams. At Southern Basalts study site limited subsurface contribution to streamflow was observed due to very low interfluvial gradients and low aquifer transmissivities that characterise the basalt geology. Assessment of groundwater-surface water interaction at this site was conducted only at the 3rd order catchment due to a limited network of groundwater boreholes. At this reach the contribution of event water was estimated between 51% and 64% for two monitored events (19 January and 20 February 2013). Groundwater contribution to streamflow through localised preferential fractured rock flow ranged between 36% and 49%.

PREFACE

I DANIEL FUNDISI declare that:

1. The presented research, except where otherwise stated, is my original work.
2. This thesis has not been submitted for any degree or examination at any other university.
3. This thesis does not contain other persons' data, pictures, graphs or other information unless specifically acknowledged as being sourced from other persons.
4. This thesis does not contain other persons writing unless specifically acknowledged as being sourced from other researchers. Where other written sources have been quoted, then :
 - 4.1 Their words have been re-written but the general information attributed to them has been referenced ;
 - 4.2 Where their exact words have been used, their writing has been placed inside quotation marks and referenced.
5. This thesis does not contain any text, graphics or tables copied and pasted from the internet, unless specifically acknowledged, and the source being detailed in the thesis and in the reference section.

Signed: 


Supervisor:

Prof. SA Lorentz

Co-Supervisor:

Dr. ES. Riddell

DATE: APRIL 2014

ACKNOWLEDGEMENTS

This research was funded by the South African Water Research Commission (WRC).

The author wishes to express heartfelt gratitude to the following people and institutions for their valuable assistance:

Professor SA Lorentz, Associate Research Professor, of the School of Agriculture, Earth and Environmental Sciences, Centre for Water Resources Research, University of KwaZulu-Natal for his invaluable advice and enthusiastic supervision throughout the research process.

Dr Edward Riddell, of the School of Agriculture, Earth and Environmental Sciences, Centre for Water Resources Research, University of KwaZulu-Natal for tirelessly being available to supervise my research work and for thorough critiquing of the write up.

Professor Piet Le Roux and Dr George Van Zijl of the University of Free State, for valuable hydrogeological input.

Dr Jaco Nel, of Groundwater Consulting Services for valuable groundwater expertise input.

Mr Robin Petersen (SANParks) for valuable critiquing and support during reference group meetings.

Mr Cobus Pretorius, Centre for Water Resources Research, University of KwaZulu-Natal, for technical laboratory advice and logistical assistance during the research process.

Ashton Van Niekerk, Faith Jumbi, Tercia Strydom, Chengetanai Mushonga, Bruce Wickam, fellow students for moral support and fieldwork assistance throughout the research process.

SANParks Scientific Services for all logistical and technical support including provision of game guards during fieldwork. Mr Anoit Mashele (SANParks) for providing game guard services and Difference Thibela for assistance during fieldwork.

In conclusion, I extend my sincere gratitude to my wife, **Esther** and children (**Pearl**, **Philothea** and **Chayil**) for their enduring support during the whole study period. Had it not been for your support, this work would have been difficult to accomplish. Lastly, I would like to thank God Almighty, for giving me strength and good health as I worked through this study.

TABLE OF CONTENTS

Contents

ABSTRACT.....	i
PREFACE.....	iii
ACKNOWLEDGEMENTS.....	iv
TABLE OF CONTENTS.....	v
LIST OF TABLES.....	viii
LIST OF FIGURES	x
LIST OF ACRONYMS AND ABBREVIATIONS.....	xiii
1. INTRODUCTION	1
1.1 Background.....	1
1.2 Rationale	2
1.3 Conceptual framework.....	4
1.4 Structure of the Thesis	6
2. LITERATURE REVIEW	7
2.1 Introduction.....	7
2.2 Hydrologic Connectivity and Catchment Function.....	8
2.3 Drivers and Controls of Hydrological Connectivity	11
2.4 Connecting Mechanisms of Surface and Groundwater Resources	12
2.5 A Review of Existing Knowledge on Hydrological Connectivity	13
2.6 Methods and Techniques of Investigating Hydrologic Connectivity.....	15
2.6.1 Electrical Resistivity Tomography (ERT)	15
2.6.2 Hydrometric techniques	17
2.6.3 Hydraulic conductivity (K)	19
2.6.4 Hydraulic gradient.....	20
2.6.5 Subsurface discharge.....	20
2.7 Environmental Tracers.....	21
2.7.1 Hydrochemistry.....	21
2.7.2 Physico-chemical parameters.....	23
2.7.3 Isotopes	23
2.8 Discussion of Reviewed Literature	25

2.9 Main challenges & gaps	26
3. METHODOLOGY	28
3.1 Study Area	28
3.1.1 Geology and drainage	28
3.1.2 Climate and vegetation.....	28
3.1.3 Supersites	29
3.2 Streamflows	36
3.2.1 Stream stage measurement.....	36
3.2.2 Stream channel surveys.....	37
3.2.3 Streamflow ratings	38
3.2.4 Subsurface flow characterisation	41
3.3 Rainfall Measurement	44
3.4 Rainfall-Runoff Analysis	45
3.5 Stream and Riparian Zone Hydraulic Head Monitoring	45
3.5 Hyporheic Zone Hydraulic Head Monitoring	46
3.6 Flow Duration Curves (FDCs).....	47
3.7 Additional Techniques to Further Understand Groundwater Stream Connectivity	48
3.8 Sampling and Laboratory Analyses	48
3.10 Tracer Analysis	51
3.11 Definition of Hypotheses	53
4. RESULTS AND DISCUSSION: HYDROMETRY	55
4. Introduction.....	55
4.1 Characterising Stream Channel Flows in the Study Sites	55
4.2 Southern Granites Rainfall-Runoff Analysis	57
4.2.1 Statistical analysis	57
4.2.2 Runoff Coefficients.....	59
4.3 Total Discharge at Southern Granites	65
4.4 Southern Basalts Rainfall-Runoff Analysis	68
4.4.1 Statistical analysis	68
4.4.2 Runoff coefficients (Rc).....	69
4.5 Flow duration curves (FDCs).....	73
4.5.1 Southern Granites FDCs	74
4.5.2 Southern Basalts FDCs	75

4.6 Summary of Hydrometric Findings	76
5. RESULTS AND DISCUSSION: TRACERS	77
5. Introduction.....	77
5.1 General Isotopic, Physico-chemical and Hydrochemical Trends in	81
Study Sites	81
5.2 Tracer Analysis at Southern Granites	86
5.3 Tracer Analysis at Southern Basalts	91
5.4 Quantifying Contribution of Different Water Sources to Streamflow	94
5.4.1 Event 1 (19 January 2013) at Southern Granites 3 rd Order Reach (SGR3).....	95
5.4.2 Event 1 (19 January 2013) at Southern Granites 1 st and 2 nd Order Reaches (SGR1 & SGR2)	98
5.4.3 Event 2 (20 February 2013) at Southern Granites 3 rd Order Reach (SGR3).....	99
5.4.4 Event 2 (20 February 2013) at Southern Granites 1 st and 2 nd Order Reaches (SGR1 & SGR2)	100
5.4.5 Three component hydrograph separation at Southern Granites 1 st order reach for..... the 19 th of January 2013 rainfall event	101
5.5 Stream Network Connectivity at Southern Granites.....	102
5.6 Event 1(19 January 2013) at Southern Basalts 3 rd Order Reach (SBAS3)	104
5.7 Event 2 (20 February 2013) at Southern Basalts 3 rd order reach (SBAS3).....	105
5.8 Results and Discussion of Electrical Resistivity Tomography (ERT) as Supplementary Data for Further Insight into Hydrological Connectivity.....	107
CHAPTER 6: SYNTHESIS.....	109
6.1 Introduction.....	109
6.2 Conceptual understanding of hydrological connectivity at Southern Granites.....	109
6.3 Quantification of Water Sources Contributing to Streamflow at Southern Granites	111
6.4 Conceptual Understanding of Hydrological Connectivity at Southern Basalts 3 rd Order Reach	113
6.5 Quantification of Water Sources Contributing to Streamflow at Southern Basalts 3 rd Order Reach	114
6.6 Limitations of the study	114
6.7 Conclusions.....	115
6.8 Recommendations.....	116
REFERENCES	118
APPENDICES	127

LIST OF TABLES

TABLE 3.1 BASE N VALUES FOR NATURAL CHANNELS (AFTER ALDRIDGE AND GARRET, 1973).....	39
TABLE 4.1 PEARSON'S PRODUCT MOMENT CORRELATION COEFFICIENT (R) AND LEVEL OF SIGNIFICANCE (P) FOR PRECIPITATION AND RUNOFF RESPONSES AT SOUTHERN GRANITES STUDY SITE.....	58
TABLE 4.2 RUNOFF COEFFICIENTS AT SOUTHERN GRANITES FOR 1 ST TO 3 RD ORDER REACHES.....	59
TABLE 4.3 STREAMBED VERTICAL HYDRAULIC GRADIENTS AT SOUTHERN GRANITES FOR 1 ST TO 3 RD ORDER REACHES.....	67
TABLE 4.4 PEARSON'S PRODUCT MOMENT CORRELATION COEFFICIENT (R) AND LEVEL OF SIGNIFICANCE (P) FOR PRECIPITATION AND RUNOFF RESPONSES AT SOUTHERN BASALTS STUDY SITE.....	69
TABLE 4.5 RUNOFF COEFFICIENTS AT SOUTHERN BASALTS FOR 1 ST TO 3 RD ORDER REACHES.....	70
TABLE 5.1A MONITORING POINTS' ACRONYMS AND SYMBOLS AT SOUTHERN GRANITES STUDY SITE.....	80
TABLE 5.1B MONITORING POINTS' ACRONYMS AND SYMBOLS AT SOUTHERN BASALTS STUDY SITE.....	81
TABLE 5.2A RAINFALL AND STREAM ISOTOPE SIGNATURES AT SOUTHERN GRANITES DURING SEPTEMBER 2012 TO MARCH 2013.....	83

TABLE 5.2B TYPICAL TRENDS OF EC, SILICA & CHLORIDE AT SOUTHERN GRANITES	84
TABLE 5.3A RAINFALL AND STREAM ISOTOPE SIGNATURES AT SOUTHERN BASALTS DURING DECEMBER 2012 TO JANUARY 2013.....	85
TABLE 5.3B TYPICAL TRENDS OF EC, SILICA & CHLORIDE AT SOUTHERN BASALTS STUDY SITES.....	86
TABLE 5.4 ISOTOPE AND HYDROCHEMICAL DATA INDICATING CONNECTIVITY POINTS AT SOUTHERN GRANITES STUDY SITE.....	90
TABLE 5.5 ISOTOPE AND HYDROCHEMICAL DATA INDICATING CONNECTIVITY POINTS AT SOUTHERN BASALTS STUDY SITE.....	92
TABLE 5.6 ESTIMATED TRIBUTARY RUNOFF TO MAIN CHANNELS AT SOUTHERN GRANITES ON JANUARY 19 AND FEBRUARY 20, 2013.....	103

LIST OF FIGURES

FIGURE 1.1 KEY COMPONENTS OF THE CURRENT STUDY	5
FIGURE 2.1 RECHARGE-DISCHARGE MECHANISMS	7
FIGURE 2.2 INTEGRATION OF HYDROLOGY AND ECOSYSTEM SCIENCE.....	10
FIGURE 3.1A MAP OF STUDY SITES.....	30
FIGURE 3.1B SOUTHERN GRANITES STUDY SITE SOILS MAP.....	32
FIGURE 3.2A INSTRUMENTATION MAP AT SOUTHERN GRANITES	34
FIGURE 3.2B INSTRUMENTATION MAP AT SOUTHERN BASALTS	35
FIGURE 3.3 SOLINST LEVELLOGGER INSTALLATION & FUNCTION.....	37
FIGURE 3.4 CONCEPT OF HYDRAULIC GRADIENT IN THE STREAMBED.....	42
FIGURE 3.5 SOUTHERN GRANITES 1 ST ORDER SUBSURFACE CROSS SECTION	43
FIGURE 3.6 HYDRAULIC CONDUCTIVITY FROM SLUG TESTS.....	44
FIGURE 3.7 CONCEPT OF STREAM-RIPARIAN ZONE INTERACTION.....	46
FIGURE 3.8 THE PRINCIPLE OF VERTICAL HYDRAULIC GRADIENT.....	47
FIGURE 3.9 ALCO SEQUENTIAL STREAMFLOW SAMPLER	49
FIGURE 4.1A CROSS SECTIONS AND RATING CURVES FOR SOUTHERN GRANITES STUDY SITE.....	56
FIGURE 4.1B CROSS SECTIONS AND RATING CURVES FOR SOUTHERN BASALTS STUDY SITE.....	57
FIGURE 4.2A SOUTHERN GRANITES STREAMFLOW RESPONSES AFTER 19 JANUARY 2013 RAINFALL EVENT.....	60
FIGURE 4.2B SOUTHERN GRANITES STREAMFLOW RESPONSES AFTER 20 FEBRUARY 2013 RAINFALL EVENT.....	61
FIGURE 4.3A MAP OF MONITORING POINTS AT SOUTHERN GRANITES; PLUS GROUNDWATER & STREAM WATER LEVEL PLOTS.....	63

FIGURE 4.3B IN-STREAM AND RIPARIAN ZONE WATER LEVELS AT SGR3 REACH OF SOUTHERN GRANITES	64
FIGURE 4.3B1 LOCATION MAP OF SGR3T AND SGR3Q SECTIONS OF THE 3 RD ORDER REACH AT SOUTHERN GRANITES STUDY SITE.....	65
FIGURE 4.4 SURFACE-SUBSURFACE FLOW RATING CURVES FOR SOUTHERN GRANITES.....	66
FIGURE 4.5 SURFACE-SUBSURFACE HYDROGRAPHS FOR SOUTHERN GRANITES FROM SEPTEMBER 2012 TO MARCH 2013.....	67
FIGURE 4.6A SOUTHERN BASALTS STREAMFLOW RESPONSES AFTER THE 19 JANUARY 2013 RAINFALL EVENT.....	71
FIGURE 4.6B SOUTHERN BASALTS STREAMFLOW RESPONSES AFTER THE 20 FEBRUARY 2013 RAINFALL EVENT.....	72
FIGURE 4.7 HYDRAULIC HEAD FOR STREAM AND GROUNDWATER AT SOUTHERN BASALTS FROM FEBRUARY TO JULY 2013.....	73
FIGURE 4.8 FLOW DURATION CURVES FOR SOUTHERN GRANITES & SOUTHERN BASALTS	75
FIGURE 5.1A MAP OF MONITORING LOCATIONS AT SOUTHERN GRANITES.....	78
FIGURE 5.1B MAP OF MONITORING LOCATIONS AT SOUTHERN BASALTS.....	79
FIGURE 5.2 ISOTOPIC TRENDS IN RAINFALL AND STREAM AT SOUTHERN GRANITES	82
FIGURE 5.3 ISOTOPIC TRENDS IN RAINFALL AND STREAM AT SOUTHERN BASALTS.....	85
FIGURE 5.4 TIME SERIES ISOTOPIC DATA AT SOUTHERN GRANITES	88
FIGURE 5.5 TIME SERIES SILICA DATA AT SOUTHERN GRANITES.....	91
FIGURE 5.6 TIME SERIES ISOTOPIC DATA AT SOUTHERN BASALTS.....	93
FIGURE 5.7 TIME SERIES SILICA DATA AT SOUTHERN BASALTS.....	94
FIGURE 5.8 $\delta D/\delta^{18}O$ PLOT 1 FOR SOUTHERN GRANITES (SGR3 REACH).....	96

FIGURE 5.9 HYDROGRAPH SEPARATION CHART FOR SGR3 REACH.....	97
FIGURE 5.10 HYDROGRAPH SEPARATION CHART FOR SGR1 & SGR2.....	98
FIGURE 5.11 $\delta D/\delta^{18}O$ PLOT 2 FOR SOUTHERN GRANITES (SGR3 REACH).....	99
FIGURE 5.12 HYDROGRAPH SEPARATION CHART FOR SGR3 REACH FOR 20 FEBRUARY 2013 EVENT.....	100
FIGURE 5.13 HYDROGRAPH SEPARATION FOR SGR1 & SGR2 REACHES.....	101
FIGURE 5.14 THREE COMPONENT HYDROGRAPH SEPARATION AT SGR1	102
FIGURE 5.15 $\delta D/\delta^{18}O$ PLOT 1 FOR SOUTHERN BASALTS (SBAS3 REACH)	105
FIGURE 5.16 TWO COMPONENT HYDROGRAPH SEPARATION FOR SBAS3 REACH FOR 19 JANUARY 2013 EVENT.....	105
FIGURE 5.17 $\delta D/\delta^{18}O$ PLOT 2 FOR SOUTHERN BASALTS (SBAS3 REACH).....	106
FIGURE 5.18 TWO COMPONENT HYDROGRAPH SEPARATION CHART FOR SBAS3 FOR THE 20 FEBRUARY 2013 EVENT.....	106
FIGURE 5.19 ELECTRICAL RESISTIVITY TOMOGRAPHY FOR SOUTHERN GRANITES.....	108
FIGURE 6.1 CONCEPTUAL MODELS AT SOUTHERN GRANITES	110
FIGURE 6.2 CONCEPTUAL MODELS AT SOUTHERN BASALTS	113

LIST OF ACRONYMS AND ABBREVIATIONS

API	Antecedent Precipitation Index
DEM	Digital Elevation Model
DGPS	Differential Global Positioning System
EM	End Member
EMMA	End Member Mixing Analysis
ERT	Electrical Resistivity Tomography
GMWL	Global Meteoric Water Line
GIS	Geographic Information Systems
ICP OES	Inductively Coupled Plasma-Optical Energy Spectrometry
KNP	Kruger National Park
RC	Runoff Coefficients
SAM	Strategic Adaptive Management
SANParks	South African National Parks
SBAS1	Southern Basalts 1 st Order
SBAS2	Southern Basalts 2 nd Order
SBAS3	Southern Basalts 3 rd Order
SGR1	Southern Granites 1 st Order
SGR2	Southern Granites 2 nd Order
SGR3	Southern Granites 3 rd Order
TPC	Threshold of Potential Concern
USGS	United States Geological Survey
VSMOW	Vienna Standard Mean Ocean Water

1. INTRODUCTION

1.1 Background

Naturally, groundwater and surface water exist in a state of interchange in various landscapes (Winter et al., 1998). Despite evident interactions between these process domains, historically their assessment has been done separately, often resulting in double accounting of the available water resource base. Recently, research has shifted towards an integrated approach which seeks to understand exchange processes between groundwater and surface water (Kalbus et al., 2006). Through this integration valuable knowledge of hydrologic connectivity is acquired providing a holistic view of water within a catchment.

Hydrological processes determine how catchments respond to storms as well as defining the extent of those responses (Uhlenbrook et al., 2005). Knowledge of these processes and how they interact is imperative to understand current and future trends of a catchment's hydrological function. This is particularly true if specific controls characterising a catchment are known, since these determine which processes dominate the catchment's hydrological response (Uhlenbrook et al., 2005). Such controls may include spatio-temporal distribution of precipitation, bedrock permeability, riverbed characteristics, soil characteristics, topography, antecedent soil moisture and vegetation distribution. Where subsurface flow is dominant, understanding waterflow paths to the catchment outlet is not an easy task (Uhlenbrook et al., 2005; Thompson et al., 2011), since subsurface controls are not readily observable. An assortment of various methods and techniques should carefully be selected to assist inference of subsurface flow dynamics.

This study was based on previous research conducted by Cullum and Rogers (2011) which developed a framework of hierarchical classification of landscapes to describe and explain the structure and function of savanna ecosystems. The framework upholds the concept that heterogeneous catchments when closely examined show patterns of organisation where scale-related controls influence the spatial variation of landscape elements. It also recognizes the pivotal role of the distribution of water in driving semi-arid savanna systems, acting both as the cause and consequence of observed patterns of soil, vegetation and topography (Cullum

and Rogers, 2011). This is primarily important in water limited ecosystems such as those commonly found in semi-arid areas, where the majority of the landscape is drained by ephemeral streams. The Kruger National Park (KNP) having a total ephemeral stream length of over 30000km compared to only 600km of perennial rivers is a typical example of the above description (O' Keefe and Rogers, 2003). Despite the fact that ephemeral streams support a vast majority of ecosystems in KNP, hydrological studies were historically exclusive to catchments drained by perennial rivers (Cullum and Rogers, 2011). For this study, therefore, it was pertinent to characterize spatio-temporal variation of hydrologic connectivity in nested catchments drained by ephemeral streams. Connectivity assessments across spatial scales were based on incremental contributing areas to stream orders on the granites and basalts, the two main geologies in KNP. The notion of spatial scales in quantifying hydrologic connectivity is essential in this study, because catchments are heterogeneous at all scales due to a diversity of landscape elements and external forcing (Tetzlaff et al., 2010). However, since catchment heterogeneity comes with very high complexity, dominant patterns should be identified within a specific framework and be used to test hypotheses in order to understand catchment functioning (Grayson and Blöschl, 2001). Distinct patterns in vegetation distribution and structure or patterns that are interpolated from measurements across spatial and temporal scales are useful in developing testable hypotheses.

1.2 Rationale

Several studies have been conducted on stream-aquifer interactions with various study goals including water resource evaluation (e.g. Ogunkoya et al., 1993; McGlynn and McDonnell, 2003; Baskaran et al., 2009; Praamsma et al., 2009; Bohte et al., 2010), contaminant transport and aquifer vulnerability to contamination (Malcolm et al., 2005) process understanding for application in models (Wenninger et al., 2008) and for identifying ecological zones suitable for fish spawning (Malcolm et al., 2005), among others. According to Winter (1998), interest in groundwater-surface water interactions has steadily increased from the 1960s where research focus was mainly on groundwater-lake interactions being influenced by rising eutrophication problems, to connectivity studies between groundwater and headwater streams in the 1990s fuelled by increases in acid rain concerns. Recently, more attention has been given towards the understanding of interactions between riparian and in-stream water which

provides valuable insight into the ecological structure and function of stream systems (Sophocleous, 2002; Mackenzie et al. 2003). These studies were conducted on different stratigraphic settings and climatic regimes using various methods thereby helping in defining different controls to hydrologic processes and their connectivity. A review of literature on groundwater- surface water interactions was carried out to get a general understanding of process behaviour under various conditions ranging from humid, semi-arid to arid climates on different geologies. Particular interest was in semi-arid environments where streamflow is ephemeral typical of the setting for the current study.

A number of important aspects underlying interactions between groundwater and surface water systems were noted from the review of literature. Stream-aquifer interactions are characterised by spatio-temporal variability (Katz et al., 1998) which is understood at least at local/hillslope scales (Soulsby et al., 2008). This variability is attributed to various controls including geology, streambed permeability, channel geometry, bedrock topography and antecedent moisture (Jencso et al., 2011). Studies have investigated the individual influence of these controls, for instance streambed topography (e.g. Harvey and Bencala, 1993) and channel geometry (e.g. Malcolm et al., 2005). This being the case, however, it has been noted that very few studies have investigated their combined and hierarchical influence across space and time (Jencso et al., 2011). This has curtailed the spatio-temporal understanding of controls to hydrological processes both within and across catchments by hydrologists. To address this shortcoming, consideration should be made for integrated approaches involving various disciplines and methodologies (Malcolm et al., 2005; Jencso et al., 2011).

Another noteworthy aspect is that though the subject of groundwater-surface water connectivity has been investigated fairly widely, most of the studies have largely been descriptive rather than quantitative (McDonnell, 2007; Jencso & McGlynn, 2011). Owing to the descriptive rather than quantitative nature of most studies, their findings have only been specific to study areas in which they were obtained with no chance of being generalised to other catchments with similar environmental conditions. This is especially the case when considering interactions across multiple scales within landscapes. As a result, there has been partial understanding of linkages between catchment structure and streamflow processes, viewed against heterogeneous landscape patches within catchments (Tetzlaff et al., 2010; Jencso and McGlynn, 2011). According to Sophocleous (2002), it is still a major challenge to

determine water exchanges between surface and groundwater systems due to heterogeneities within catchments and the problem of integrating measurements at various scales.

1.3 Conceptual framework

This study sought to define spatio-temporal mechanisms by which dominant hydrological processes are connected or disconnected in the context of prevalent climatic and geological conditions. Differences in stream-aquifer/stream-hillslope interactions based on incremental contributing areas to stream orders were investigated on the granitic and basaltic geologies. This was done with the aim of understanding the abiotic template that drives ecosystems in the study area across spatial and time scales. Temporal scales are important considering that the study area is semi-arid and thus characterized by variable rainfall with distinct seasonal distribution. Spatial scales, to capture the influence of heterogeneous landscape elements on processes that subsequently determine a catchment's hydrological response. This understanding is expected to guide management decisions in KNP and the broader lowveld with respect to people, animal and plant water use functions that promote sustainable water resource use for the foreseeable future. For instance, informed management decisions as to how much of a specific animal population is allowable per unit area given a predictable water resource base and associated biomass levels, can better be implemented. Meaningful predictions of water resources can be done through modelling only if there is quantified baseline or historical hydrological information. Pringle (2003) posits that the current understanding of how hydrologic connectivity influences natural ecological integrity is poor due to the extent and magnitude of anthropogenic activities that often occur before such understanding is acquired. As such, the knowledge gained in KNP is useful for extrapolation to altered catchments with similar climatic conditions to influence management decisions with respect to land use policy and water resources development.

The key aspect of this study is to identify time-variant (event and pre-event) contributing water sources to total runoff and how these are controlled or driven by geology and rainfall input as summarized in Figure 1.1. When determined, interactions between hydrological processes will provide a basis for the general understanding of catchment functioning in the study areas. Catchment hydrologic responses to climate forcing (e.g. rainfall) trigger

geomorphic responses that result in catchment morphological changes. For instance, discharge hydrographs are feedbacks of the magnitude and intensity of rainfall input, as sediment transport and deposition are to stream power. Vegetation distribution and structure also form effective feedbacks to either sustained water availability or shortlived water flow along flow paths. The catchment hydrologic response and the morphology of channel networks and interfluvies are closely linked phenomena over space and time scales (Vivoni et al., 2003). Feedbacks between pattern and process are highly relevant in defining the critical role of water in ecological, geomorphological and pedological processes within a catchment (Sivapalan, 2005). As such, identifying these process-pattern feedbacks is essential to get a deeper understanding of how hydrologic connectivity influences catchment function.

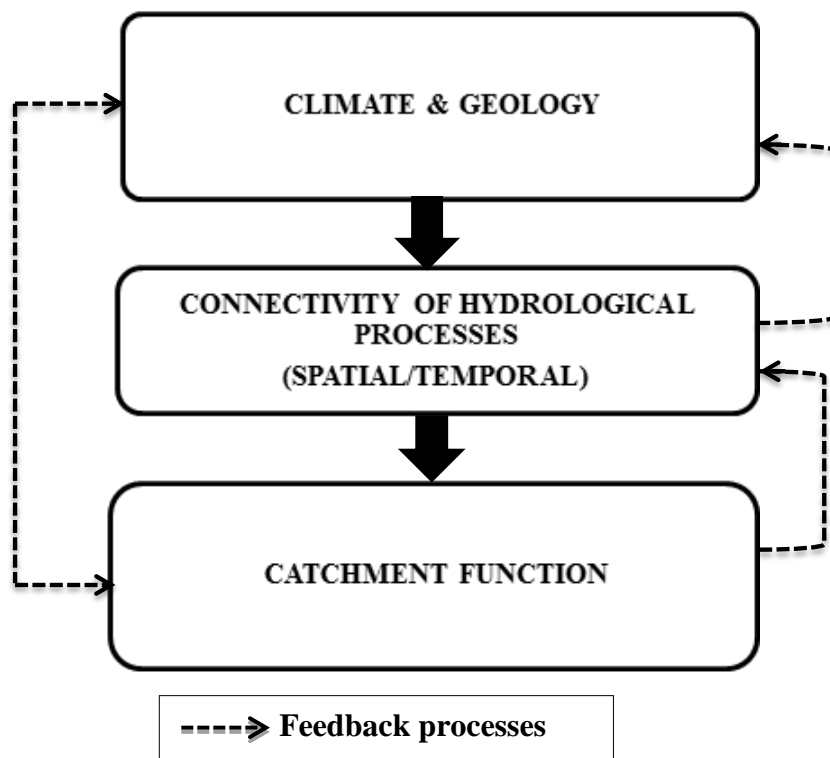


Figure 1.1 Schematic representation of key components constituting the current study

Viewing the vital role of water in semi-arid ecosystems, the need to understand its connectedness across spatio-temporal scales cannot be over emphasized. With this in mind, the essence of this thesis is summarized by the following key question and specific objectives:

Main research question:

- How is the stream connected to groundwater across nested incremental contributing areas (1st to 3rd order) on different geologies?

Specific objectives:

For each geology and incremental contributing area:

- Define mechanisms of groundwater-surface water interaction (i.e. stream gains and losses) during and immediately after rainfall events
- Quantify periods and sites of connection/disconnection during and immediately after rainfall events.
- Quantify groundwater-surface water contribution to streamflow during and immediately after rainfall events.

1.4 Structure of the Thesis

This thesis is structured in such a way that Chapter 2 presents the literature review which assisted in the selection and development of methodology for this study. Chapter 3 gives the setting of the study area or baseline data and hypothesis development as well as providing detailed description of materials and methods used. In Chapter 4 the characterization of catchment hydrological processes and responses is given in light of hydrometric analysis findings. Chapter 5 tests hypotheses developed from analysis of hydrometry using isotopic, hydrochemical and physico-chemical environmental tracers. A synthesis of results reflecting on the key research question and hypotheses of this study shall be presented in Chapter 6. This last chapter culminates with statement of limitations of study, further research suggestions and implications of findings to water resources management within and outside the Kruger National Park.

2. LITERATURE REVIEW

2.1 Introduction

Multiple definitions of connectivity exist across and within disciplines. For the purpose of this study some working definitions of hydrologic connectivity were selected. Herron and Wilson (2001) define the term as the efficiency with which runoff moves from source areas to streams and then through the stream network. Michaelides and Chappell (2009) view hydrologic connectivity as a measure of the degree of coupling between different components of the hydrological cycle, specifically the coupling of surface and groundwater flows. According to Tetzlaff et al. (2010) this term refers to the presence of a continuous saturated zone that links different landscape elements to the catchment outlet. From Pringle's (2003) perspective this term is taken to mean the hydrologically mediated transfer of mass, momentum, energy, or organisms within or between compartments of the hydrological cycle. It is portrayed from these definitions that precipitation into catchments follows defined pathways dictated by the structure of catchments (topography, soils & vegetation), prevailing climatic conditions. The influence of anthropogenic activities cannot be ruled out since these alter catchment structure through different land use practices. It is also evident from these definitions that hydrologic connectivity as a state and/or process of interaction of fluxes between surface and groundwater domains conveying mass (water and solutes) and energy to a catchment outlet. Figure 2.1 summarises the concept of how interactions occur between the afore-mentioned process domains.

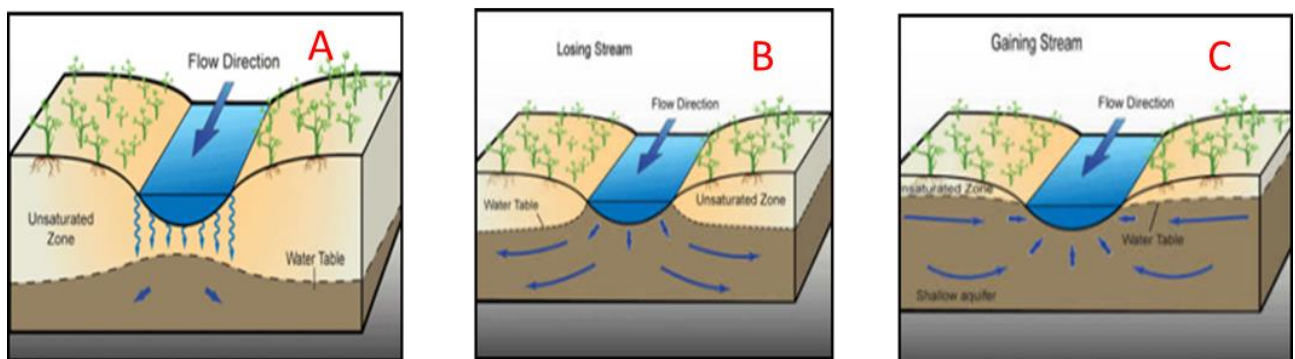


Figure 2.1 Recharge-discharge mechanisms (after Winter, 2007)

Groundwater-stream interaction is demonstrated by natural recharge and discharge processes, through the streambed and hillslope interface. Recharge occurring through channel leakage gives rise to losing or influent streams. Losing streams have water surface elevations that lie above aquifer water table which result in water seeping through streambeds to indirectly recharge groundwater aquifers. Stream A has an unsaturated zone under it while stream B overlies a saturated zone, but both streams are similarly losing. Stream A is typical of ephemeral streams (event-driven) while stream B epitomizes intermittent streams (only flowing seasonally). Conversely, groundwater discharge into channels results in gaining or effluent streams, as in stream C. Gaining streams are usually perennial with flows that typically occur all year round. While a gaining stream can be described as having a saturated connection to the aquifer a losing stream may either have a saturated or an unsaturated connection to the aquifer (Winter, 2007). The direction of fluxes between groundwater and streams commonly varies spatially and temporally along a stream reach and is influenced by the scale of analysis (Ivkovic, 2008).

The nature and extent of groundwater-stream interactions determine whether or not headwaters upstream of catchments are entirely transmitted through channels to downstream points. This phenomenon is what Nadeau and Rains (2007) describe as stream network connectivity or connectivity along streams. Longitudinal linkages are defined by upstream-downstream as well as tributary-trunk relationships (Fryirs et al., 2007). Notably streams can be gaining in one reach while experiencing transmission losses in another (Kalbus et al., 2006). When gaining, an increase in downstream discharge occurs whereas transmission losses result in a reduction of downstream flow (Beven and Hornberger, 1982; Tal et al., 2012).

2.2 Hydrologic Connectivity and Catchment Function

The term ‘function’ has plural meanings in environmental science denoting either processes, roles, services or the operation of whole systems (Schroder, 2006). With respect to catchments, ‘function’ can broadly be classified into hydrological, geomorphological, pedological and ecological functions which essentially, are interconnected functions. The collective response of a catchment as a result of the interaction of component processes is

termed catchment functioning (Bloschl et al, 2013). A catchment's component processes include the partitioning, transmission, storage and release of water, energy and matter into different pathways and storage areas (Bloschl et al, 2013). How these processes are connected within the catchment is controlled by thresholds and feedbacks over space and time scales. The controls and feedbacks governing hydrologic behaviour reflect inherent variability in catchment physiography and climate forcing across spatio-temporal scales (Wagener et al, 2008).

Inference of how connected hydrological processes are within catchments can be achieved by observing vegetation distribution patterns which tend to coincide with water distribution especially in water limited semi-arid environments. As such integrated studies between hydrology and ecology (vegetation structure & distribution) mutually assist either discipline in dealing with their respective research questions (Rodriguez-Iturbe, 2000; Schroder, 2006). The above observation concurs with Mackenzie et al. (2003), who noted that the fluvial geomorphology of the Sabie River in KNP is a critical component of the riparian vegetation distribution patterns. Thus hydrologic, geomorphic and ecological processes tend to undergo a process of co-evolution to produce patterns of self-organisation (Tetzlaff et al., 2010). For instance, riparian and wetland areas in the semi-arid environments usually show concentrations of woody, evergreen vegetation more than any other part within catchment landscapes due to moisture and nutrients availability conveyed by the interaction of hydrological processes. Hillerislambers et al. (2001) further support this notion through their study which revealed the formation of patterns in semi-arid areas portrayed by positive feedback between plant densities, local water infiltration coupled with the spatial redistribution of runoff water.

Similarly the soils of a catchment have an interactive relationship with its hydrology. The partitioning, transfer and storage of water (i.e. catchment hydrologic function) can be traced by studying soil properties across space and time scales since soils are products of water-related physical and chemical processes (Van Tol et al., 2013). The distribution of particular soils with discernible properties gives an indication of a catchment's hydrological response and it forms the basis of hydopedology (Lin et al., 2006). When correctly interpreted, the spatial variation of soil properties associated with the interaction of soils and water can serve as indicators of dominant hydrological processes (Van Tol et al., 2010). Pedologists, therefore, have the capacity to contribute valuable information to the science of hydrology by

interpreting and relating soil properties to catchment hydrological behaviour (Lin et al., 2006). Hydrologists agree that the spatial variety of soil properties significantly influences the connectivity of hydrological processes but their major challenge is the skill to gather and interpret soil information (Van Tol et al., 2010). The importance of integrating hydrology and soil science demonstrated in the above discussion can be achieved through interdisciplinary studies involving pedologists and hydrologists. Integrating hydrology and other science disciplines (e.g. ecology and pedology) as already described, will provide better understanding of hydrologic processes that characterise the catchment's hydrologic function.

Nuttle (2002) agrees that coupling hydrologic and ecosystem science is vital for understanding catchment function which in turn is vital to inform sustainable water management decisions. This is schematically presented in Figure 2.2.

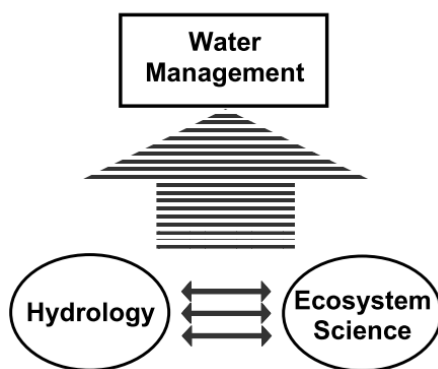


Figure 2.2 Integration of hydrology and ecosystem science (adapted from Nuttle, 2002)

In addition to interdisciplinary approaches, Tetzlaff et al. (2007) posit that a better understanding of catchment function can be obtained through use of tools and methodologies that present integrated perspectives of how catchments route water across spatio-temporal scales. This can be achieved through coupling multi-scale traditional techniques with integrated methods such as tracer analysis, geophysical surveys, remote sensing and modelling tools including Geographic Information Systems (GIS) and hydrologic models (Tetzlaff et al., 2010). For instance, hydrochemical tracers and geophysical surveys can provide integrated insights into emergent hydrological processes and how these are influenced by different landscape elements (Tetzlaff et al., 2007).

Analysing the chemistry of water from surface, subsurface and groundwater zones gives an indication of how flowpaths are integrated within these process domains. Quantifying water transit time distributions from tracer data within catchments leads to better understanding of the functioning of catchments. According to McDonnell et al. (2010) the modelling of transit times provides new insight to catchment functioning since transit times portray how catchments retain and release water and solutes thereby setting up biogeochemical conditions. Transit time distributions enable inference into dominant processes and catchment function by relating catchment responses to catchment characteristics including soils, vegetation, topography and climate. Integrated insight for understanding emergent behaviour of complex mixing processes and flowpaths within catchments can also be gained through quantifying transit times for water from rainfall input to the moment it reaches the stream (MacKinnon and Tetzlaff, 2009). Tracer determined transit times and flowpaths can further be used to inform distributed, physically-based hydrologic models which integrate catchment characteristics and processes to better understand the functioning of catchments (MacKinnon and Tetzlaff, 2009; McDonnell et al., 2010).

2.3 Drivers and Controls of Hydrological Connectivity

Studies have shown that hydrologic connectivity depends on several factors such as rainfall intensity, catchment wetness, vegetation characteristics, soil properties, geology, surface and bedrock topography (e.g. Buttle et al., 2004; Jencso et al., 2009; McGuire and McDonnell, 2010). These controls cause hydrologic connectivity to vary spatially and temporally thus reflecting geographic differences in key forcing factors and catchment characteristics. Interpreting these differences requires an understanding of catchments as evolving systems where climate and landscape organisation interact in different ways in response to external forcing to influence hydrological processes (Tetzlaff et al., 2010). However, since catchments are enormously complex and heterogeneous concentration should initially be on dominant or first order controls that influence observed heterogeneity (Wagener et al., 2008).

Antecedent soil moisture prior to a rainfall event plays an important role in initiating runoff and in ensuring continuity of flow to the stream outlet. Catchments in semi-arid areas, which often experience clearly demarcated seasons, have low antecedent moisture during dry

seasons and high in wet seasons. Consequently, hydrologic connectivity often fluctuates with these changes in seasons as well as episodically during and between rainfall events. As McGuire and McDonnell (2010) posit, a clear seasonality of a catchment accentuates connectivity presence and absence.

Soil properties in a catchment also determine hydrologic connectivity between constituent parts of the basin. These include soil macropores, soil layering and soil depth. Macropores are formed and developed by various mechanisms which include subsurface erosion, animal burrows, live and decayed plant roots as well as surface bedrock fractures. Noguchi et al. (1999) assert that connection of macropores can possibly occur over relatively long slope distances creating considerable waterflow pathways.

The influence of topography on water fluxes cannot be overemphasized. Having bearing on catchment slopes or gradients, topography poses as an important control on flow direction. Micro-topography also determines whether flow should occur or not, as some water should contribute to depression storage before it can flow to downslope areas. However, it has been noted in recent studies that surface and subsurface topography should be considered separately, since their effects on waterflows are distinctly different (Costa et al., 2012). While surface topography mainly influences surface flows, bedrock topography controls local hydrological gradients and has significant impacts on flows in the vadose zone.

2.4 Connecting Mechanisms of Surface and Groundwater Resources

Various mechanisms facilitate the interaction of groundwater and surface water within and between nested catchments. These include subsurface lateral flow occurring either through soil/bedrock interfaces or through soil material underlain by a layer of low hydraulic conductivity. Surface water can be connected to groundwater aquifers by infiltrating the soil and weathered zone matrices or directly through fractures or macropores as preferential flow (Sophocleous, 2002). Stormflow can be distinguished from baseflow in that baseflow occurs due to the sole contribution of groundwater discharge from persistent, slowly varying sources (Sophocleous, 2002) into streams and this keeps streams flowing during dry periods. Subsurface flow that enters streams quick enough to contribute to event-response is known as subsurface stormflow or quickflow (Sophocleous, 2002). According to Beven (1989)

interflow can be defined as near-surface flow occurring within the soil profile and enters a stream channel within the time frame of a storm hydrograph. Interflow was isotopically observed to sometimes contribute to stormflow response through a displacement or translatory process in which event water displaces or bumps onto stored subsurface water pushing it towards stream channels (Beven and Germann, 1982; Sklash and Farvolden, 1979). If the rate of interflow entering a saturated area from upslope exceeds that of interflow leaving the area, excess interflow returns to the surface as return flow.

2.5 A Review of Existing Knowledge on Hydrological Connectivity

Several studies have been conducted on groundwater-surface water interaction with various study goals including (i) the understanding of hydrological processes (e.g. McCartney et al., 1998; Burns et al., 2001; Bohte et al., 2008; Wenninger et al., 2008; Riddell et al., 2013) (ii) water resources evaluation and management (e.g. Ogunkoya et al., 1993; McGlynn and McDonnell, 2003; Baskaran et al., 2009; Praamsma et al., 2009; Bohte et al., 2010), and (iii) monitoring hyporheic fluxes to identify ecological zones suitable for fish spawning (Malcolm et al., 2005). Although this subject has been investigated fairly widely, most of the studies have largely been descriptive rather than quantitative (McDonnell, et al., 2007; Jencso and McGlynn, 2011). This has resulted in research findings that are site-specific with no chance of being generalised to other catchments with similar environmental conditions. As a result, there has been partial understanding of linkages between catchment structure and function.

Research studies (e.g. Bracken and Croke, 2007; McGuire and McDonnell, 2010) have generally shown that subsurface flow is the dominant mechanism in forested or vegetated catchments, however, specific flowpaths, transit and residence times and sources of water are not well understood. Devising new approaches needed to determine and quantify hydrological process linkages remains the most pressing challenge in environmental hydrology (Ali and Roy, 2009).

Stream-aquifer interactions are characterised by spatio-temporal variability (Katz et al., 1998) which is understood at least at local/hillslope scales (Soulsby et al., 2008). Since management decisions are made at catchment scale, recent research has shifted towards upscaling from smaller research plots to larger mesoscale catchments. Due to process complexity and

catchment heterogeneity upscaling often requires identification of dominant processes evident at catchment scale rather than attempting to capture all small scale variability and complexity (Tetzlaff et al., 2010). Tracers (e.g. Uchida et al., 2005) and geophysical surveys (Wenninger et al., 2008) were noted to be useful for conceptualising smaller scale catchment processes which can be used for upscaling studies. Applying these techniques at a multi-scale level in nested catchments yields useful results which inform hydrological model building and allows unanticipated or emergent responses to be identified (e.g. Soulsby et al., 2008).

The variability of hydrological responses within and between catchments is attributed to plural controls influenced by heterogeneous catchment characteristics such as geology, streambed permeability, surface and bedrock topography, antecedent moisture, vegetation characteristics, and soil properties (Jencso et al., 2011; Van Tol et al., 2013). Studies have been done to investigate individual influence of these controls, for instance streambed topography (e.g. Harvey and Bencala, 1993) and local channel geomorphology (e.g. Malcolm et al., 2005). However, it is noted that very few studies have comparatively investigated the combined and hierarchical influence of these controls across space and time scales (Jencso et al., 2011). Despite existing inter-catchment variability, comparative studies make it possible to discern similar functional patterns between catchments which could be used to formulate and test generic hypotheses that are applicable to other catchments, especially ungauged basins (Wagener et al., 2008). Earlier approaches that characterised and catalogued enormous heterogeneity and complexity of catchment processes have produced findings that are not generic for prediction in ungauged basins (PUB) (McDonnell et al., 2007). As such contemporary approaches advocate the exploration of sets of organising principles (McDonnell et al., 2007) which relate catchment hydrology to vegetation distribution (e.g. (Nuttle, 2002; Blöschl et al., 2013) or to soil properties (e.g. Van Tol et al., 2013). The concept of identifying organizing principles is actually a paradigm shift from emphasizing reproduction of process complexity to that of simplifying complex systems by identifying patterns or dominant processes that explain the existence of those complexities (Sivapalan, 2005). Organizing or optimality principles form diagnostic generalization tools and analytical frameworks that act as a basis for cross-scale characterisation and prediction (MacKinnon and Tetzlaff, 2009).

The community of hydrological scientists still has not realized the Dooge (1986) vision of searching for new macroscale laws that will assist in predictions in ungauged basins

(McDonnell et al., 2007). Other studies advance the concept of providing a common hydrologically significant classification framework through assessing and mapping catchment form, climate and function (Wagner et al., 2008). When achieved such a framework provides insight into causal relationships between the afore-mentioned aspects (form, climate and function) thereby increasing predictive power through rational testing of hypotheses about similarity/dissimilarity of hydrological systems (Wagner et al., 2008). Tested hypotheses can lead to theories or models which when proven can be established as laws with wide applicability.

Integrated approaches involving various disciplines and methodologies (e.g. tracers, geophysical surveys, remote sensing and hydrological models in addition to hydrometry) are recommended in literature for better understanding of how catchments respond to rainfall events (Lorentz et al., 2008; Jencso et al., 2011). Involving experts from other disciplines such as geologists, ecologists and engineers enhances better understanding of catchment functioning and the underlying governing processes (Rodriguez-Iturbe, 2000). Progressive implementation of adaptive analytical tools and procedures enables the field of catchment hydrology to develop robust methodologies and understanding that takes cognisance of global change impacts with respect to climate and land use changes (Van Beek et al., 2003).

2.6 Methods and Techniques of Investigating Hydrologic Connectivity

Several methods and techniques have been used to investigate and test the connectivity of hydrological processes (Scanlon, 2002). These include electrical resistivity tomography (ERT), hydrometric techniques, hydrochemical and isotopic tracers and hydrological modelling. Various results under diverse climatic and physiographic conditions were obtained and each technique's limitations and strengths noted. Taking cognisance of strengths and limitations of different methods, integrated approaches to catchment studies are being viewed as a means to better understand catchment process behaviour since one method's limitation is addressed by the strength of another (Uhlenbrook et al., 2005; Crook et al., 2008).

2.6.1 Electrical Resistivity Tomography (ERT)

One of the challenges of studying streams is to understand and quantify subsurface properties (Crook et al., 2008). Most studies have employed point measurements which include

installing piezometers and trenches at selected locations in the streambed. These have not fully achieved the intended goals especially in channels that are characterised by highly heterogeneous streambeds (Crook et al., 2008). Geophysical techniques bridge this gap by providing subsurface streambed sediment and lithological information with spatial continuity. According to Uhlenbrook et al. (2005) electrical resistivity surveys have been conducted for decades in hydrogeological or geotechnical investigations and have recently been used to solve problems in environmental hydrology. Earlier studies have used ERT for various purposes including definition of soil water dynamics (Koning, 2006), characterisation of substream sediments (Crook et al., 2008), understanding hillslope lithology in order to define and upscale key hydrological processes (Lorentz et al., 2008) and for the hydrological characterisation of a wetland system (Riddell et al., 2012). These studies have revealed the effectiveness of ERT in providing deeper understanding of subsurface profiles including the identification of hydro-geomorphic controls to water fluxes.

ERT is conducted by injecting electric current into the ground through an array of current electrodes and then measuring the resultant potential difference through pairs of potential electrodes. The choice of which array to use depends on what sort of subsurface data needs to be obtained in a study, for instance deep lithological or shallow subsurface information. Varying the position and sequence of current and potential electrodes along transects, results in the acquisition of subsurface measurements of different spatial (horizontal and/or vertical) resolution. The current (I) and voltage (V) values obtained from these measurements are used to calculate apparent resistivity for subsurface materials using the following equation (Loke, 1999):

$$P_a = kR, \quad (2.1)$$

where p_a is apparent resistivity, R is resistance obtained by dividing voltage by current (Ohm's law) and k is the geometric factor.

True resistivity values are then obtained by inverting the apparent resistivity values using 2D Electrical Resistivity and Induced Polarisation Inversion software (RES2DINV).

2.6.2 Hydrometric techniques

The monitoring of water levels in the stream, subsurface piezometers and groundwater boreholes is essential for determining hydraulic gradients across spatial scales (Cey et al., 1998). Coupled with subsurface hydraulic conductivities, hydraulic gradients can be useful in calculating fluxes within and between process domains (Harvey et al., 1996; Landon et al., 2001; Baxter and Hauer, 2011). The data obtained from hydrometric techniques can be used to determine whether river reaches are effluent (gaining) or influent (losing). Losses and gains occurring within river reaches have been noted for influencing streamflow reduction and increase, respectively (Nadeau and Rains, 2007).

□ Streamflow characterisation

Streams are natural conveyances of water which are exposed to the atmosphere. The component of the force of gravity in the direction of motion is the driving force of waterflow in streams. The geometry of stream channels is geomorphologically determined by the long term history of sediment load and water discharge. Each stream balances channel erosion, sediment transport and deposition in the context of its physiographic and climatic settings (Harrelson et al., 1994). Therefore, to understand streamflow and its controlling variables the characterisation of stream channel longitudinal and cross sectional profiles is essential, especially in ungauged catchments. Several studies have been conducted to characterise channel networks and interfluvial physiographic and lithological settings using methods that include theodolite surveys to determine channel cross section areas (Riddell et al., 2011), geophysical surveys to understand subsurface lithology for identification of hydrological processes (Wenninger et al., 2008) and steel probe cross section surveys to determine subsurface cross section areas (Mansell and Hussey, 2005). With channel surface and subsurface cross sectional areas, estimation of streamflow and subsurface discharge can be done using the slope-area method (Herschy, 1985) and Darcy formula (Younger, 2006), respectively.

□ **Stream discharge**

Stream discharge can be calculated using the continuity equation by multiplying channel cross sectional area and the flow velocity in the channel. The cross sectional area is obtained through surveys as already explained in Section 2.6.2 (a). Flow velocity can be measured directly or indirectly. Direct methods include tracer dilution method, floating object method, velocity-area method, mid-section and mean section methods. Details of these methods are documented in literature (e.g. Carter and Davidian, 1989). During floods, it is practically difficult to measure flow velocities using direct methods due to (Herschy, 1985; Carter and Davidian, 1989):

- The threat posed by extremely high flows accompanied by transport of debris and large logs.
- Damaged infrastructure such as impassable roads and bridges that hinder access to gauging stations.
- Knowledge of impending floods might not be available well in advance to allow hydrographers to reach gauging sites before or at the time to peak.

Owing to the predicaments just outlined, indirect methods are commonly used to compute flow velocity. One such method is the slope-area method (Herschy, 1985), which is normally employed after the flood has passed. This method requires knowledge of the energy gradient or water surface slope, hydraulic radius and the character of the streambed which helps in the selection of a suitable roughness coefficient (Chow, 1959; Herschy, 1985). Computation of flow velocity then occurs using either the Chezy or Manning's equation (Herschy, 1985).

For practical purposes Manning's equation is preferred to the Chezy equation for its simplicity in application as well as for a proven record of reliable results over the years (Herschy, 1985).

Determination of a channel's Manning's roughness coefficients calls for the understanding of roughness adjustment factors and knowledge of typical channels whose roughness is already documented (Chow, 1959; Arcement and Schneider, 1984; Sturm, 2001). Channel roughness adjustment factors including characteristics of in-stream/ floodplain vegetation, channel

geometry, in-stream obstructions and sinuosity should be considered when estimating Manning's roughness coefficients (Cowan, 1956).

□ **Stage-Discharge Relationship**

Flow is an important variable required in hydrological analysis but its continuous measurement at a river reach is not practically feasible due to high operating costs (DHV and DELFT, 1999). Conversely, stage can relatively be measured and monitored with relative ease. River discharge at a section is related to its corresponding stage (DHV and DELFT, 1999). This rating relationship is used to determine discharges from observed stages at a river reach. Discharge is not always a unique function of stage, but other variables such as streambed slope, channel roughness and shape also play an important role in the relationship.

2.6.3 Hydraulic conductivity (K)

Streambed hydraulic conductivity is an important parameter required in order to quantify the magnitude and spatial distribution of groundwater-surface water interactions (Landon et al., 2001). The estimation of streambed hydraulic conductivities can be done using several methods including slug tests (e.g. Bouwer and Rice, 1976; Baxter et al., 2011), pumping tests conducted near streams (e.g. Landon et al., 2001), chemical tracer experiments (e.g. Harvey et al., 1996), aquifer grain size method (e.g. Landon et al., 2001) and constant head permeameter tests (e.g. Landon et al., 2001). In a comparative study of in-stream methods for estimating streambed hydraulic conductivity, Landon et al. (2001) found that the making of adequate measurements along the stream channel matters more than the actual method used, so that spatial variability can be captured. Thus for any selected method to determine K, provided it is used in locations that adequately represent the heterogeneity along the streambed, the data will be useful to quantify groundwater-surface water interactions at different places along the channel.

The knowledge of horizontal hydraulic conductivity of streambed sediments enables one to calculate subsurface discharge when the hydraulic gradient between two points on the traversed aquifer is known. This is particularly important in catchments that are drained by

ephemeral streams with short-lived surface flows that culminate into subsurface discharge between rainfall events.

2.6.4 Hydraulic gradient

Monitoring water levels in piezometers and wells installed in hillslopes, riparian zone and in streambeds is the standard method to estimate hydraulic gradients (Kalbus et al., 2006). Differences in hydraulic head between nested piezometers and their horizontal distances can be used to calculate hydraulic gradients which in turn help to determine horizontal fluxes in porous media.

Vertical components of groundwater flow are calculated from piezometer nests with piezometers set at different depths in the same location. Vertical hydraulic gradient (VHG) are then calculated from the head difference between piezometers and the difference in piezometer depths (Kalbus et al., 2006). Alternatively, VHG can be calculated through dividing the difference between stream stage and water level in a piezometer which is installed in the streambed, by the length of the piezometer screen (Baxter et al., 2011). Positive vertical hydraulic gradient values indicate groundwater discharge into the stream whereas negative values show loss of water from the stream into the ground (USGS, 2001; Baxter et al., 2011). Hydraulic gradients assist to infer possible existence or absence of connectivity between hillslopes and streams or between streams and streambed aquifers (Jencso and McGlynn, 2011). Water levels can either be read manually or using automated pressure transducer systems.

2.6.5 Subsurface discharge

Knowledge of a porous medium's hydraulic conductivity, hydraulic gradient and cross sectional area makes the quantification of subsurface flow possible using Darcy's Law (Younger, 2006): Multiplying the above-mentioned quantities gives subsurface discharge. Subsurface cross sections are obtained either through the use of geophysical surveys or by

driving steel probes into the streambed to the hard rock across a stream channel (Mansell and Hussey, 2011).

2.7 Environmental Tracers

Environmental tracers are natural or manmade chemicals or isotopic substances that can be measured in various water samples in order to understand catchment or hillslope hydrologic properties (Plummer, 2003). Natural environmental tracers exist in the atmosphere or in soils and are incorporated into precipitation and into water that infiltrates to recharge groundwater aquifers. The use of environmental tracers is known for its effectiveness in defining interactions of water fluxes thereby assisting to inform the development of catchment hydrological models (Burns et al., 2001; Lambs, 2003; Haria and Shand, 2006; Soulsby et al., 2008; Wenninger et al., 2008). Through use of tracers small scale heterogeneity can be integrated to build a bigger picture of dominant catchment-scale hydrological processes. This is possible without the need to extrapolate or to formulate additional assumptions in a bid to understand catchment behaviour (Kendall and Caldwell, 1998). Uses of environmental tracers include identification of streamflow generation mechanisms, testing hydrological conceptual models developed through hydrometry, and to quantify contributions of different water sources to total streamflow (McGuire et al., 2005). Environmental tracers commonly used in hydrological studies include stable isotopes (e.g. $\delta^2\text{H}$ and $\delta^{18}\text{O}$), hydrochemical parameters (e.g. Cl^- , Ca^{2+} , Mg^{2+} , K^+ , Na^+), and physico-chemical parameters such as electrical conductivity (EC), pH and salinity.

2.7.1 Hydrochemistry

Chemical signatures of groundwater, subsurface and surface water in terms of concentrations can be used to understand hydrological processes (Sundaram et al., 2009). Hydrogeochemistry is useful to estimate recharge, discharge and mixing or connectivity of fluxes from different sources. Since groundwater-surface interactions are complex, a multi-parameter approach involving chemical, isotopic, hydraulic and geophysical techniques is often advantageous for a better understanding of underlying processes (Sundaram, 2009).

▪ Cations

Cations are positively charged metallic ions while anions are negatively charged non-metallic ions found in solution as dissolved components of their compounds. Major cations and anions are those that commonly exist in high concentrations almost always exceeding 1mg/L (Younger, 2006). Examples of major cations include calcium (Ca^{2+}), magnesium (Mg^{2+}), sodium (Na^+) and potassium (K^+). Steady concentrations of major cations are introduced to different domains through rainwater as well as through dissolution of minerals in soil and bedrock (Sundaram et al. 2009). In more basic igneous rocks such as basalts, Ca^{2+} and Mg^{2+} are obtained from weathering of anorthitic plagioclase ($\text{CaAl}_2\text{Si}_2\text{O}_8$) and diopsidic pyroxene ($\text{CaMgSi}_2\text{O}_6$), while in acidic igneous rocks such as granites common sources of these cations are Biotite mica ($\text{K}(\text{MgFe})_3(\text{Si}_3\text{Al})\text{O}_{10}(\text{OH})_2$) and hornblende ($\text{Ca}_2\text{Mg}_4\text{Al}_2\text{Si}_7\text{O}_{22}(\text{OH})_2$) (Younger, 2006). Silicate weathering is also a common source of K^+ and Na^+ . As the silicate compounds dissolve to release major cations concurrent precipitation of clay minerals occur which traps much of SiO_2 and all aluminium deposits in them (Younger, 2006).

▪ Anions

Major anions include chloride (Cl^-), sulphate (SO_4^{2-}) and bicarbonate (HCO_3^-). Rainwater is the most common source of Cl^- , accounting for about 20mg/L. Sodium is one of the least reactive solutes which can also be obtained in small amounts from halite and sylvite compounds. According to Kirchner et al., (2001), chloride is an effective chemical tracer due to its non-reactive nature under typical catchment conditions.

▪ Dissolved silica (SiO_2)

Dissolved silica is a common component of many rocks such as quartz in sandstones and unconsolidated sand deposits. It is obtained through the dissolution of silicate minerals as discussed for Ca^{2+} and Mg^{2+} . Silica is known for being less reactive hence its common application in hydrograph separation and other tracer studies (Shanley et al., 2002)

2.7.2 Physico-chemical parameters

Electrical conductivity (EC) is an indirect method of measuring salinity which is one of the most common and convenient tracers in catchment hydrology (Sundaram et al., 2009). A combination of cations and anions described above, accounts for the extent of electrical conductivity by water samples from different sources.

2.7.3 Isotopes

Oxygen isotopes (^{18}O & ^{16}O) and those of hydrogen [protium (^1H), deuterium (^2H) are the common stable isotopes used to understand hydrological processes. Radioactive isotopes such as radon and tritium (^3H) are also sometimes used in hydrological studies. Various reasons exist that make stable isotopes useful tools in tracing water and solutes in a catchment. These include the fact that (Kendall and Caldwell, 1998; Liebundgut et al., 2009):

- Stable isotopes are integral constituents of water molecules and are not dissolved solutes.
- They are conservative, retaining their distinct fingerprints, in reactions with catchment materials.
- They provide proof of hydrologic connection despite any hydraulic measurements or models to the contrary, for instance, when water from isotopically distinct sources (e.g. rain) is found along a flowpath.

□ Reporting isotope data

Stable isotope compositions of light elements such as oxygen, hydrogen, carbon, nitrogen and sulphur are normally presented as delta (δ) values which are reported in units of parts per thousand denoted as (‰) or permil relative to a standard of known composition. Calculation of delta values is governed by the following equation (Kendall and Caldwell, 1998):

$$\delta \text{ (in ‰)} = (R_x/R_s - 1) * 1000 \quad (2.14)$$

where R = ratio of heavy to light isotope (e.g. $^{18}\text{O}/^{16}\text{O}$) while R_x and R_s are the ratios in sample and standard respectively.

Delta values are always prefixed by a positive or negative sign where a positive value means that the sample isotopic ratio is higher than that of the standard (enriched with respect to the heavier isotope). Conversely, a negative value shows a lower isotopic ratio for the sample than for the standard (depleted with respect to the heavier isotope). For example, a $\delta^2\text{H}$ value of +10‰ implies that the $^2\text{H}/^1\text{H}$ ratio of the sample is 1% higher than that of the standard. Isotopic compositions of samples analysed on mass spectrometers are reported against an international reference standard known as the Vienna Standard Mean Ocean Water (VSMOW). Usually samples are analysed simultaneously with the reference standard or with some internal standard developed by a laboratory and calibrated relative to the international standard.

□ **The Global Meteoric Water Line (GMWL)**

Earlier research (e.g. Craig, 1961) revealed that oxygen and hydrogen stable isotopes show similar variation during fractionation processes of most meteoric waters. The observed covariant relationship known as the Global Meteoric Water Line (GMWL) is described by the following equation (Craig, 1961):

$$\delta^2\text{H} = 8 \delta^{18}\text{O} + 10 \quad (2.15)$$

The GMWL is a regression line obtained from the isotopic analysis of precipitation samples that provides a reference against which local differences in water may be compared. The slope and intercept of the GMWL equation are useful in the analysis of isotopic systematics of groundwater, surface water and rain as components of the hydrological cycle (Kendall and Caldwell, 1998). When analysing water samples the data should immediately be plotted on a $\delta^2\text{H}$ versus $\delta^{18}\text{O}$ diagram to see whether it plots on the GMWL. Perfect plots lie exactly on the GMWL. Evaporated water samples plot below GMWL, have a slope of less than 8 and are enriched in heavier isotopes (δD and $\delta^{18}\text{O}$). Water samples that have not undergone

evaporation are said to be depleted in the heavier isotopes and they plot above the GMWL (Kendall and Caldwell, 1998).

When water evaporates, isotopic molecules (H_2^{16}O ; HDO & H_2^{18}O) distribute themselves such that heavier molecules (HDO & H_2^{18}O) are concentrated in the remaining liquid while the vapour will have higher concentrations of lighter H_2^{16}O molecules (Kendall and McDonnell, 1998; Liebundgut et al., 2009). This information on isotopic composition of certain forms of precipitation enables the quantification of their importance in the hydrological cycle. The isotopic composition of raindrops is determined by two major factors which are the isotopic composition of the condensing parent vapour and environmental temperature. The composition of the condensing vapour derives from the meteoric history of the original air mass such as upward losses by precipitation and additions from evapotranspiration (Kendall and McDonnell, 1998; Liebundgut et al., 2009).

□ **Hydrograph separation using environmental tracers**

Several studies have been conducted to separate streamflow components using environmental tracers in different climatic and physiographic environments. Most studies conducted in perennial rivers in different climatic environments have shown greater contributions of pre-event water (old water) to streamflow than event water (rainfall) contributions (e.g. Sklash and Farvolden, 1979; Burns et al., 2001; McGlynn and McDonnell, 2003; Bohte et al., 2010). However, other studies found event water contribution dominating the pre-event component (e.g. McCartney et al., 1998; Brown et al., 1999; Riddell et al., 2013). Various trends have been noted across scales with respect to the contributions of event and pre-event water sources (Shanley et al., 2002). Very few hydrograph separation studies have been done particularly in ephemeral streams in semi-arid areas (e.g. Mulholland, 1993).

2.8 Discussion of Reviewed Literature

Reviewed literature has shown the necessity of catchment scale studies on hydrologic connectivity to further contribute understanding of hydrological processes which is necessary for the development of hydrological models. Various controls on hydrologic connectivity

have been identified including geology, channel morphology, surface/bedrock topography, vegetation characteristics, antecedent moisture and rainfall intensity. However, it is little known how these controls actually influence groundwater-surface water interaction. In addition, very few comparative studies have been conducted to determine the influence of a control such as catchment geology.

Tracers such as Cl, Si, EC, ^{18}O , and ^2H have been proven effective in defining sources and pathways of water-flows in a catchment as well as in informing hydrological modelling. Therefore, one can confidently use these tracers in similar studies to understand water fluxes from different process domains within catchments. It has also been noted that water levels in piezometers and boreholes are useful in determining hydraulic gradients, hydraulic conductivities of aquifers using slug tests as well as for subsurface and groundwater sampling.

Integrating hydrometric and tracer techniques help to understand hierarchical controls to connectivity. This implies that multi-disciplinary studies involving combined expertise from hydrologists, hydrogeologists, hydropedologists, engineers to ecologists yield a better understanding of hydrological processes and catchment function.

2.9 Main challenges & gaps

Reviewed literature revealed challenges and gaps in hydrologic connectivity studies as follows:

- Catchment scale controls on streamflow generation are poorly understood.
- Few studies quantified groundwater-surface water interaction across scales hence findings are site specific and difficult to generalise.
- Little work has been done to understand spatio-temporal differences and drivers of hydrologic connectivity across nested catchments.
- Few studies have investigated the combined influence of geology and rainfall intensity on hydrologic connectivity.
- In particular no quantification of the contribution of different water sources to streamflow has so far been done in ephemeral streams of the Kruger National Park.

- Above all, it has been revealed through literature that integrating various methods provides better understanding of catchment hydrology, since weaknesses of one method are overcome by the strength of another.

3. METHODOLOGY

3.1 Study Area

3.1.1 Geology and drainage

The Kruger National Park (KNP) has a north–south longitudinal geologic alignment, consisting mainly of granites to the west and basalts to the east with patches of shale and sandstone sandwiched between them (O’Keeffe and Rogers, 2003; Cullum and Rogers, 2011). This longitudinal stretch of geology is dissected by 5 main river systems (Luvuvhu, Letaba, Olifants, Sabie and Crocodile) with a west–east flow direction across it (O’Keeffe and Rogers, 2003). These major river systems have their origin outside the park in the Klein or Northern Drakensburg Escarpment and they pass through landscapes under diverse land use practices ranging from forestry, irrigated crop and citrus fruit agriculture to communal mixed farming. Conversely, smaller drainages originate in and end within the boundaries of the park in low rainfall areas resulting in them being ephemeral streams. O’Keeffe and Rogers (2003) further observe that the occurrence of intrusive dykes of dolerite, patches of gabbro and minor faults add heterogeneity and complexity to the geological template of the park.

3.1.2 Climate and vegetation

KNP is generally semi-arid with a rainfall range falling between 440-740mm per year (Venter and Gertenbach, 1986). A north-south rainfall gradient of 450-650mm/year exists (O’Keeffe and Rogers, 2003) with an east-west gradient of between 400 and over 600mm per year (Cullum and Rogers, 2011) in the KNP. Seasonal rainfall is experienced within KNP, with November to March being wetter months while April to October constitutes the drier period. KNP is situated in the savanna biome of South Africa which is a semi-arid system where water plays a pivotal role in many biotic and geomorphic processes.

The diversity of vegetation in KNP varies with underlying geology, rainfall amounts and faunal activity (particularly of large herbivores such as elephants). Some parts of the park are still under pristine conditions while others have been altered by human interference adding to

the spatial variability in the occurrence and diversity of vegetation. Due to higher rainfall, deeper and more diverse soils, the southern parts of KNP have varied woody vegetation species which are also influenced by hillslope position and geology (Cullum and Rogers, 2011).

3.1.3 Supersites

Two research sites (coined “Supersites” by Cullum and Rogers, 2011) falling within KNP’s dominant geologies, were the focus of this study. Figure 3.1 shows the Southern Granites (Stevenson Hamilton) and Southern Basalts (Nhlowa) study sites, which shall henceforth be referred to only as Southern Granites and Southern Basalts, respectively. Three nested catchments at each study site which were based on 1st to 3rd order incremental contributing areas were delineated for this study. At the Southern Granites incremental areas for the nested catchments are 0.3km², 0.9km² and 1.5km² for 1st to 3rd order, respectively. On the other hand nested catchments at Southern Basalts have incremental areas of 15.4km², 31.6km² and 47.8km².

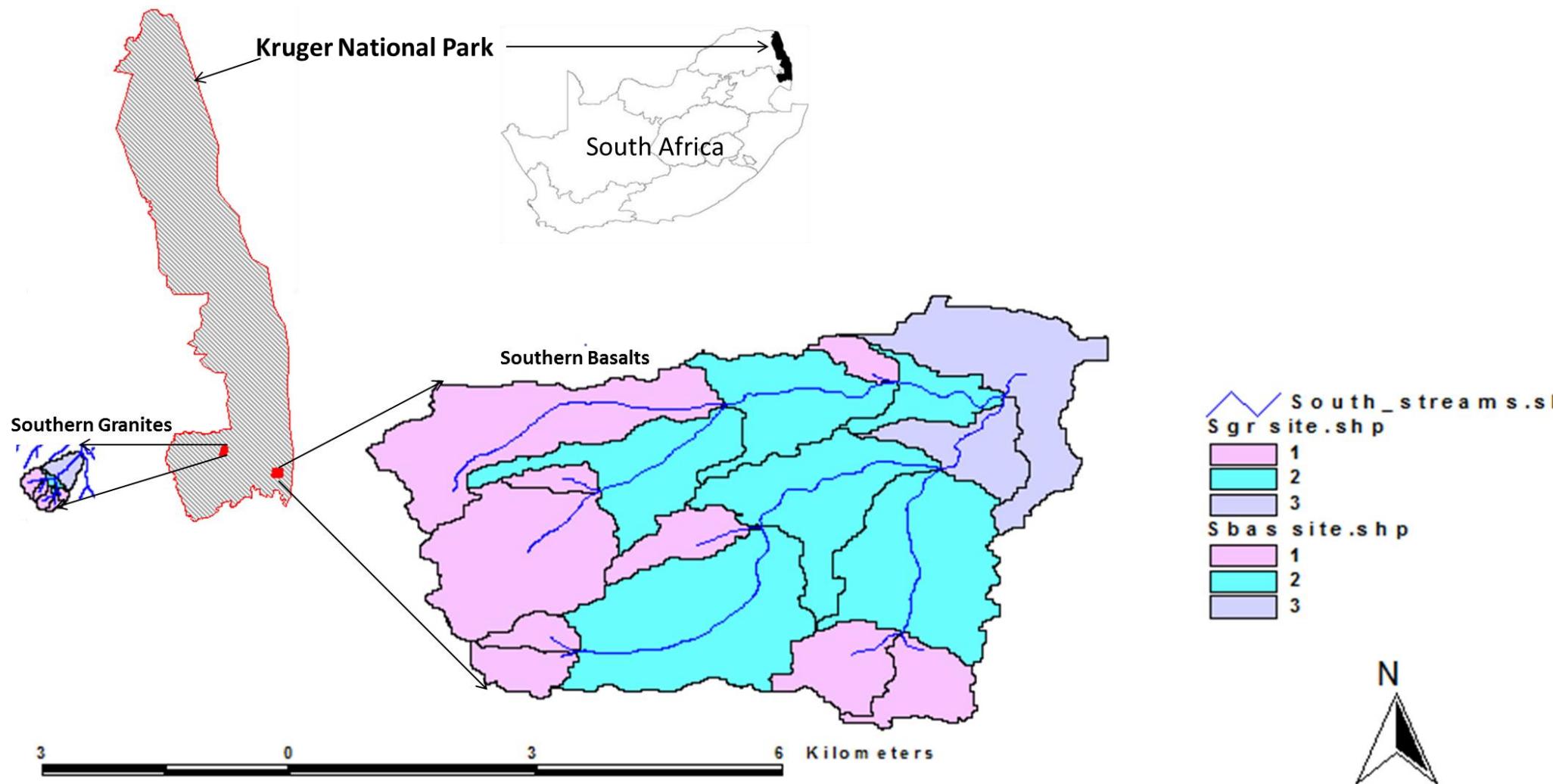


Figure 3.1A Map of study sites, Southern Granites and Southern Basalts. Labels 1,2 and 3 represent contributing areas for 1st, 2nd and 3rd stream orders, respectively.

□ Southern Granites Catchment Characteristics

The topography is characterised by steeper slopes (3.2%) from headwaters decreasing downstream to 2.3% at the 3rd order. A high stream density dissects the underlying granite geology. Channels of lower order streams are deeply incised with steep banks as evidence of active sediment evacuation that occurs during storms. Higher order stream channels are shallow and often contain woody vegetation and massive sand deposits along streambeds and within the floodplain. The floodplain widens and becomes more defined downstream towards higher stream orders. Soil depth also increases from lower to higher order catchments. Information on soil forms was taken from Le Roux et al. (2011). The crests and midslopes are convex straight dominated by soils of the Mispah (Ms), Glenrosa (Gs) and Cartref (Cf) forms in the catchments of 1st, 2nd and 3rd order streams (Le Roux et al., 2011). The footslopes have Sterkspruit (Ss), Milkwood (Mw), Bonhiem (Bo) and Mayo (My) soils (Le Roux et al., 2011). It is covered with grass and scattered patches of trees. *Acacia nilotica* tree species dominate footslopes and midslopes. Sodic sites are common on the midslopes increasing in area towards the 3rd order catchment. Combretum apiculatum and Combretum zeyher dominate the woody vegetation on the crests. Figure 3.1B summarises the functional distribution of soils at the Southern Granites study site. The soil map shows that the 1st and 2nd order catchments are dominated by interflow soils. Hydropedological responses of interflow soils are characterised by predominant lateral fluxes either within the A/B horizon or on the soil bedrock interface (Van Tol et al., 2013). The 3rd order is dominated by recharge soils which do not have any morphological indication of saturation hence promoting vertical fluxes through the soil profile (Van Tol et al., 2013) except at the sodic site where either shallow or saturated responsive soils dominate. Shallow responsive soils have limited storage which results in overland flow after rainfall events, whereas saturated responsive soils show morphological evidence of long periods of saturation and are characterised by saturation excess overland flow (Van Tol et al., 2013). The long-term mean annual precipitation (MAP) is 550.4mm (SANParks Scientific Services, 2013).

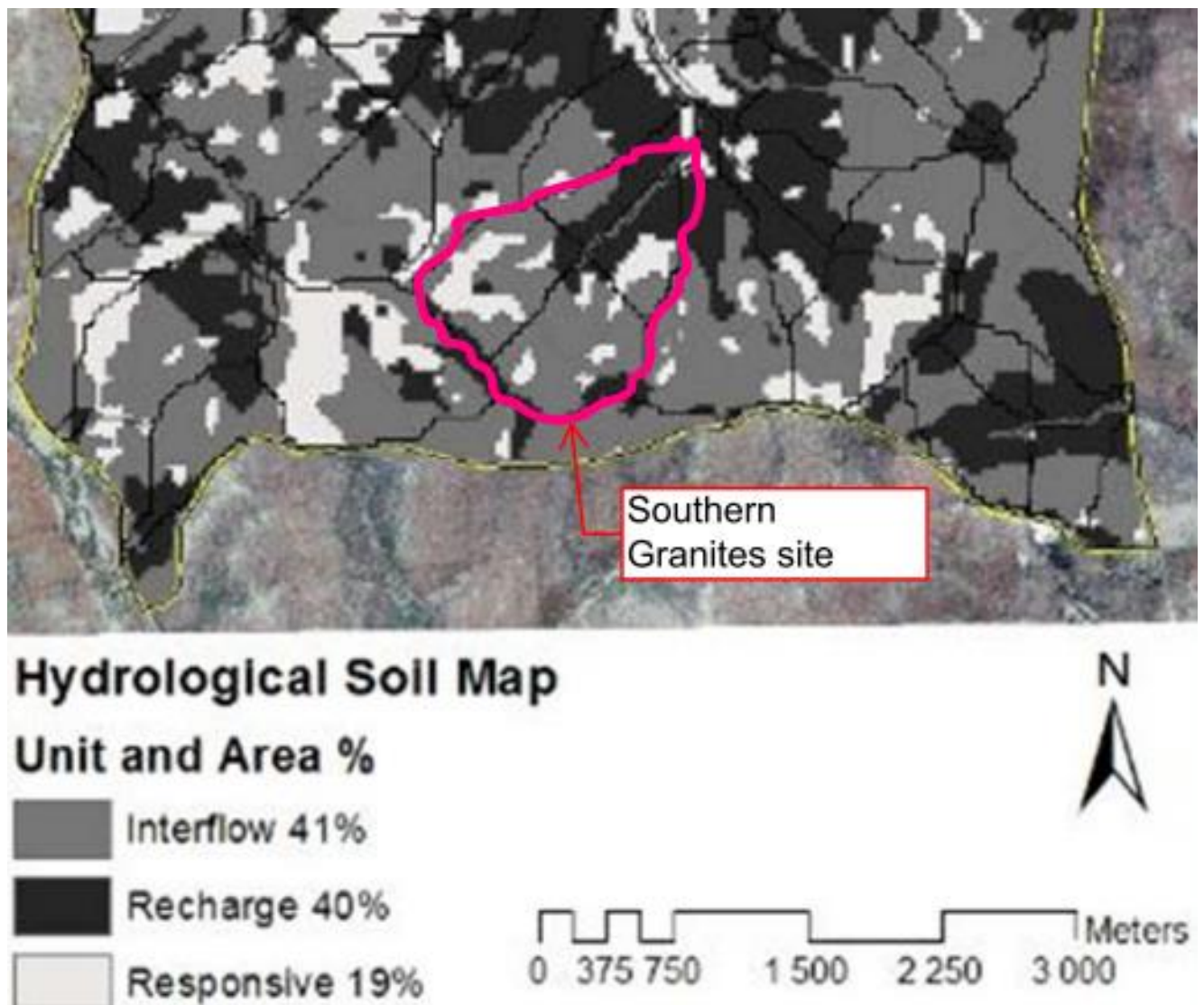


Figure 3.1B Southern Granites soil map showing distribution of soils according to their perceived hydrologic function (after Van Zijl and Le Roux, In Press).

□ Southern Basalts Catchment Characteristics

This site shows a flat topography and low stream density dissecting the underlying basalt geology. The headwater stream channels are less incised than higher order ones which are also wider. Sporadic pools are observed along stream channels and these get more pronounced at higher order reaches. This site has dense grass cover interspersed with trees dominated by *Sclerocarya birrea* and *Acacia nigrescens* species. The soils at this study site decrease in depth from headwaters towards the 3rd order catchment. Information on soil forms was taken from Le Roux et al. (2011). Dominant soil forms for 1st and 2nd order catchments

are Shortland and Mispah/Glenrosa on crests and midslopes. The footslopes have the Mayo, Milkwood and Bonheim soil forms. At the 3rd order catchment the hillslope crest has Shortland and Coega soils while the midslope has Mispah/Glenrosa and Milkwood/Mayo soils. On the footslope Milkwood and Mayo soils occur. No in-depth soil classification was done for this site hence no site-specific soil map is available. The long-term mean annual precipitation (MAP) is 602.6mm (Scientific Services, 2013).

According to Smit et al (2013) the selection of the supersites was done in line with specific agreed criteria by SANParks Scientific Services representatives and supersites' researchers, as follows:

- The research sites should contain hillslope vegetation and soil patterns that commonly recur throughout a land system.
- They must be delimited by catchment boundaries, recognising the importance of water distribution to the intrinsic operation of a wide range of ecological processes.
- The research sites should be third-order catchments, allowing ecological patterns to be observed at a minimum of three scales associated with different stream/catchment orders.
- They must contain as few anomalous features as possible such as kopjes, dykes, dams and roads that would substantially disrupt the flow of water across and through the landscape.
- They should be easily accessible (i.e. close to roads and research facilities/camps).

□ Catchment monitoring networks

Assessment of dominant hydrological processes in groundwater, vadose zone and surface water domains were conducted at three catchment scales that are based on 1st to 3rd order contributing areas. Streamflows were monitored for a period of 15 months (January 2012 to April 2013) while sampling for hydrochemical and isotopic analysis was done for 7 months (September 2012 to April 2013) at each of the study sites. Figures 3.2A and 3.2B show instrumentation maps for the Southern Granites and Southern Basalts study sites.

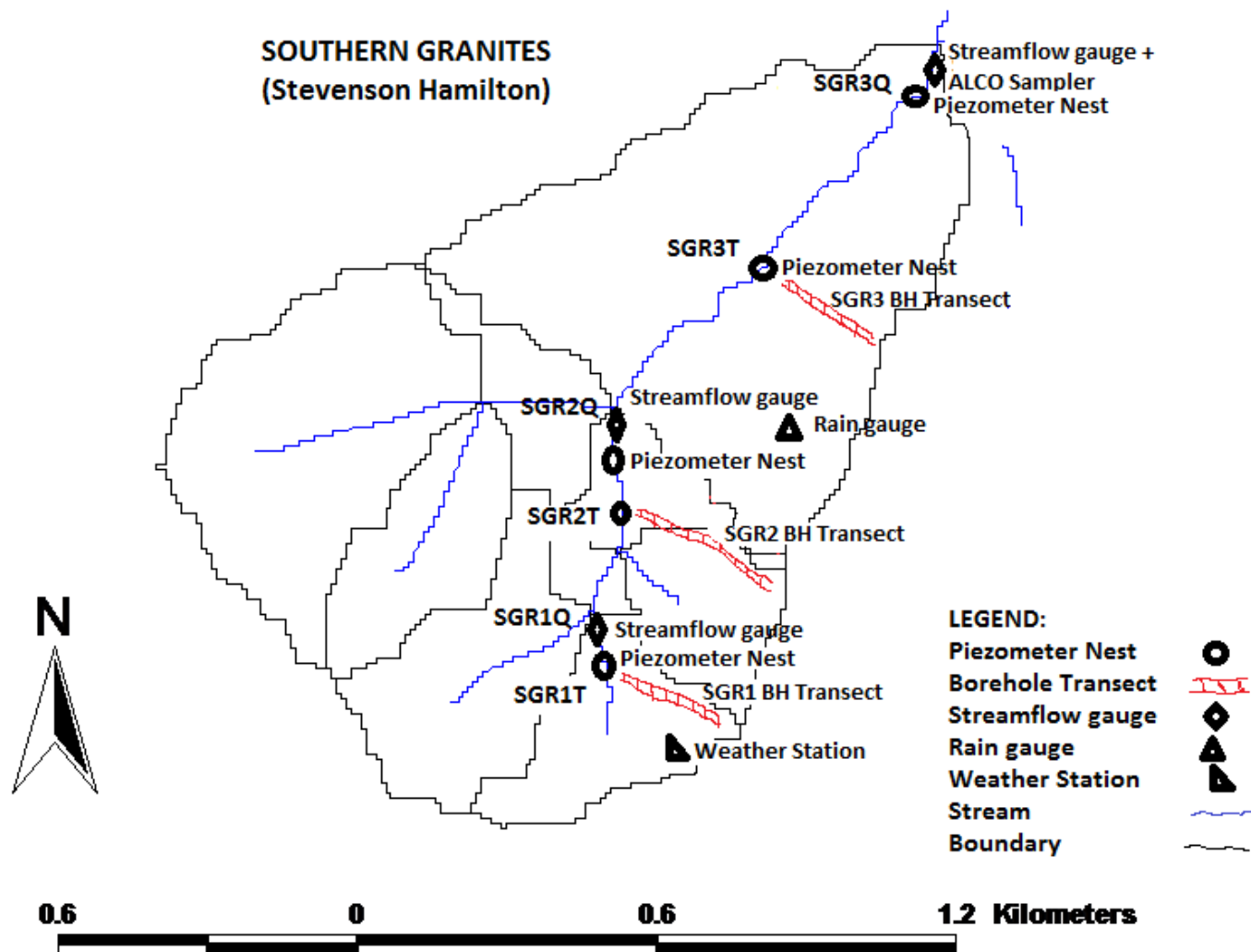


Figure 3.2A Southern Granites instrumentation map (BH = borehole; Q = streamflow gauge; T = transect).

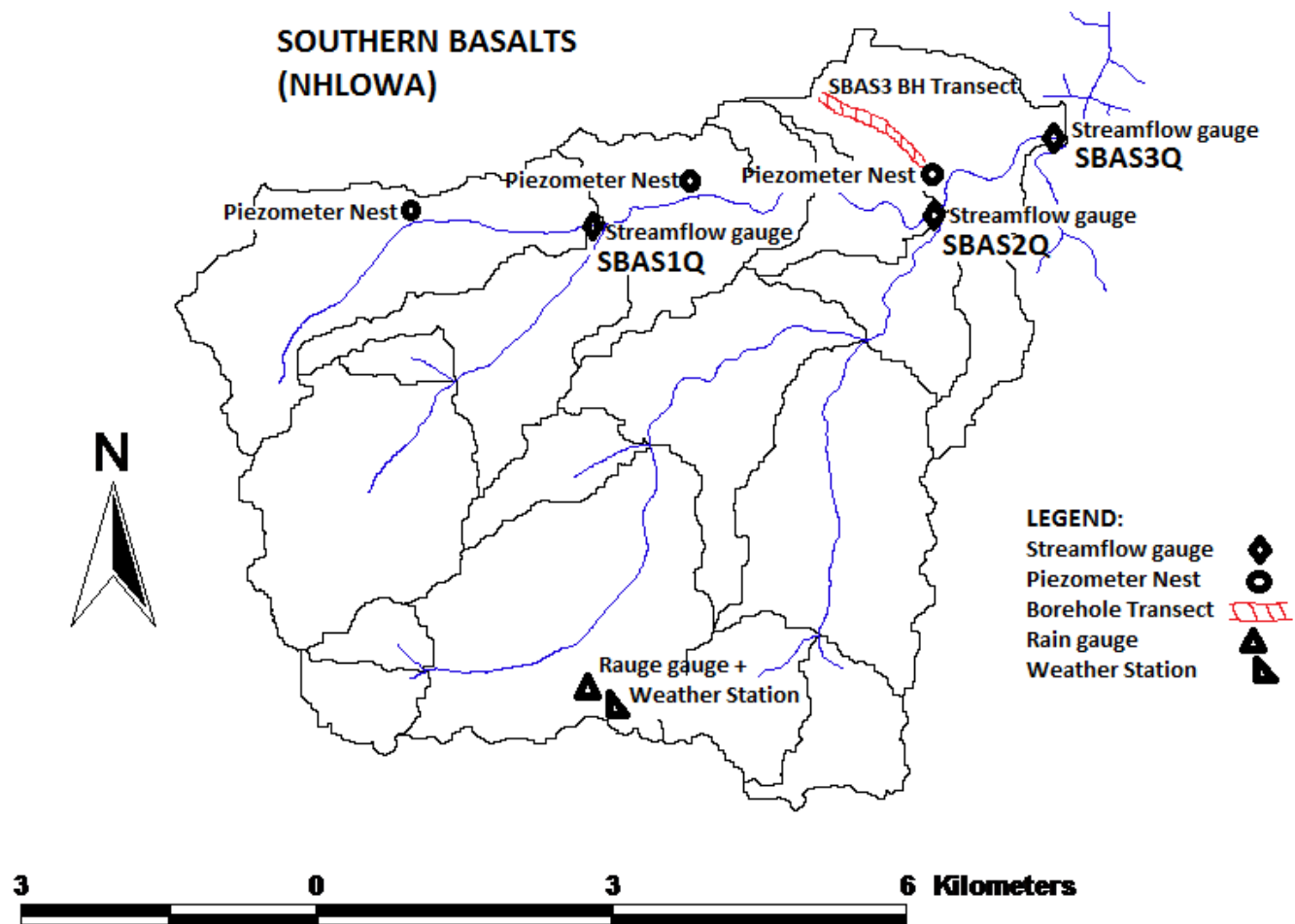


Figure 3.2B Southern Basalts instrumentation map (BH = borehole; Q = streamflow gauge; T = transect).

3.2 Streamflows

3.2.1 Stream stage measurement

Sub-catchment outlets were identified and ground-truthed (GPS) using a combination of aerial imagery (recent GoogleTM Earth) overlaid with a stream-order network derived from 25m disaggregated 90m ASTER DEM data (provided by Cullum and Rogers, 2011). SolinistTM Levellogger Junior water level data loggers were installed at the outlet of each 1st to 3rd order catchments for real-time stream stage monitoring. These loggers were installed in a way that helped to prevent damage by animals by placing them inside perforated polyvinyl chloride (PVC) piezometers which were in turn placed inside perforated metal casings of larger diameter (Figure 3.3). The piezometer tops were then covered by plastic caps with holes that allowed free water movement but concurrently concealing the loggers from animals. The loggers were set to log at 5 minute time steps which enabled acquisition of reasonably high temporal resolution stage data sets. This type of logger has a measuring accuracy of 0.0001m (Solinist©, 2008). It uses a high quality piezoresistive silicon pressure transducer packaged in a stainless steel housing for high accuracy and stability and has a zirconium nitride (ZrN) coating to resist corrosion (Solinist©, 2008). A combination of barometric and water pressure is recorded from which a corresponding water level equivalent is derived (Figure 3.3). Actual water levels were then obtained by compensating for barometric pressure using a SolinistTM Barologger which was placed at a weather station on site to obtain barometric pressure readings (Figures 3.2A and 3.2B). The stages obtained from levelloggers were calibrated against a datum (stream bed surface) in each catchment and used to compute observed discharges at the outlet of incremental subcatchments. Since this study was carried out in ephemeral streams, the measured stage had two components one for subsurface water (negative stage) and the other for surface water (positive stage). This was done in order to determine the significance of subsurface flows in these ephemeral drained catchments.

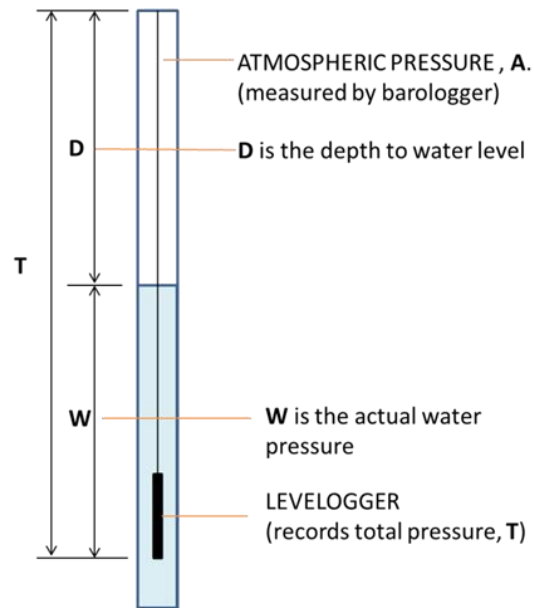


Figure 3.3 Solinst Levellogger installation and schematic on how water pressure (W) is calculated from total pressure (T) and atmospheric pressure (A) for determination of actual water level ($W = T$ minus A).

3.2.2 Stream channel surveys

Longitudinal and cross sectional surveys were conducted for three rated reaches in the first to third order stream channels at each site using a DT5A SOKKIA surveyor's theodolite and a stadia rod. Before taking any measurements the theodolite was positioned at a point clear of obstructions for a minimum of 100m on either side of the instrument. Once positioned, the instrument was levelled up using an in-built levelling mechanism. The height of the instrument (HI) was determined by adding reference point elevation for each surveyed reach, to the backsight (BS) stadia reading. Elevations of surveyed transects were calibrated against a datum (metres above mean sea level, mamsl) determined from Google Earth satellite imagery for the study catchments. Elevation differences were read off from the stadia rod through the theodolite telescope. Calibrated elevation values, HI values and horizontal distances were fed into a Concalcs HydroToolBox Excel Spreadsheet program (Renshaw, 2010) from which channel and flood plain cross sections were constructed and streambed slope for surveyed reaches were calculated. See Appendix I. Channel longitudinal profile elevations and horizontal distances were measured and recorded with subsequent plotting of

streambed slope profiles for the reaches. The streambed slope for a rated reach was calculated as the change in elevation over known horizontal distances as follows:

$$\text{Channel slope} = \frac{\Delta y}{\Delta x} \quad (3.1)$$

Where Δy = change in elevation, and

Δx is the change in horizontal distance of the reach.

The change in flow velocity in the channel reaches was observed to be gradual. Therefore, the energy slope was essentially equated to the water surface slope as well as to the slope of the streambed (Chow, 1959).

3.2.3 Streamflow ratings

The slope-area method which is widely used to estimate flows in natural channels (Herschy, 1985) was used to calculate discharges at the outlet of each sequential stream order (1st – 3rd order). In order to use the slope-area method knowledge of the channel cross section area, channel energy slope and an estimate of the channel roughness coefficient for the reach was a pre-requisite. The first two hydraulic variables were determined as described in the preceding section hence details of channel roughness coefficients follow in this section.

▪ Manning's Roughness Coefficients (n)

Manning's roughness coefficients for rated reaches were estimated using Cowan (1956)'s equation as follows:

$$n = (n_b + n_1 + n_2 + n_3 + n_4) m \quad (3.2)$$

where n_b is a base value of n for a straight, uniform, smooth natural channel;

n_1 is a correction factor for the effect of surface irregularities;

n_2 is a value depicting channel cross sectional area variations in shape and size;

n_3 is a value for flow obstructions in the channel;

n_4 is a value for vegetation and flow conditions;

m is a correction factor for the meandering of the channel.

Base n values (n_b) were obtained by first classifying channel sections as stable or sand channels. Stable channels are shown by firm soils, gravel, cobbles, boulders or bedrock on the streambed that enables the channel to maintain its geometry for wide ranges of flow. Conversely, sand channels are those with vast supplies of sand ranging from 0.2 to 2mm in diameter (USGS, 2008). Having determined the channel class, base n values were then selected from Table 3.1. The base n values selected for this study and corresponding adjustment factors are presented in Appendix II.a.

Table 3. 1 Base n values for natural channels (modified after Aldridge and Garret, 1973)

Bed material	Median size of bed material (mm)	Base 'n' value
Sand channels	0.2	0.012
Fine sand	0.3	0.017
	0.4	0.02
	0.5	0.022
	0.6	0.023
	0.8	0.025
	1.0	0.026
Coarse sand	1.0 - 2	0.026-0.035
Stable channels & flood plains		
Firm soil e.g. clays	--	0.025-0.032
Gravel	2-64	0.028-0.035
Cobble	64-256	0.030-0.050
Boulder	> 256	0.040-0.070

Since the selected base n values are for straight channels with relatively uniform flow conditions, they were adjusted for the roughness increasing factors (n_1 to n_4) including the meandering effect (m) as given in Equation 3.2. These factors physically define what is observed in field reconnaissance surveys done in the study catchments. Compound cross sections at the Southern Granites 3rd order and Southern Basalts 1st order reaches were each sub-divided into 3 subsections according to visible abrupt changes in roughness conditions.

Compound channels are those consisting of channel and floodplain subsections marked by distinct roughness or geometric changes (USGS, 2008). Accordingly, identified subsections of the floodplain were assigned different n values as determined by prevalent physical characteristics influencing streamflow processes. A similar approach was also taken for the Southern Basalts 1st and 2nd order stream reaches. In addition to on-site visual observation and judgement in selecting vegetation (n_4) adjustment factors for flood plains, use was made of photographs of flood plains with verified n values (Yochum and Bledsoe, 2010) which appeared to have similar characteristics with floodplains in study areas. The characteristics included general vegetation types (e.g. grasses, brush or trees), and vegetation density.

▪ **Stage-Discharge relationships**

With information on channel slope (S), cross section area (A), roughness coefficients (n) and stage, channels were rated at every stream order outlet up to the third order. This was done in an Excel Spreadsheet program in which the HydroToolbox Excel Add-In (Renshaw, 2010) was used to compute the wetted perimeter and cross sectional area. These were incorporated into Manning's equation to calculate flow velocity as follows:

$$V = \frac{1}{n} R^{2/3} S^{1/2} \quad (3.3)$$

where v is flow velocity; n is Manning's roughness coefficient; R is hydraulic radius and S is bed slope. Computed velocities were then converted to estimated discharges using the continuity equation:

$$Q = AV \dots\dots\dots (3.4)$$

Where Q is discharge in m^3/s ; A is cross section area and V is flow velocity.

Rating curves were constructed from minimum possible stage with increments of 0.0001m up to maximum observed stages in each catchment plotted against estimated discharges. Polynomial rating equations fitted to these curves were subsequently programmed into a Microsoft Access database to compute actual observed discharges of main streams within 1st to 3rd order spatial scales. Details of channel ratings are presented in Appendix I.a.

- **Calibration of streamflows**

Observed data obtained from direct current ratings conducted in January 2012 were used to calibrate flows obtained using the slope-area method. The direct current meter and slope-area method discharge data were plotted together and Manning's roughness coefficients (n) were adjusted until a perfect fit was achieved for all catchment outlets.

3.2.4 Subsurface flow characterisation

Subsurface flows depend on the hydraulic conductivity of the porous medium, its cross sectional area as well as the hydraulic gradient between the points over which the flow occurs. The flow rate or specific discharge was calculated from Darcy formula as follows:

$$V = -K \frac{dh}{dl} \dots \dots \dots (3.5)$$

where V is the flow rate or velocity; K is the hydraulic conductivity or permeability of the porous medium, and $\frac{dh}{dl}$ is the hydraulic gradient.

Hydraulic gradients were calculated by dividing observed head differences (dh) between nested piezometers installed within stream channels by the distance between the piezometers (dl). Figure 3.4 illustrates this concept.

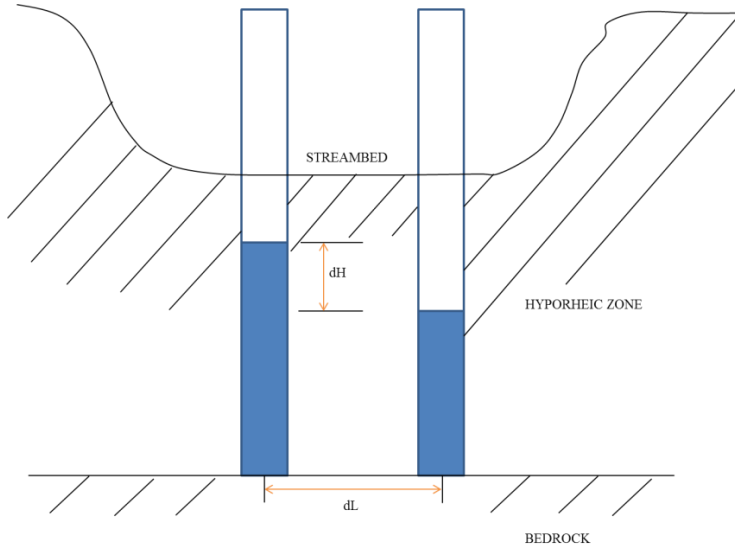


Figure 3.4 Schematic showing the concept of lateral hydraulic gradient in the streambed alluvium.

Subsurface discharge (Q) was then calculated using Darcy equation as follows:

$$Q = -KA \frac{dh}{dl} \quad (3.6)$$

where Q is the subsurface discharge; A is the cross sectional area of streambed aquifer; and V is the flow rate computed using Equation 5 as already described.

Equation (3.6) was applied across incremental subsurface depths obtained using the steel probe method (Mansell and Hussey, 2011). Steel probes were driven into the streambed until resistance or refusal was experienced, which was assumed to mark the beginning of the bedrock. The driven lengths of steel probes were measured using a measuring tape to give the depth from streambed surface to underlying bedrock. When plotted against the channel width, these depths will produce total cross sectional areas from which theodolite surveyed channel areas are subtracted to obtain subsurface areas only. One such cross section is presented in Figure 3.5. Further understanding of subsurface lithology was obtained from Electrical Resistivity Tomography (ERT) surveys conducted along streambed channels. Logged water levels were plotted with a rating to obtain observed subsurface discharge.

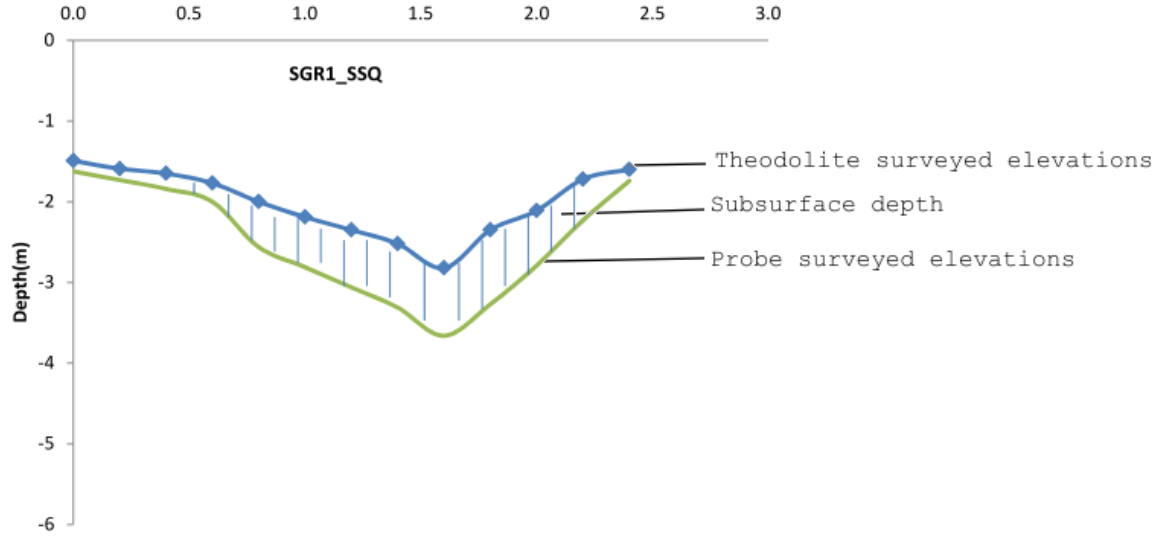


Figure 3.5 Southern Granites 1st order subsurface cross section. (SGR1_SSQ = Southern Granite 1st order subsurface cross section).

Streambed hydraulic conductivities were estimated from falling head slug tests data obtained from installed streambed piezometers (Baxter et al., 2011, Freeze and Cherry, 1979). The slug tests were done by quickly adding known volumes of water to dry monitoring piezometers and then using the rate at which water level falls to calculate K. Where piezometers had some water, a known volume of water was removed from the piezometer and the rate of water rise or recovery was recorded. Computations were done using the Bouwer and Rice (1976) equation as follows:

$$K = \frac{rc^2 \ln\left(\frac{Re}{r_w}\right)}{2L} \frac{1}{t} \ln \frac{y_0}{y_t} \quad (3.7)$$

where K is the hydraulic conductivity; r_c is inside radius of piezometer if water level is above perforated area; R_e is the effective radius over which y is dissipated; r_w is the horizontal distance from well centre to original aquifer (radius of casing plus thickness of gravel pack); the term $\frac{1}{t} \ln \frac{y_0}{y_t}$ is obtained from the best fitting straight line in a plot of $\ln y$ against t (See Figure 3.6).

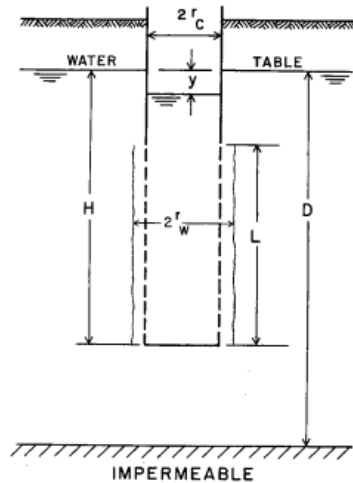


Figure 3.6 Schematic showing dimensions used to calculate hydraulic conductivity from slug tests (Bouwer and Rice, 1976)

3.3 Rainfall Measurement

TexasTM and DavisTM tipping bucket rain gauges were installed at Southern Granites and Southern Basalts respectively, to measure event-based rainfall assumed to be representative of the rainfall received by all 1st to 3rd order catchments. The rain collectors have funnels of size 0.254mm and are set to log at event increments of 0.1mm at Stevenson Hamilton and 0.2mm at Nhlowa study sites. Tipping bucket rain gauges were essential since they enabled the calculation of rainfall intensities which are crucial in comparative connectivity studies. Bulk rain gauges were also installed on study sites for the collection of rain samples for use in isotopic and hydrochemical tracer analyses. However, due to problems of evaporation closely monitored rain gauges 10km and 12km from site for Southern Granites and Southern Basalts respectively, were finally used for isotope and hydrochemical analysis. This is a potential area of uncertainty in isotope analysis arising from the amount and altitudinal effects that are based on the concept of rain-out. However, the anticipated error is assumed acceptable since the mean rainfall isotopic ($\delta^{18}\text{O}$) distribution across the KNP region is generally uniform (Abiye et al., 2013).

3.4 Rainfall-Runoff Analysis

The relationships between rainfall and runoff characteristics of three separate events were statistically examined. Pearson's product moment correlation coefficient (r) was used to determine linear dependencies between rainfall and runoff dynamics. Identified dependencies were tested using the t -test in order to ascertain the level of significance (p) at which these relationships were valid.

Runoff coefficients were calculated using total runoff volumes for the three selected events to further understand the general reaction of study sites to rainfall events. The analysis was done for a day's runoff volume obtained in response to that day's preceding rainfall event for each site. The following equation was used (Blume et al., 2010):

$$\text{Runoff Coefficients (R}_c\text{)} = \frac{\text{runoff volume(mm)}}{\text{rainfall depth(mm)}} \quad (3.8)$$

3.5 Stream and Riparian Zone Hydraulic Head Monitoring

Monitoring of hydraulic head in boreholes, piezometers and stream was done in order to determine places of potential lateral connectivity between deep groundwater, hillslope vadose zone and the stream. Water levels in riparian zone boreholes and piezometers as well as in piezometers installed in the streambed were primarily considered since connectivity of processes within these domains (riparian zone and stream) was the key issue being investigated. However, where data from these domains was not adequate to fully understand hydrological responses, boreholes and piezometers located further in the midslope and crest positions were also considered. Piezometer installations were on three transects within 1st to 3rd order contributing areas. Higher water levels in the riparian zone wells compared to the stream suggest fluxes from hillslope into stream (gaining), whereas lower levels in riparian zone wells relative to the stream suggest a losing reach (Figure 3.7). Water levels were measured after every rainfall event in addition to a fortnightly monitoring routine.

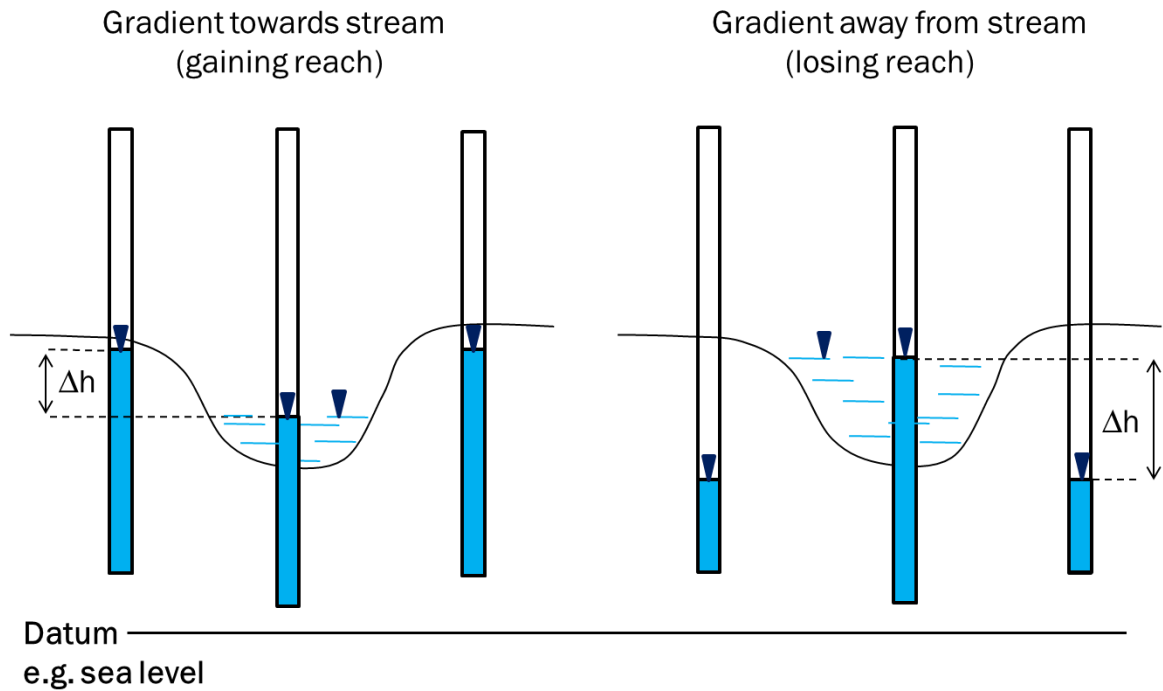


Figure 3.7 Schematic of riparian zone and stream piezometers used to determine potential lateral connectivity (gains or losses)

3.5 Hyporheic Zone Hydraulic Head Monitoring

Vertical hydraulic gradient (VHG) and streambed hydraulic conductivity (K_h) helped to quantify hyporheic exchange between streambed alluvium and stream. Vertical hydraulic gradient is a dimensionless quantity that is positive under upwelling conditions and negative under downwelling conditions (Kalbus et al., 2006; Baxter et al., 2003; Lee et al., 1980) as illustrated in Figure 3.8. The following equation (Baxter et al., 2003) was used to calculate VHG:

$$\text{VHG} = \frac{\Delta h}{\Delta l} \quad (3.8)$$

where Δh is head difference between water level in piezometer and water level in the stream channel; Δl is the piezometer depth from streambed surface to the first opening of piezometer screen.

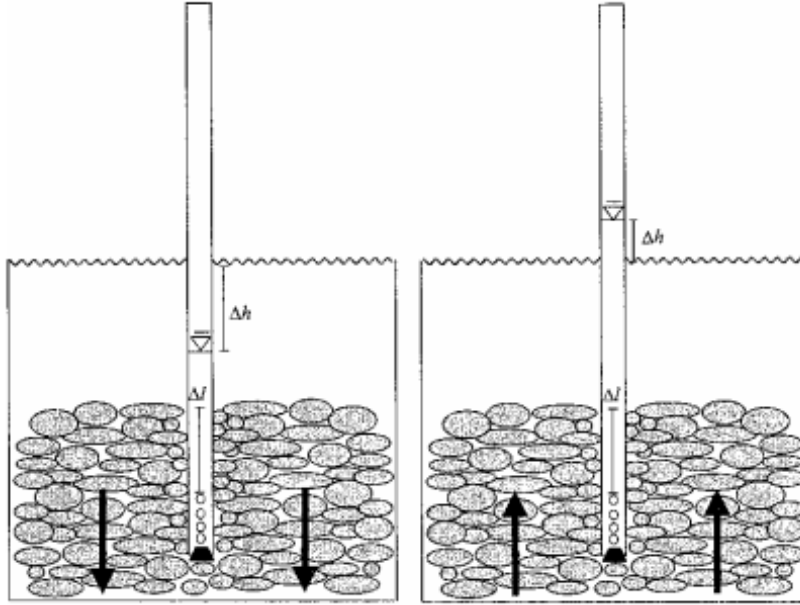


Figure3. 8 Principle of VHG with downward facing arrows indicating downwelling or losing while the upward facing show upwelling or gaining (adapted from Baxter et al., 2003)

3.6 Flow Duration Curves (FDCs)

Flow duration curves (FDC) are tools used to depict streamflow characteristics in a single curve for a range of discharges. Castellarin et al., (2007) define an FDC as a cumulative frequency curve showing the percentage of time during which specific streamflow magnitudes are equalled or exceeded in a given period of time. In order to understand the relationship between the magnitude and frequency of streamflow in the study sites, FDCs were constructed. Viewed across scales this relationship helped to determine stream network connectivity for the three scales from 1st to 3rd order stream reaches. Flow duration curves were plotted from time series streamflow data for the period from September 2012 to March, 2013. Streamflow data was first arranged in descending order and ranked with the largest flow value ascribed rank number 1 while the least flow value was ranked last. The frequency of occurrence or exceedance probability was then calculated using the following formula:

$$F = 100 * \left(\frac{R}{N+1} \right) \quad (3.9)$$

where F is the frequency of occurrence (expressed as % of time a particular flow is exceeded or equalled), R is the rank and N is the number of streamflow observations.

3.7 Additional Techniques to Further Understand Groundwater Stream Connectivity

- **Electrical Resistivity Tomography (ERT)**

ERT surveys were done using a SAS1000 ABEMTM Terrameter (Loke, 1999) and its switching unit in early February 2013 (very wet period) and mid-March 2013 (drier period). Probe locations were captured using a Differential Global Positioning System (DGPS) of the TrimbleTM ProXRS Asset Surveyor brand. Elevation data was differentially corrected against available TrigNET (<http://www.trignet.co.za>) beacon data. The protocol used was a combined Schlumberger Long and Short array, which used in combination provide both horizontal and vertical sensitivity, in order to capture both near-surface and deep lithological profiles and moisture dynamics. Fixed transects were used where probes were left in place for the whole survey period in order to hold geological conditions constant and leave moisture as the only variable parameter. This was done to understand stream morphological controls as well as to trace temporal moisture variations in the subsurface. Any changes in resistivity were attributed to moisture differences since geology was held constant by fixing probe positions.

Inversion of apparent resistivity values was done using RES2DINV programme (Loke, 1999). Pseudosections were plotted and bad data points exterminated. Profiles were refined to RMS errors below 30% to finalise the modelling process. Profiles depicting streambed heterogeneities indicated by different resistivity values were obtained and topographically corrected using corrected DGPS points.

3.8 Sampling and Laboratory Analyses

Surface water from streams, groundwater from boreholes and subsurface water from riparian and streambed piezometers were routinely sampled fortnightly at first and then weekly during the peak rainfall period from January to February, 2013. In addition to the routine sampling, samples were also collected after every rainfall event. This was done to get the signature of processes between rainfall events as well as during stormflow periods. Sampling before and after rainfall events was crucial to determine time-variant water sources contributing to total runoff, commonly denoted as event and pre-event components in two component hydrograph separations using tracers. Piezometers were purged first before a sample could be collected in

order to ensure fresh subsurface samples which are free from direct rain or enriched ponded water. Surface water samples were grabbed from streams. Groundwater was sampled at 10m specific depth intervals using a sampler with a calibrated extension. This was done in order to capture signatures at different depths which could be influenced by changes in aquifer properties such as presence of a fracture.

At the third order of the Southern Granites study site, grab samples augmented samples obtained from an ALCO automatic streamflow sampler which was manufactured by the Centre for Water Resources Research at the University of KwaZulu-Natal (Figure 3.9). This sampler is controlled by a CR200 Campbell ScientificTM datalogger which measures stage, calculated as a pressure via a CS450 sensor after every 10s. The data logger was programmed to trigger the sampler to collect a sample when the stage surpasses a threshold change of 5cm head. The rationale for the 5cm threshold was to allow all the 20 bottles in the sampler to be used in an average event where head change in the stream would be +/-50cm.

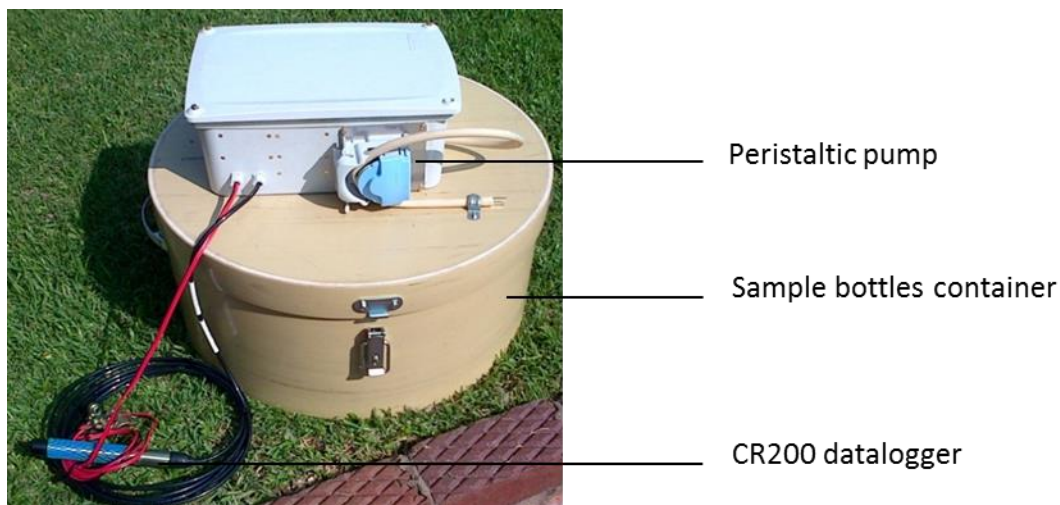


Figure3.9 ALCO 20-bottle sequential sampler built by the Centre for Water Resources Research at the University of KwaZulu-Natal.

Physico-chemical parameters which included electrical conductivity (EC), temperature and pH were measured using a calibrated PC5 Testr 35 Multi-Parameter instrument as soon as the sample was collected in the field.

Samples collected in clean plastic bottles which were filled to the brim and tightly closed to prevent evaporation and any exchange of vapour with the atmosphere, were carried in cooler bags and stored in refrigerators prior to being analysed. These samples were analysed for stable isotopes (^2H and ^{18}O) and for major cations and anions (K^+ , Mg^{2+} , Na^+ , Cl^- , Ca^{2+}) and dissolved silica (SiO_2). The analyses were done at the Chemistry and Hydrology laboratories of the University of KwaZulu-Natal. Stable isotope analysis was done using a Los Gatos Research (LGR) DT-100 Liquid Water Laser Isotope Analyser following International Atomic Energy Agency (IAEA) guidelines and results obtained were reported relative to an international standard, the Vienna Standard Mean Ocean Water (VSMOW). This equipment is capable of analysing a maximum of 30 prepared samples at a time and completes analysing within a total of 21 hours. Analytical errors using this equipment are $\pm 0.3\text{‰}$ for oxygen and $\pm 1.0\text{‰}$ for hydrogen. Standard solutions were run concurrently with the prepared samples for the analysis of $\delta^2\text{H}$ and $\delta^{18}\text{O}$ isotopes.

The mixing of components or sources of streamflow was distinguished by analysing the assortment of isotope concentrations from various sources including rainfall and the stream on an $\delta^{18}\text{O}/\delta^2\text{H}$ plot. These concentrations are plotted as differences (delta values) between sample values and the Vienna Standard Mean Ocean Water (VSMOW). Isotope delta values are expressed as parts per thousand (‰), also denoted as permil.

Cation analysis was done using Inductively Coupled Plasma-Optical Energy Spectrometry (ICP OES) equipment. This equipment is capable of analysing a maximum of 180 prepared samples at a time completing them within a total of 4 hours. It is highly automated such that relatively unskilled people can use it following methods or standardised procedures set by specialists. Its analytic precision is $\pm 0.3\text{mg/L}$.

Chloride was analysed using HACH DR/2000 Spectrophotometer which measures concentrations with a precision of $\pm 0.3\text{ mg/L}$. This equipment can analyse one sample at a time. The chloride in the sample reacts with mercuric thiocyanate forming mercuric chloride and liberating thiocyanate ions. Thiocyanate ions react with ferric ions forming an orange thiocyanate complex whose amount is proportional to the chloride concentration (HACH, 2000).

3.10 Tracer Analysis

Tracer analysis was done through time series hydrochemical and isotopic plots to capture and interpret trends in chemical parameter and isotopic signatures. Lumped plots of $\delta^{18}\text{O}$ and $\delta^2\text{H}$ values on x and y axes respectively, were conducted relative to the GMWL to identify possible mixing of different water sources. Quantification of component contributions to total runoff was accomplished through hydrograph separations using $\delta^2\text{H}$, $\delta^{18}\text{O}$, Cl, EC and Si which have notably been used in previous studies and produced reliable results.

□ Hydrograph separation

Hydrochemical and isotopic tracers were used to quantify components of streamflow based on the following assumptions (Liebundgut, 2009; Hoeg, 2000, Rice and Hornberger, 1988):

- There are significant differences between tracer concentrations of different components.
- Tracer concentrations do not change in space and time, and any changes that occur can be explained.
- Contributions of an additional component must be negligible or that its concentration must be similar to that of another component in the sample.
- Tracers must mix well and conservatively, without readily reacting with other chemicals.

These assumptions were met in that isotopic ($\delta^{18}\text{O}$) values and concentrations of EC and Si were distinct for different water sources which included surface water from streams, subsurface and groundwater from piezometers and boreholes respectively, and that their ranges were not significantly variable for each source (standard deviation of ± 0.01).

□ Two component hydrograph separations

These were conducted for discharges observed at three gauging stations across nested spatial scales that are based on stream orders. This enabled spatio-temporal comparative analysis of streamflow components which was successfully done at Southern Granites where a comprehensive network of monitoring equipment was in place. At Southern Basalts study site hydrograph separations were done only for the third order reach which had groundwater boreholes and streamflow monitoring stations.

Given complete mixing of two components, pre-event (QP) and event water (QE) with CP and CE respective concentrations in a total streamflow, QT, with a concentration, CT, mass balance equations for water and tracer were solved as follows (Uhlenbrook and Hoeg, 2003):

$$QT = QP + QE \quad (3.10)$$

$$CT*QT = CP*QP + CE*QE \quad (3.11)$$

These relationships enabled percentage contributions of components to be calculated thus:

$$QP = QT * \left[\frac{CT - CE}{CP - CE} \right] \quad (3.12)$$

$$QE = QT * \left[\frac{CT - CP}{CE - CP} \right]. \quad (3.13)$$

The pre-event concentration was taken from a subsurface sample collected a day before the rainfall event being investigated.

□ Three component hydrograph separation

A three component hydrograph separation model was used to partition total runoff into three components with two conservative tracers, EC and $\delta^{18}O$ using Ogunkoya and Jenkins (1993) model. Full chemical-isotopic mass balance equations were solved as follows:

$$CT_{\delta^{18}O} = QR.CR_{\delta^{18}O} + QSS.CSS_{\delta^{18}O} + QG.CG_{\delta^{18}O} \quad (3.14)$$

$$QT.CT_{EC} = QR.CR_{EC} + QSS.CSS_{EC} + QG.CG_{EC} \quad (3.15)$$

where, QR is the proportion of incident precipitation; QSS is the proportion of soil water; QG is the proportion of groundwater; CT, CR, CSS and CG are concentrations of total runoff, incident rain, soil water and groundwater respectively. Given the above, the proportions QR, QSS and QG were calculated as follows:

$$QR = \frac{-(CT_{d180} - CG_{d180})(CSS_{EC} - CG_{EC}) + (CT_{EC} - CSS_{EC}) - (CSS_{d180} - CG_{d180})}{(CSS_{d180} - CG_{d180})(CR_{EC} - CG_{EC}) - (CSS_{EC} - CG_{EC})(CR_{d180} - CG_{d180})} \quad (3.16)$$

$$QSS = \frac{(CT_{d180} - CG_{d180})(CR_{EC} - CG_{EC}) - (CT_{EC} - CG_{EC}) - (CR_{d180} - CG_{d180})}{(CSS_{d180} - CG_{d180})(CR_{EC} - CG_{EC}) - (CSS_{EC} - CG_{EC})(CR_{d180} - CG_{d180})} \quad (3.17)$$

$$QG = 1 - QR - QSS \quad (3.19)$$

3.11 Definition of Hypotheses

Desktop analysis and field reconnaissance of study areas helped in the definition of hypotheses which were tested through hydrometric and environmental tracers' data. Hypothesis testing provided better understanding of the connectivity of hydrological processes thus assisting in addressing research objectives as stated in Chapter 1. With the key objective of assessing stream-groundwater connectivity across nested catchments on different geologies (granites and basalts), the following hypotheses were developed:

□ Southern Granites

- 1st and 2nd order stream reaches were hypothesized as connected to groundwater as gaining reaches particularly during rainfall events. Soil bedrock interflow and near-surface macropore flow were conceptualised as the dominant connecting mechanisms. This assertion was based on the fact that these lower order reaches are deeply incised channels which are flanked by steeper hillslopes.

- The 3rd order reach (SGR3) was hypothesized as the threshold at which the stream switches from gaining to increasingly losing thereby acting as a groundwater recharge point. However, limited soil interflow augmented by near-surface macropore flow were conceptualised to connect the stream to interfluvies at least during rainfall events. This speculation was based on the observation that this higher order channel has a shallow and broad macro-channel or floodplain populated with large evergreen woody vegetation.

□ **Southern Basalts**

- It was hypothesized that stream channels (1st to 3rd order reaches) are largely disconnected from interfluvies due to very low hillslope gradients (1.4%) and prevalent clay-rich vertic soils that impede free drainage across all scales.
- The 3rd order reach was, however, hypothesized to be gaining from groundwater aquifers through localised fractured rock preferential flow. This assertion was based on persistent pools observed along this 3rd order reach which contained water several weeks after the 1st and 2nd order reaches had dried up.

4. RESULTS AND DISCUSSION: HYDROMETRY

4. Introduction

This chapter presents results of the characterisation of surface and subsurface streamflow processes across spatial and temporal scales on both the Southern Granites and Southern Basalts. Potential sites and periods of hydrologic connectivity are identified whose verification shall be presented in Chapter 5 using hydrochemical and isotopic signatures of samples collected in these catchments.

4.1 Characterising Stream Channel Flows in the Study Sites

Stream stage measurements logged using Junior Solinst™ Leveloggers were plotted with a rating to get discharge for surveyed reaches. The rating curves and corresponding cross sections are presented in Figures 4.1A and 4.1B for Southern Granites and Southern Basalts, respectively. Subsurface fluxes at Southern Granites were also rated and the cross sections and rating curves are presented in Appendix I.b.

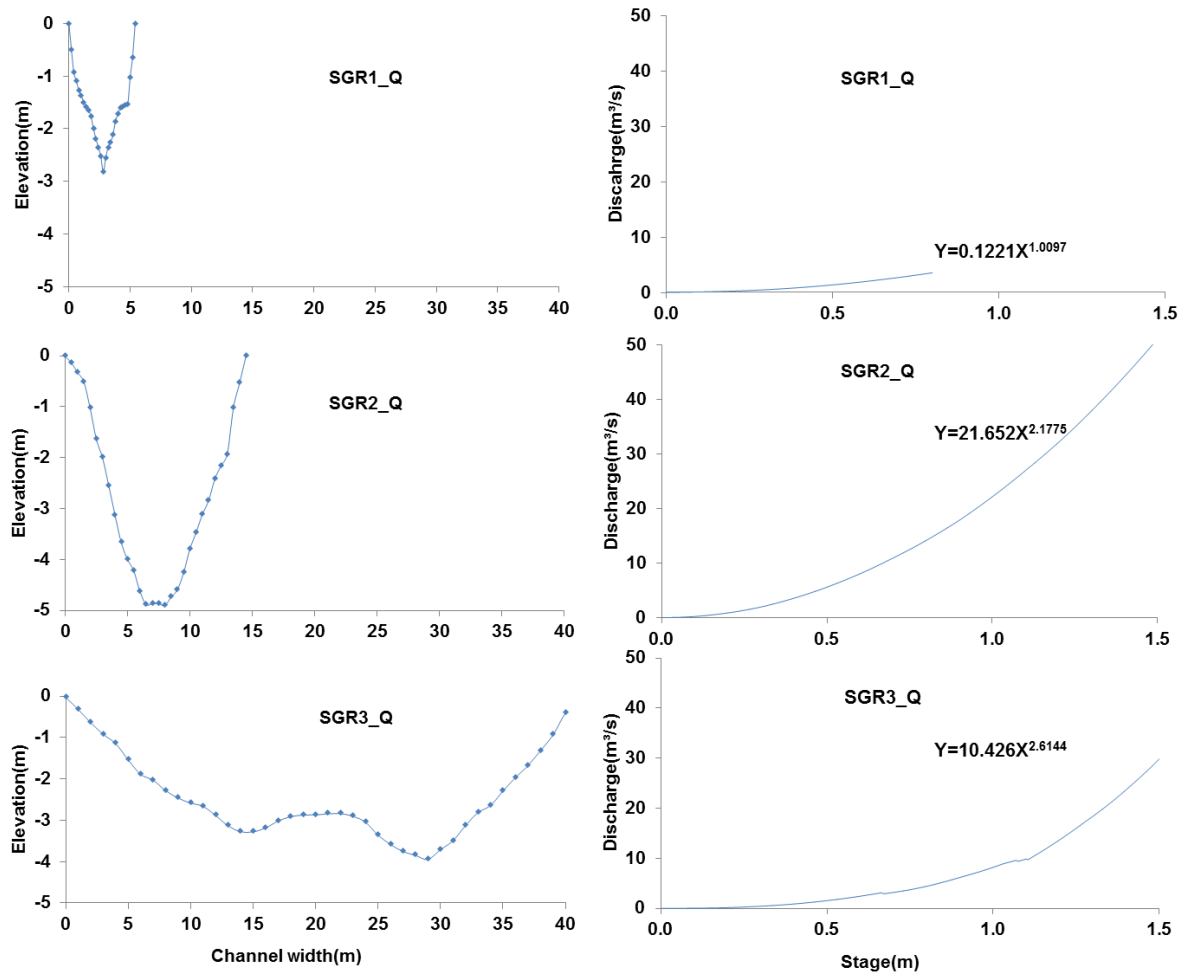


Figure 4.1A Cross sections and rating curves for incremental channels at Southern Granites study site.

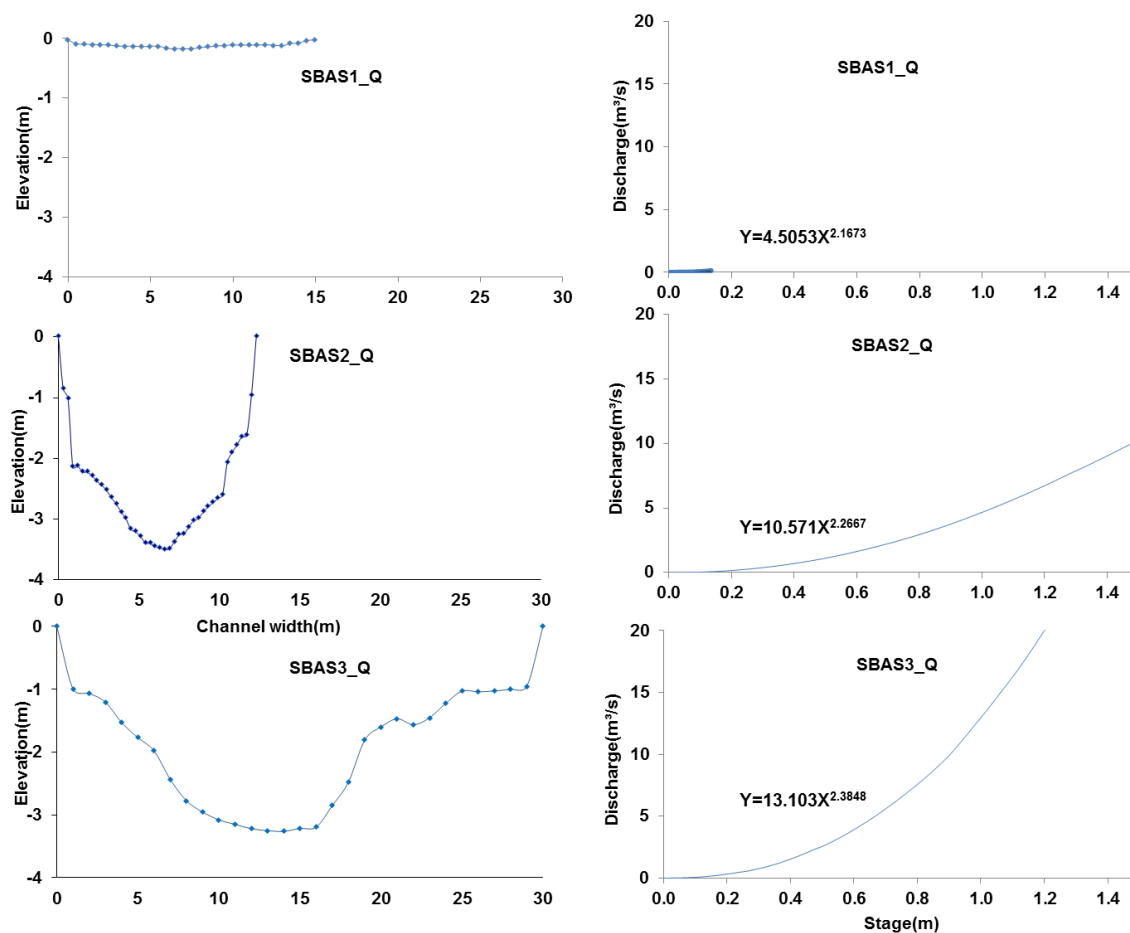


Figure 4.1B Cross sections and rating curves for incremental channels at Southern Basalts study site.

4.2 Southern Granites Rainfall-Runoff Analysis

4.2.1 Statistical analysis

In order to get a better understanding of linkages between rainfall, runoff responses and soil moisture dynamics, an analysis of three events over an hourly time-step which occurred on 2012/12/26, 2013/01/19 and 2013/02/20 respectively, was conducted. This analysis helped to establish relationships between rainfall and runoff using Pearson's product moment correlation coefficient (r) with the level of significance (p). The correlation factors are presented in Table 4.1.

Table 4.1 Pearson's product moment correlation coefficient (r) with level of significance (p, in parenthesis) showing precipitation and runoff responses of three events at Southern Granites during the period from December 2012 to February 2013

	Precip. Duration	Precip. Amount	Precip. Int _{mean}	Precip. Int _{max}	Precip API ₇	Runoff Delay time	Runoff Rising Time	Catchmen t Area	Runoff Peak Discharge
Precip. Amount	0.805 (0.153)								
Precip. Int _{mean}	-0.474 (0.322)	0.139 (0.450)							
Precip. Int _{max}	-0.668 (0.232)	-0.097 (0.465)							
Precip. API ₇	0.517 (0.303)	0.924 (0.068)	0.508 (0.307)	0.291 (0.395)					
Runoff Delay time	0.547 (0.186)	-0.055 (0.211)	-0.174 (0.438)	-0.988** (0.013)	-0.434 (0.339)				
Runoff Rising Time	0.500 (0.320)	-0.206 (0.322)	-0.474 (0.322)	-0.253 (0.409)	-0.999** (0.001)				
Runoff Peak Discharge	0.498 (0.430)	0.915 (0.297)	0.527 (0.180)	0.312 (0.346)	0.999** (0.001)			0.999** (0.003)	
Runoff Volume	0.482 (0.319)	0.913* (0.05)	0.543 (0.292)	0.331 (0.380)	0.999** (0.003)	-0.457 (0.329)	-0.587 (0.272)		0.999** (0.000)

** Significant to the 0.01 level

* Significant to the 0.05 level

The occurrence of high precipitation depths has been identified to cause high runoff volumes and subsequently moderate peak runoff discharges ($r = 0.913$; $p = 0.05$ and $r = 0.915$; $p = 0.297$, respectively). High antecedent precipitation index (API), which is a proxy for catchment antecedent soil moisture conditions was found to cause short rising times between the start of runoff response and peakflow ($r = -0.999$; $p = 0.001$). The volume of generated runoff also showed a strong dependency on antecedent soil moisture conditions ($r = 0.999$; $p = 0.003$). Since volume of generated runoff positively correlates with antecedent soil moisture, it indicates the important role played by pre-event water for the generation of runoff at Southern Granites study site. The significance of high rainfall intensity for runoff generation was revealed through causing short runoff delay times following rainfall events ($r = -0.988$; $p = 0.013$). Peakflow discharges were also observed to vary incrementally with increasing catchment scale ($r = 0.999$; $p = 0.003$). Calculation details for these correlations are presented in Appendix III.

4.2.2 Runoff Coefficients

Having identified the linear relationship between rainfall and runoff depths in this catchment runoff coefficients (Rc) were calculated using total runoff volumes as a proportion of total rainfall depths for the same events (Blumme et al., 2010). The results are presented in Table 4.2.

Table 4.2: Southern Granites Runoff Coefficients for 1st to 3rd order reaches

EVENT DATE	SGR1Q(Rc)	SGR2Q(Rc)	SGR3Q(Rc)	RAINFALL(mm)	API- ₇
2012/12/26	6.66	2.70	0.06	55.3	52.3
2013/01/19	18.18	27.52	40.74	95.7	130.96
2013/02/20	2.37	0.17	1.04	27.9	50.44

As shown in Table 4.2, runoff coefficients increase with increasing precipitation depths for the analysed events which upholds the positive correlation determined using Pearson's correlation coefficient (r). For the moderate rainfall events (27.9mm to 55.3mm) during low antecedent soil moisture conditions (API = 52.3 and 50.44, respectively) Rc values decreased from SGR1 to SGR3 indicating increasing transmission losses at these higher order reaches (Blume et al., 2010).

A closer look at two such events is presented here to single out these relationships and how they influence hydrologic connectivity at Southern Granites site. Observed discharges for this supersite show short-lived, event driven responses. This is indicated by sharp peaks and steep recession curves on the hydrographs (Figure 4.2A and 4.2B). Peakflow discharges for the three scales from 1st to 3rd order contributing areas on the granitic geology show an incremental change in magnitude for the events of 19 January and 20 February 2013.

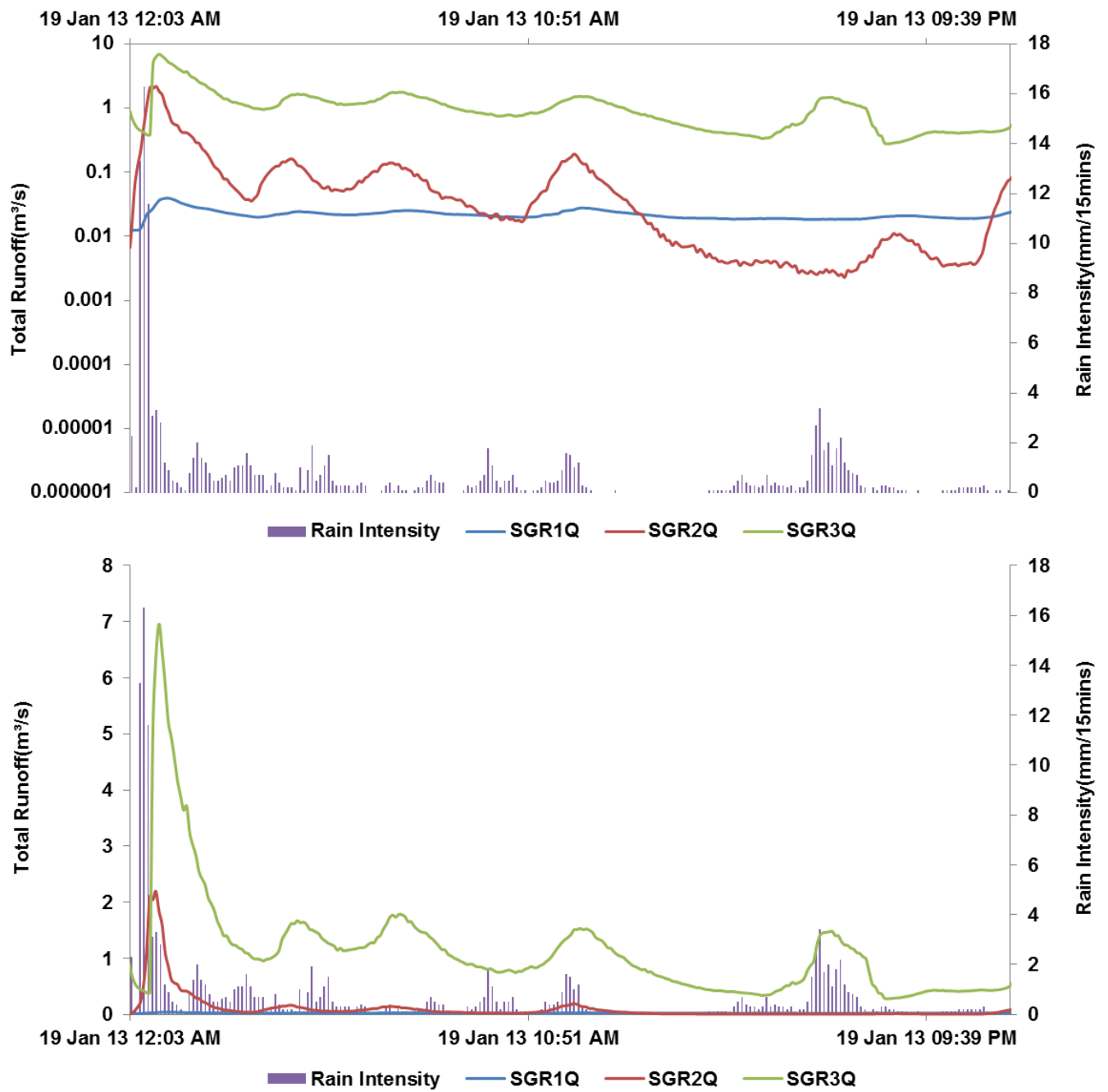


Figure 4.2A Southern Granites streamflow responses following the rainfall event on the 19th of January 2013.

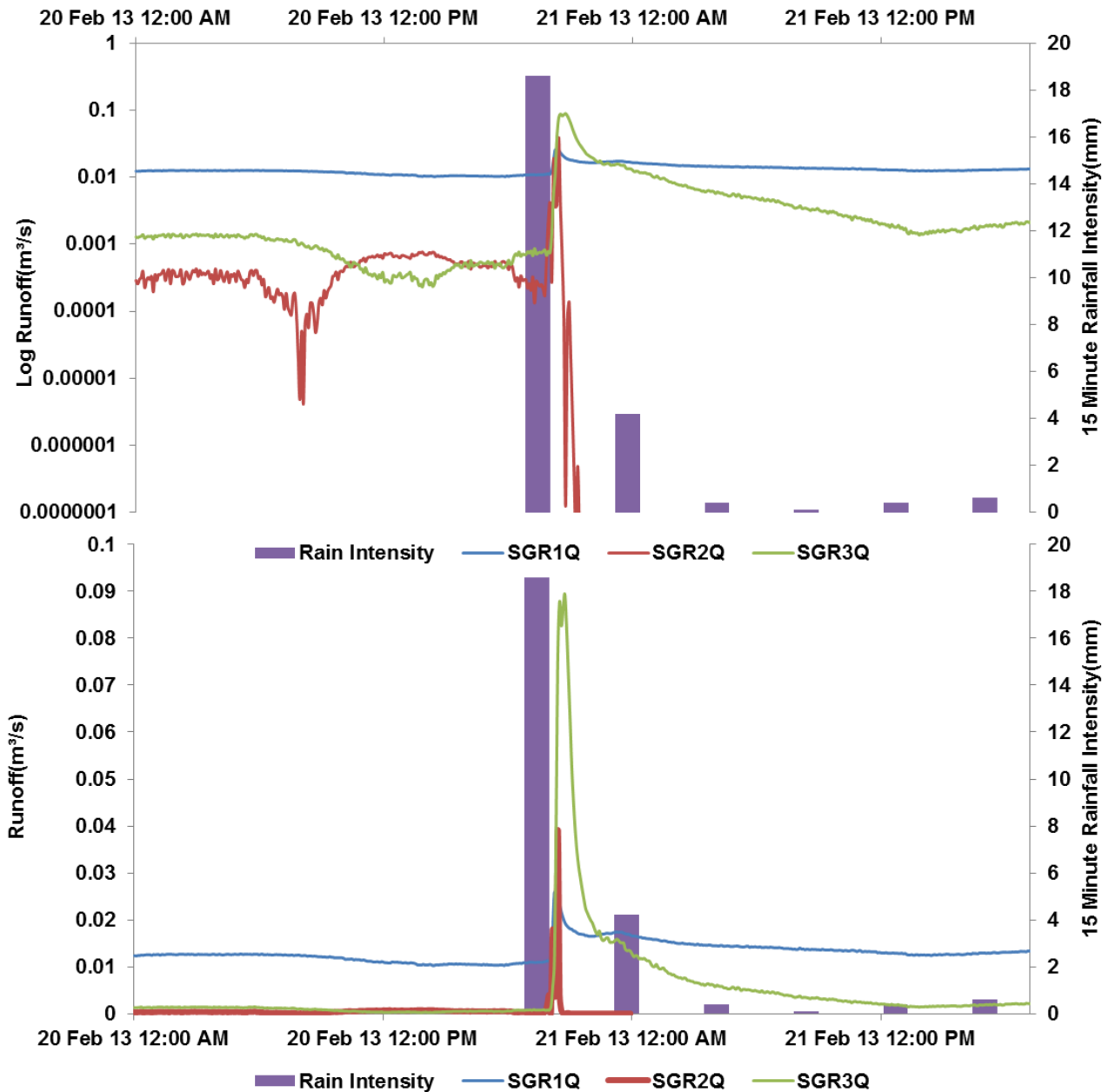


Figure 4.2B Southern Granites streamflow responses following the rainfall event on the 20th of February 2013.

The incremental changes in peakflows at Southern Granites uphold the hydrological principle that discharge increases downstream due to subsequent increases of flow velocity and channel width-to-depth ratio for connected stream networks (Chow, 1959). This apparent increase in magnitude of streamflow responses with scale shows that larger contributing areas play a pivotal role in influencing streamflow processes at this site. Streamflow recession after the January 19, 2013 event was very rapid at SGR2 followed by SGR3. This implies increasing transmission losses at these reaches and in particular at SGR2 where an almost

complete cessation of surface flow occurred rapidly and prior to the other reaches. Lower borehole hydraulic heads compared to the stream support the idea that SGR2 and SGR3 reaches are potentially losing to groundwater (Figure 4.3A). A 32cm increase in water level in the 28m riparian borehole following this large rainfall event supports the notion that SGR2 losses contribute to groundwater recharge. Although an SGR2 crest borehole also experienced a 7m rise in head, this did not set up a hydraulic gradient towards the stream. In addition, installation errors involving improperly sealed steel casing were noted for the SGR2 Crest boreholes such that the observed 7m response is viewed with scepticism. The fact that SGR3 reach does not gain from groundwater is also shown by ever lower borehole hydraulic heads relative to the stream at this scale (refer to Figure 4.3A). In fact, the rest of the boreholes in this catchment indicate hydraulic gradients that are parallel to the stream towards higher order streams beyond the 3rd order spatial scale (See Appendix II.d). Water levels at SGR3T monitoring transect (Figure 4.3B) in riparian zone and in-stream piezometers show hydraulic gradients inclined away from the stream towards the hillslope. Even after a sizable rainfall event in April 2013, (35mm) the reach is still portrayed as losing through the stream bank interface.

However, further down the same reach at the catchment outlet (SGR3Q), hydraulic head differences suggest the possibility of alternate gaining and losing stream behaviour (Figures 4.3B and 4.3B1). Between rainfall events the in-stream piezometer had lower water levels than the riparian one, suggesting lateral flow towards the stream, hence potentially gaining. This was also the case during periods of moderate rainfall (e.g. 40-45mm in early January, 2013) where water levels increased in both piezometers but still with a lower elevation in the in-stream piezometer. The assertion that the stream possibly gains from the hillslope at some point along this reach was initially suggested by hydro-pedological surveys (Le Roux et al., 2011) that identified certain soils on this section as interflow soils. Large, high intensity rainfall events typical of the January 2013 95.7mm event were observed to promote gaining trends as hillslope hydraulic heads were maintained above those of the stream. Such trends persisted until water levels equilibrated following which the stream switched to a losing status in response to potential increases in the soil water deficit of adjacent hillslope soils.

Persistent flows at SGR1, as seen in Figure 4.2B suggest an additional water source apart from event contribution, indicating that this reach is gaining from groundwater or via shallow sub-

surface hillslope processes at least during rainfall events. This assertion is supported by a one metre hydraulic head difference between the stream and a shallower (17m) groundwater borehole at the hillslope crest of this transect following a 95.7mm rainfall event on the 19th of January, 2013 (See Figure 4.3A). Events with exceptionally large precipitation depths as the one in question should be viewed as key thresholds that determine interaction between groundwater and streams, since smaller events or even moderate ones (e.g. a 55.3mm event on the 26th of December 2012) did not result in similar groundwater responses. In addition to being a large rainfall event, the 19th of January event had a high peak rainfall intensity of 16.3mm/15min (Figure 4.2). A rapid runoff response followed this high intensity rainfall event with a delay time of only 12 minutes from start of rainfall event to inception of runoff in the stream. As such the role of rainfall intensity in runoff generation as well as in triggering connectivity between groundwater and the stream, cannot be overemphasized. The fact that only the SGR1 Crest17m shallow borehole responded suggests that groundwater contribution is through the weathered rock aquifer overlying a consolidated hardrock. The deeper SGR1 Crest 103m borehole that penetrate the hard rock aquifer always had lower hydraulic heads than the stream for this period (Figure 4.3A).

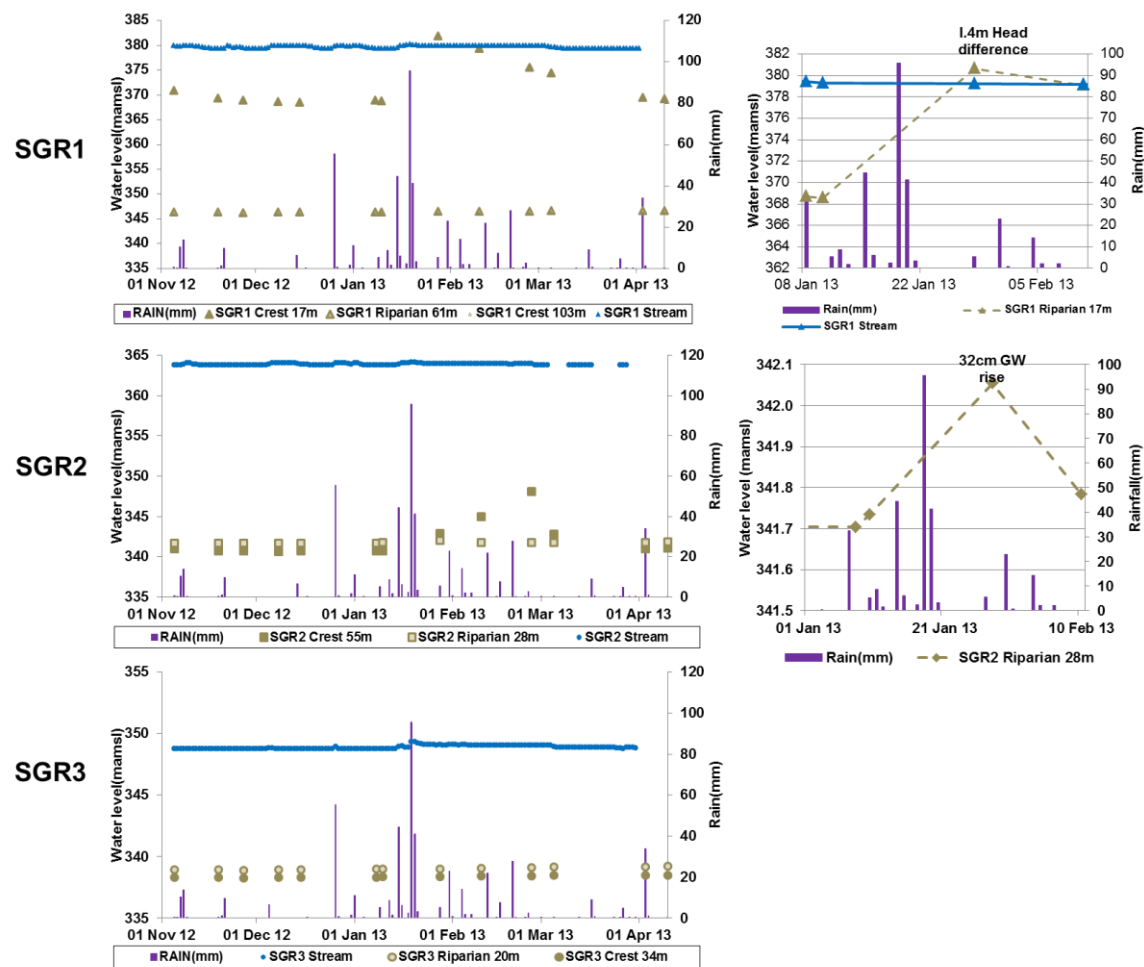
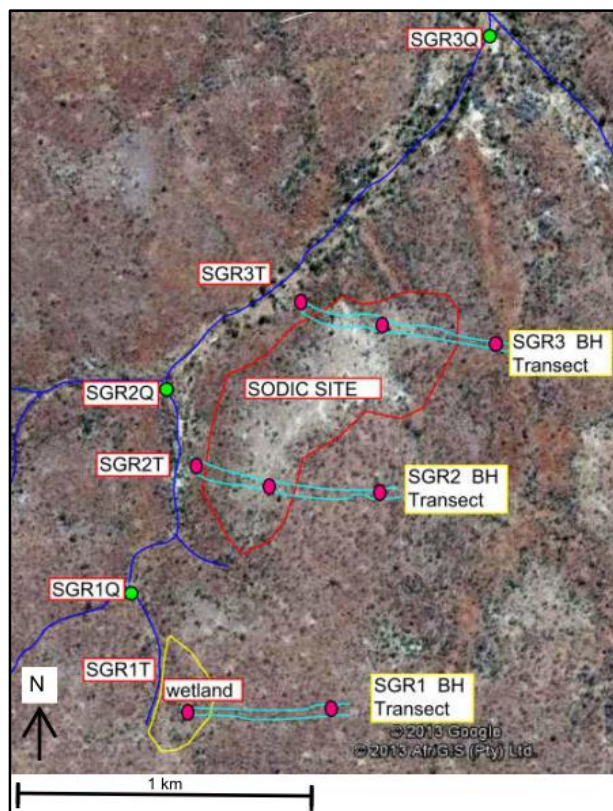


Figure 4.3A Southern Granites monitoring points map (extreme left), groundwater and stream water levels (middle) monitored from November 2012 to April 2013. Plots at the extreme right show enlarged points where responses were observed at SGR1 and SGR2 reaches (BH = groundwater; blue = stream water level; green = groundwater levels).

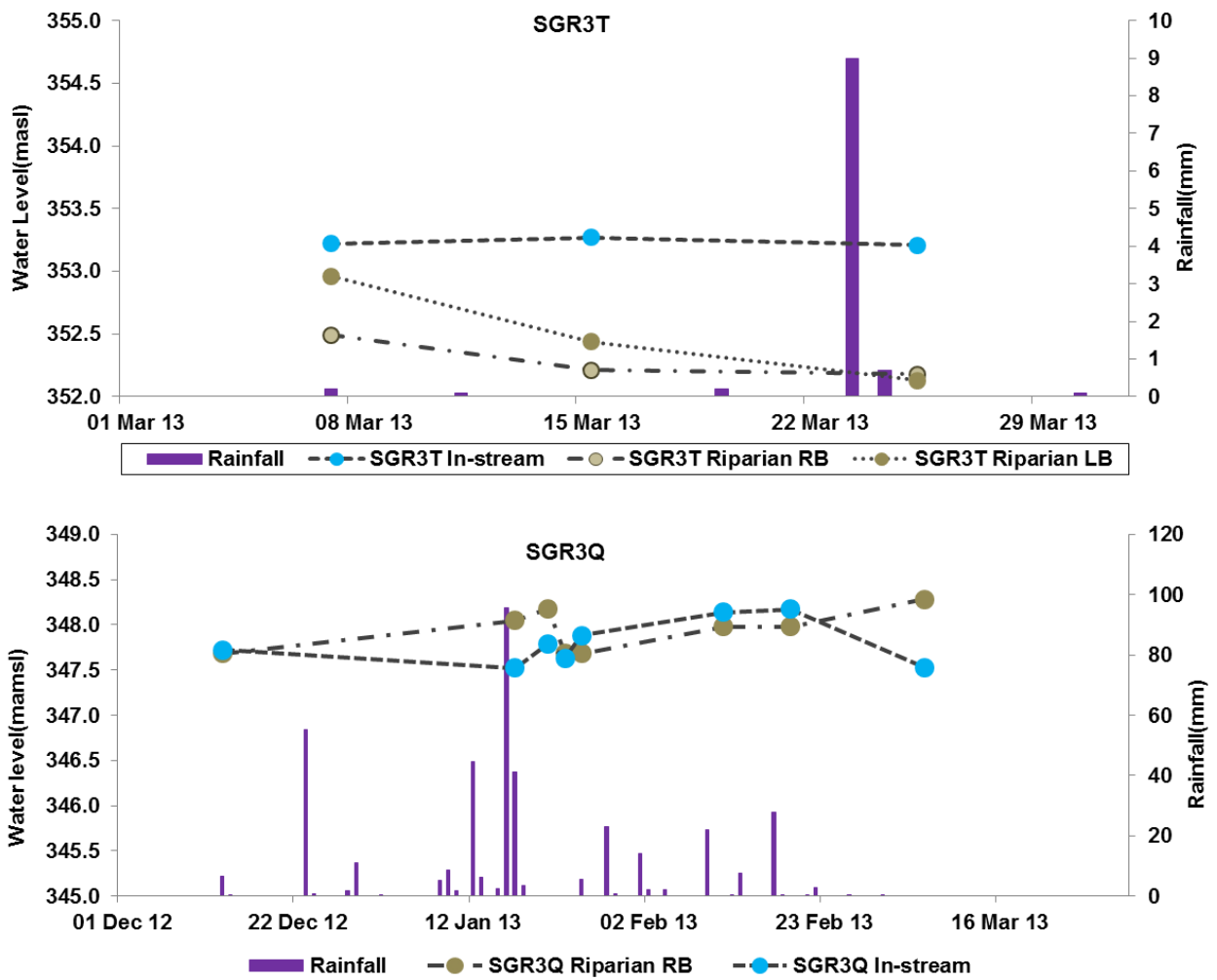


Figure 4.3B: In-stream and riparian zone piezometer water levels at SGR3T during the month of March 2013 and at SGR3Q (from December 2012 to March 2013) at Southern Granites. (SGR3T refers to a monitoring transect at the 3rd order reach; SGR3Q is the catchment outlet of the same 3rd order reach; RB =right stream bank and LB = Left stream bank).

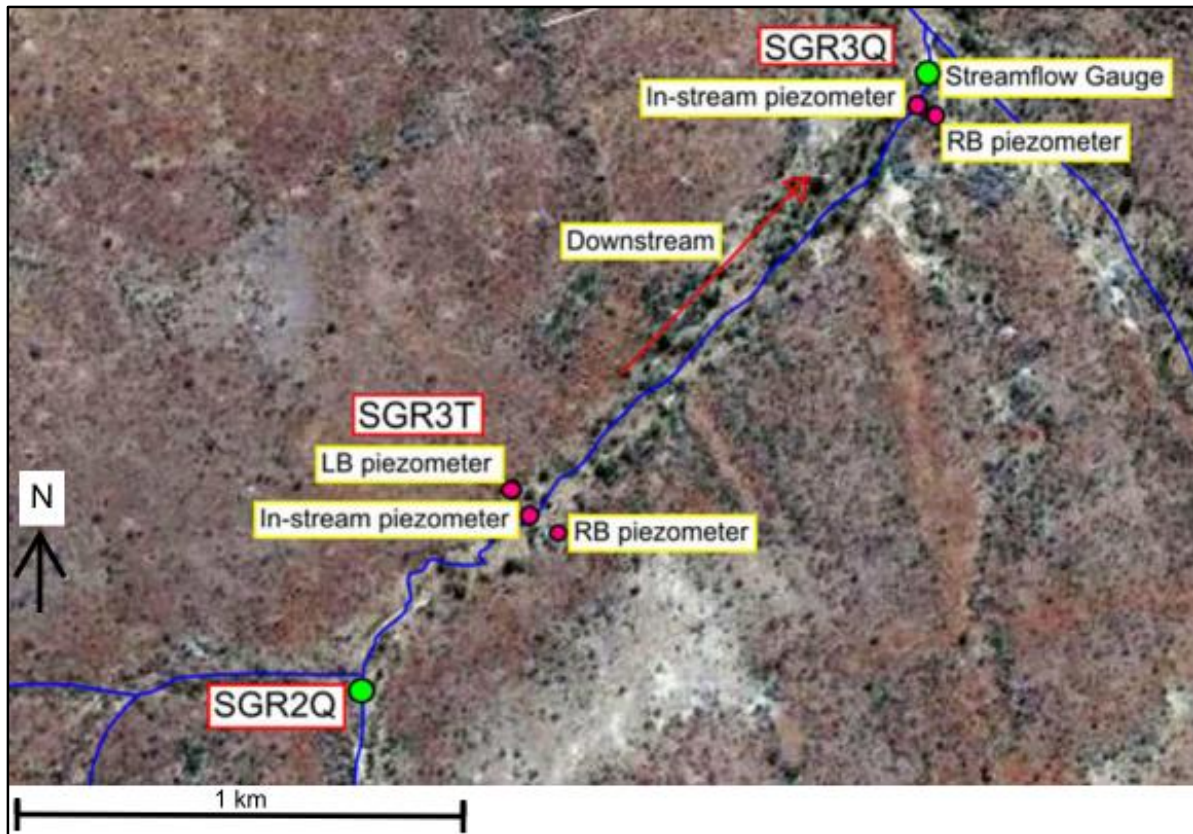


Figure 4.3B1 Location map of SGR3T and SGR3Q reaches at the Southern Granites site.

4.3 Total Discharge at Southern Granites

Fluxes in the subsurface alluvium of the streambed were rated and resultant rating equations combined with those of the surface water to give combined surface-subsurface discharge ratings. These are presented in Figure 4.4. Separate subsurface flow rating curves are presented in Appendix I.

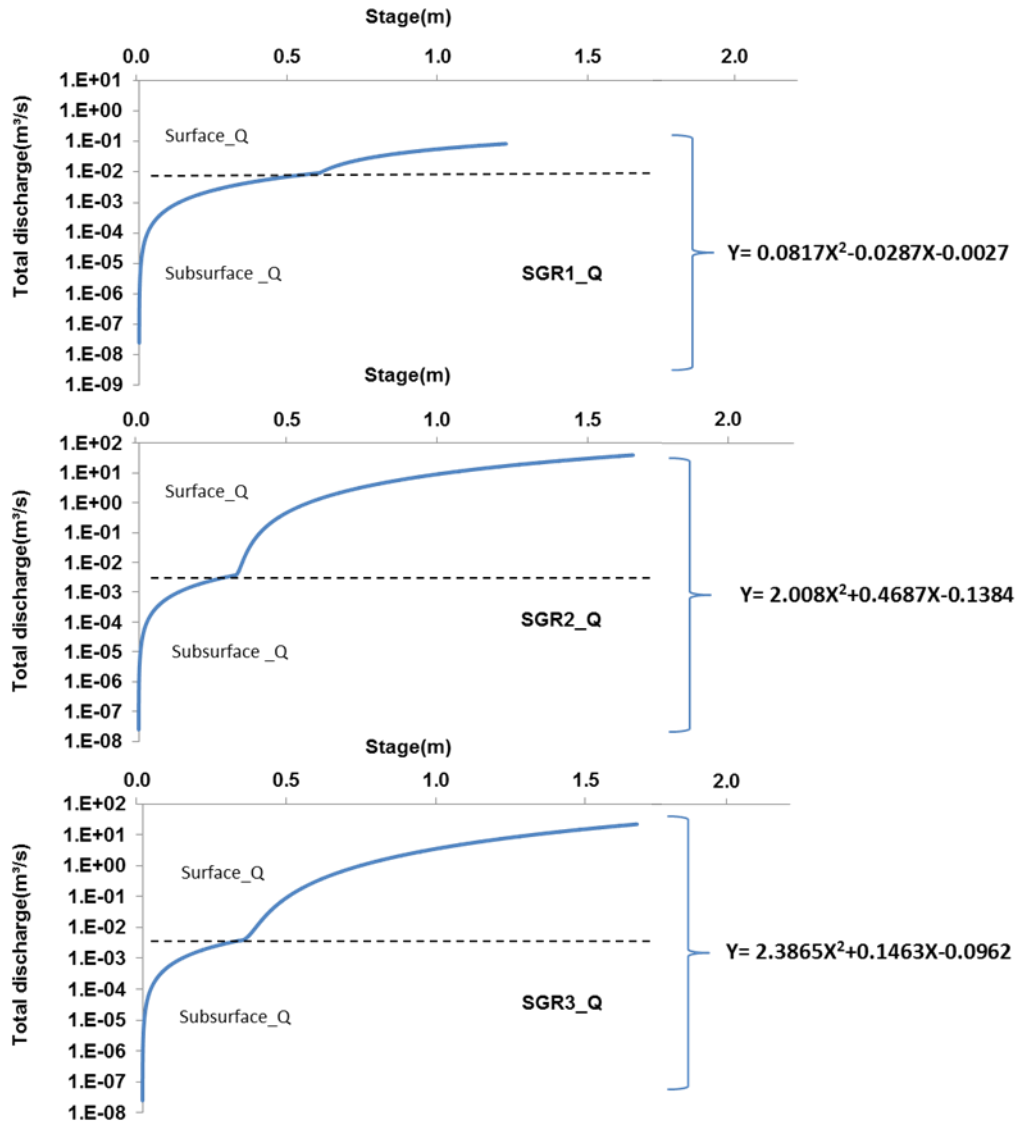


Figure 4.4: Total discharge rating curves for Southern Granites 1st to 3rd order reaches. (Below dotted line = subsurface rating curve; above dotted line = surface flow rating curve).

Characterising subsurface discharge at Southern Granites provided insight into the role played by this hydrological component in the catchment's ecohydrological functions. The pattern of subsurface fluxes perfectly fits into the total discharge hydrographs suggesting subsurface flow as a continuation of surface flow recession into the subsurface alluvium. In essence, subsurface water adds to the total catchment water resource that is integral for ecological requirements such as sustaining aquatic and terrestrial biota. SGR1 discharges appear more persistent than at higher spatial scales suggesting that this reach is in contact with some groundwater source (Figure 4.5). This observation which was earlier supported by borehole water levels, also tallies with vertical hydraulic gradient values calculated from

streambed piezometer water levels (Table 4.3). SGR1 shows upwelling with a positive VHG (+2.3408) while SGR2 and SGR3 reaches had negative VHGs indicating down-welling or infiltration losses. These vertical components of streambed fluxes are mean values obtained following the 19th of January 2013 rainfall event. These values provide further support that the SGR1 reach is gaining while SGR2 and SGR3 reaches are losing. Details of VHG calculations are presented in Appendix II.c. This headwater reach also had sustained flows than the higher spatial scales (SGR2 & SGR3) during the drier November to December, 2012 (Figure 4.5). This observation suggests the contribution of an additional water source to total stream runoff at SGR1 which is apparently absent at the higher order reaches.

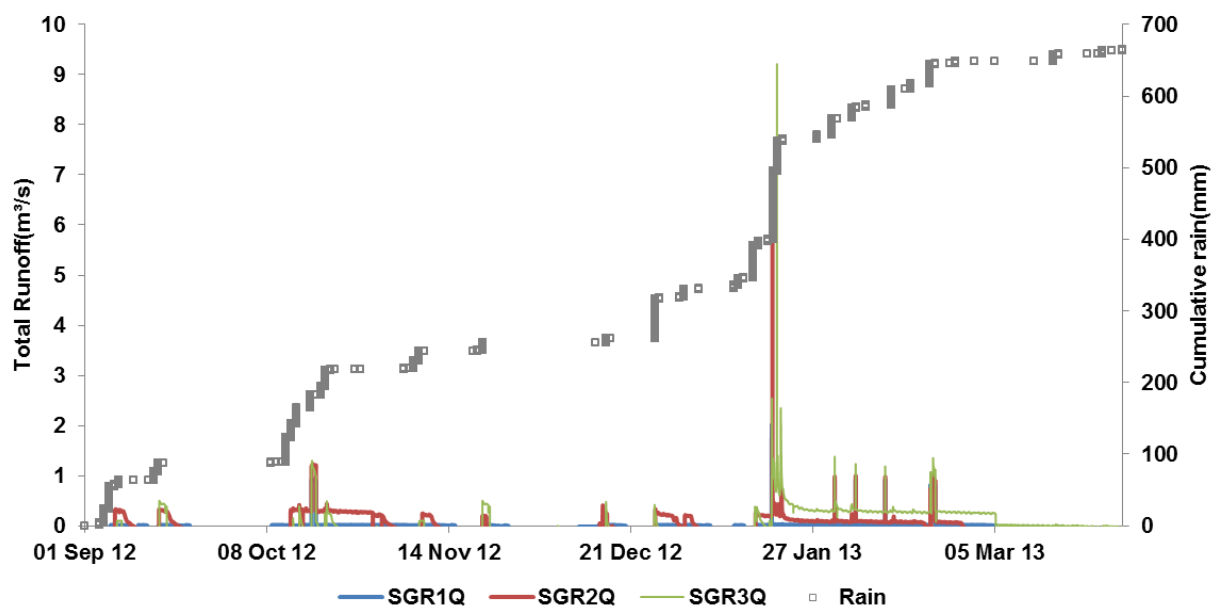


Figure 4.5: Total discharge (combined surface and subsurface) hydrographs at Southern Granites during the period, September 2012 to March 2013.

Table 4.3: Shows vertical hydraulic gradients (VHG) monitored following the January 2013 rainfall event within streambeds of 1st to 3rd order stream channels at Southern Granites site.

Stream reach	SGR1	SGR2	SGR3
VHG Value	2.3408	-0.7575	-0.2834

(SGR1 –SGR3 = Southern Granites 1st to 3rd order reaches)

4.4 Southern Basalts Rainfall-Runoff Analysis

4.4.1 Statistical analysis

A similar analysis of rainfall-runoff characteristics was done for Southern Basalts study site to identify relationships between these important hydrological parameters (Table 4.4). High precipitation depth was found to be positively correlated to runoff volume strongly influencing the magnitude of runoff peak discharge ($r = 0.999$; $p = 0.000$ and $r = 0.999$; $p = 0.001$, respectively). A strong dependence of runoff volume on maximum precipitation intensity was identified ($r = 0.999$; $p = 0.000$). As anticipated, high rainfall intensities resulted in short delay times and such high intensities positively correlated with short duration rainfall events ($r = -0.999$; $p = 0.003$ and $r = -0.970$; $p = 0.029$). The role of antecedent soil moisture conditions, represented by API, on runoff delay times and rising times was notably significant ($r = -0.994$; $p = 0.006$ and $r = 0.923$; $p = 0.001$, respectively). High soil moisture conditions were revealed to cause high runoff volumes and high peak discharges ($r = 0.999$; $p = 0.001$ and $r = 0.999$; $p = 0.001$, respectively). These observations on soil moisture conditions show the importance of pre-event water for the generation of runoff in this catchment.

Table 4.4: Pearson's product moment correlation coefficient (r) with level of significance (p in parenthesis) for rainfall and runoff characteristics of three events at Southern Basalts monitored during December 2012 to February 2013.

	Precip. Duration	Precip. Amount	Precip. Int _{mean}	Precip. Int _{max}	Precip API ₇	Runoff Delay time	Runoff Rising Time	Catchment Area	Runoff Peak Discharge
Precip. Amount	0.919 (0.073)								
Precip. Int _{mean}	-0.313 (0.391)	0.088 (0.469)							
Precip. Int _{max}	-0.970* (0.029)	0.987* (0.012)							
Precip. API ₇	0.899 (0.303)	0.999 (0.068)	0.134 (0.452)	0.881 (0.102)					
Runoff Delay time	0.230 (0.314)	-0.998** (0.002)	-0.999** (0.003)	-0.928 (0.058)	-0.994** (0.006)				
Runoff Rising Time	0.076 (0.231)	-0.464 (0.445)	-0.227 (0.419)	-0.037 (0.487)	-0.923** (0.001)				
Runoff Peak Discharge	0.897 (0.076)	0.999 (0.256)	0.132 (0.330)	0.879 (0.086)	0.999** (0.001)			0.903* (0.04)	
Runoff Volume	0.999** (0.001)	0.999** (0.000)	0.089 (0.468)	0.999** (0.000)	0.999** (0.001)	-0.174 (0.438)	-0.465 (0.326)		0.999** (0.001)

** Significant at the 0.01 level

*Significant at the 0.05 level

4.4.2 Runoff coefficients (Rc)

The runoff coefficients for the Southern Basalts are presented in Table 4.5. Increasing Rc values were observed with increasing precipitation depths for the events in question. A linear relationship across spatial scales was noted on the dates where high soil moisture conditions were estimated using API as the surrogate. This signifies the importance of antecedent soil moisture on connectivity of channel networks at this catchment. Low soil moisture increases infiltration capacity and subsequent infiltration losses implying less water getting to downstream reaches under these conditions. However, incidence of high intensity rainfall under low soil moisture conditions can connect channel networks as the rainfall rate exceeds infiltration rate (saturation from above).

Table 4.5: Southern Basalts Runoff Coefficients for incremental stream reaches.

EVENT DATE	SBAS1Q(Rc)	SBAS2Q(Rc)	SBAS3Q(Rc)	RAINFALL(mm)	API ₇
2012/12/16	0.01	0.78	1.28	10	36.4
2013/01/19	0.73	2.18	2.62	70.8	108.62
2013/02/20	0.01	0.005	0.01	5.4	35.02

In order to closely link identified relationships to interactions of hydrological processes, two of the analysed events are presented in Figures 4.6A and 4.6B. Streamflow responses on the basalt geology are flashy as shown by sharp rising limbs and steep recession curves. Incremental changes in peak stream runoff with increasing stream orders is proof of stream network connectivity at least during and following high intensity rainfall events. This suggests the influence of scale in runoff generation where larger contributing areas result in pronounced runoff responses. Field surveys revealed the presence of persistent pools along channel networks, especially at the 3rd order where there is the possibility of groundwater contribution to streamflow (See Appendix IIe for location of pools). These pools were observed to have water for a period exceeding two months after the last rainfall event at this 3rd order reach. Events of high intensity clearly play a pivotal role in enhancing runoff responses as well as in facilitating hydrologic connectivity. A 10mm/15min rainfall rate on the 19th of January 2013 corresponded to a peakflow of 8.7m³/s showing close correlation between rainfall and runoff response.

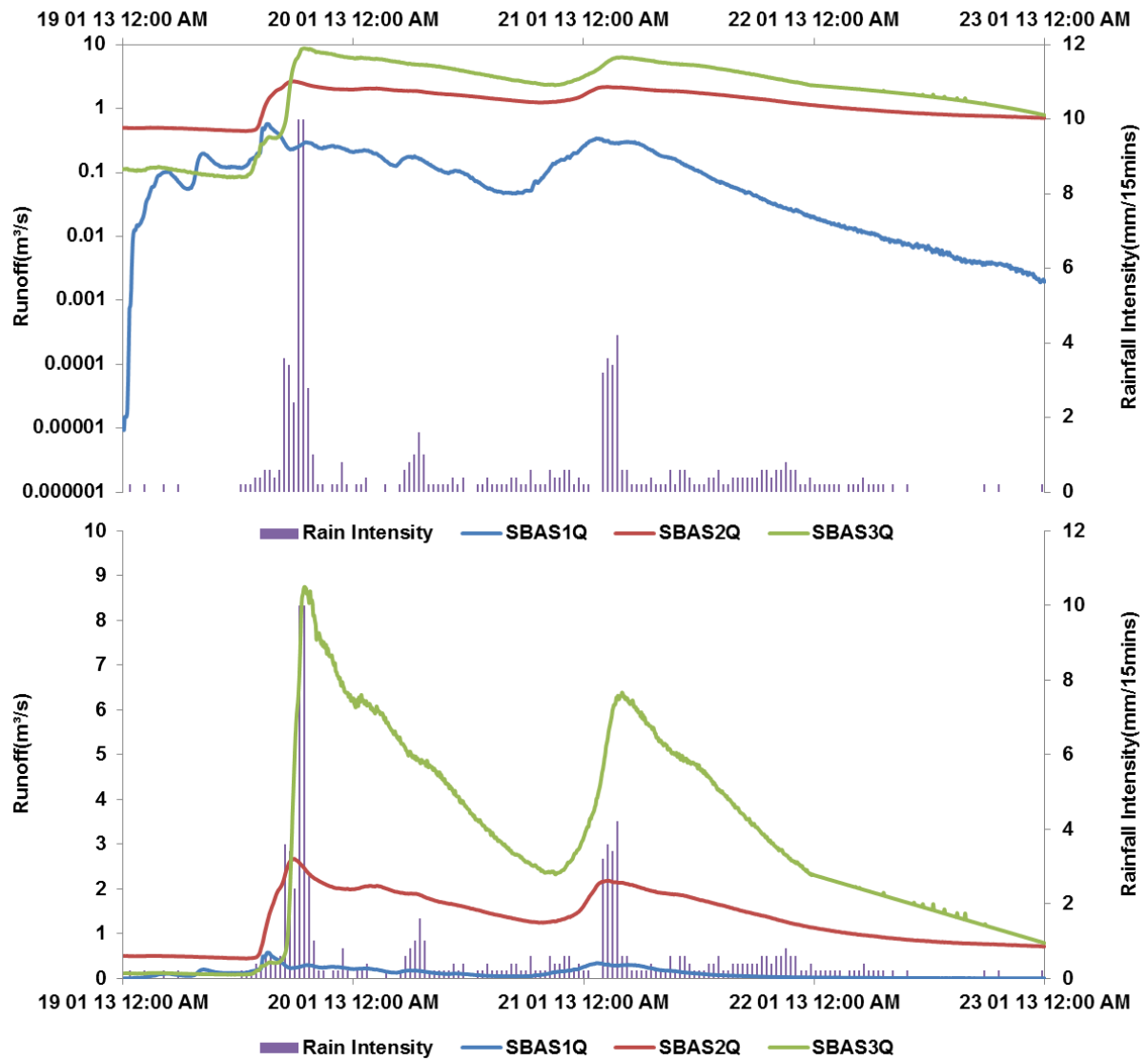


Figure 4.6A Southern Basalts streamflow responses following the rainfall event on the 19th of January 2013.

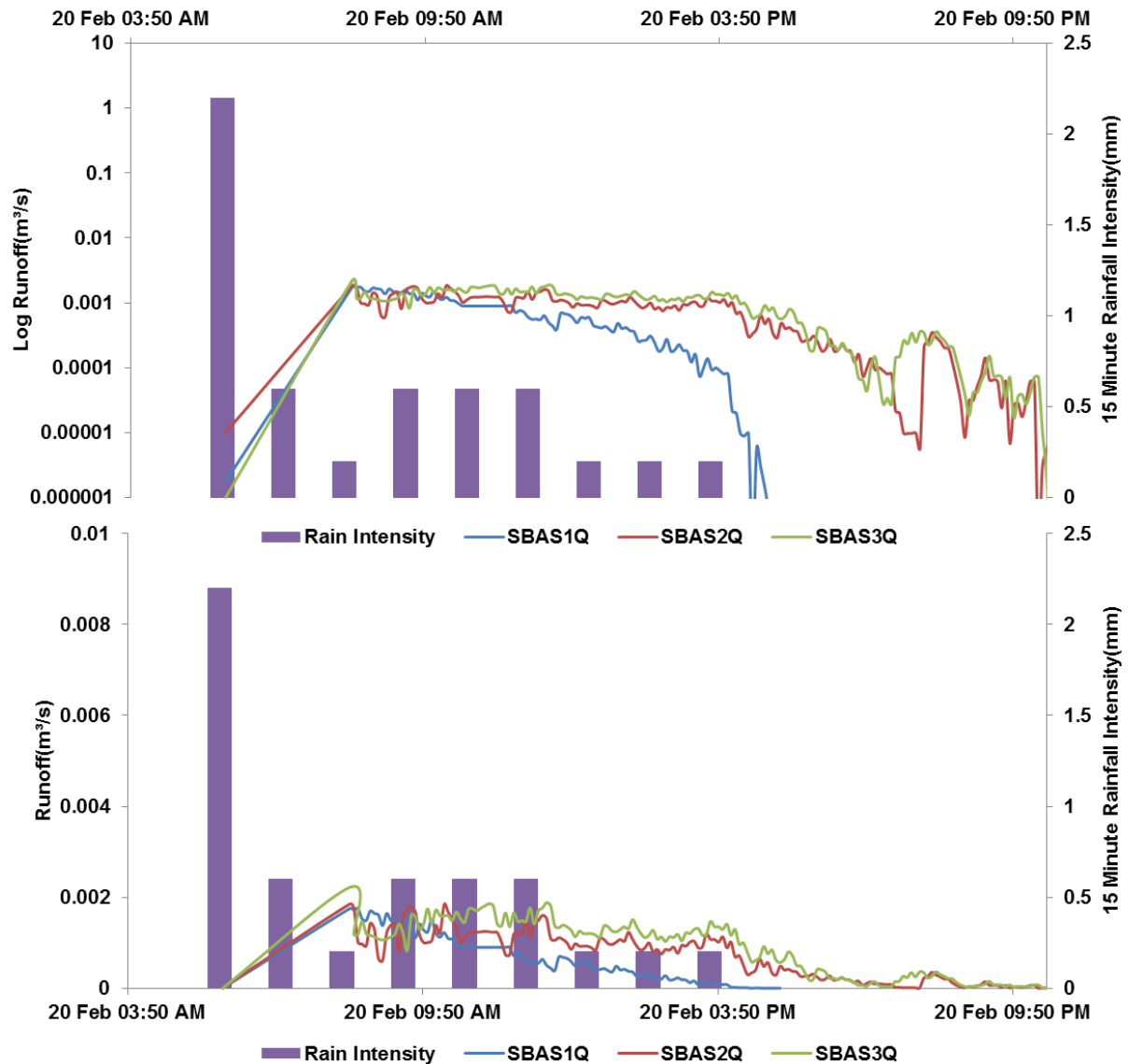


Figure 4.6B: Southern Basalts streamflow responses following the 20th of February 2013 rainfall event.

No subsurface discharge rating was done at the Southern Basalts catchment since this geology is characterised by very shallow soils where subsurface fluxes were presumed to be negligible. Compounding the difficulty for free drainage is the presence of vertic soils which are characterised by very low hydraulic conductivities. The few piezometers driven into the subsurface at this catchment confirmed the insignificant role of subsurface fluxes by being dry most of the time. As such stream-aquifer interaction was only characterised between streamflow processes and the deep groundwater zones at the 3rd order catchment only. With the lowly permeable vertic soils groundwater connectivity to the stream was perceived to occur through localised exposed fractures within the aquifer. A 9m water level difference

between crest boreholes and the stream at SBAS3 was observed during February to March 2013 which indicates a significant hydraulic gradient between boreholes and the stream (Figure 4.7). This provides further support of possible contribution of groundwater to the stream at this 3rd order reach of Southern Basalts study site.

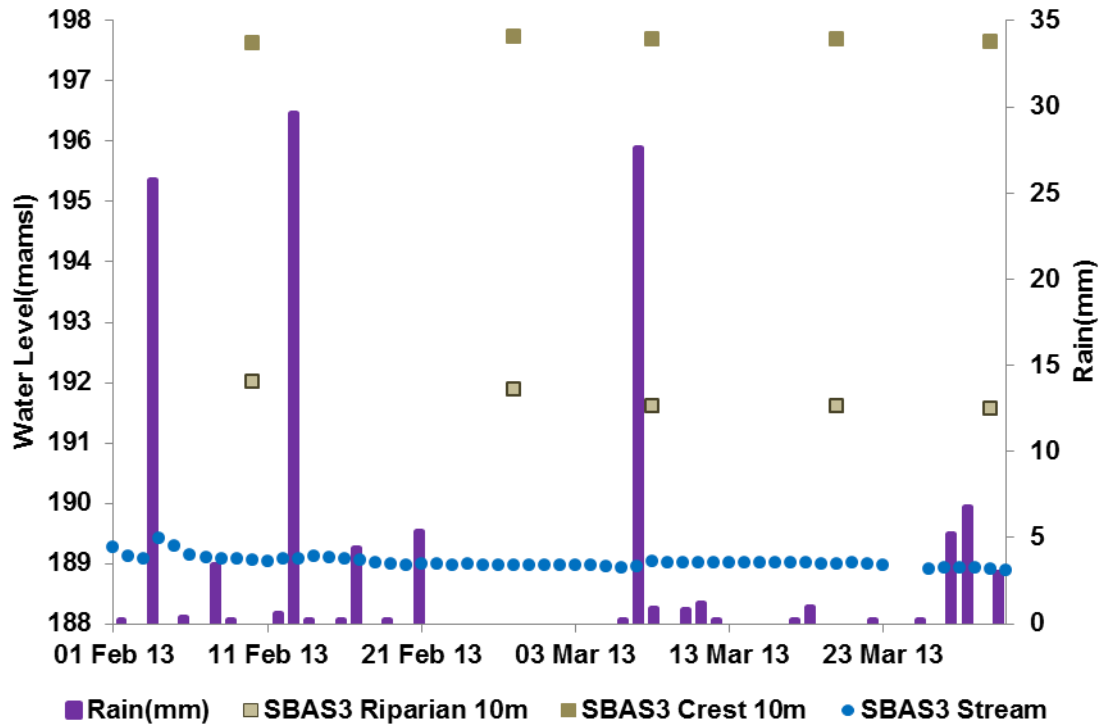


Figure 4.7: Hydraulic head differences between crest boreholes, riparian boreholes and the stream at Southern Basalts 3rd order reach during the period February to March 2013.

4.5 Flow duration curves (FDCs)

Analysing the percentage of time observed discharges are equalled or exceeded in different reaches within stream networks provided important indicators of stream network connectivity in study sites. The ensuing FDCs were calculated and plotted as functions of mean daily streamflow depths in millimetres per second (mm/s) for the period from September 2012 to March 2013.

4.5.1 Southern Granites FDCs

The flashy, ephemeral nature of streamflow on the granite geology is clearly portrayed in Figures 4.8 where the shape of flow duration curves show extremely concave shapes that are cut off at lower tails (Yokoo and Sivapalan, 2011). On this granitic geology, the first order subcatchment (SGR1) had persistent above zero (minimal), mean daily event-driven flow depths for 45% of the time in the period from September 2012 to March 2013. Conversely, at SGR2 and SGR3 reaches, respectively, surface flows were absent (below 0mm/s) between 85% and 75% of the time for the period under discussion. The highest percentage exceedance of at least just-above-zero flows at SGR1 further supports that this reach is gaining from groundwater sources. The SGR2 stream channel with no surface flow 85% of the time following rainfall events further supports the fact that this reach experiences pronounced transmission losses between rainfall events. The SGR3 reach showed flows for only 25% of the time in this period which indicate that this stream is increasingly losing between rainfall events. High rainfall intensity allows all reaches to be connected during the high flow regime indicated by extremely concave shapes of the FDCs (Figure 4.8) with exceedance probability of less than 5% for the period from September 2012 to March 2013. Mid-range flow regimes (intermittent) for these reaches are dampened by a combination of high ET demand and very permeable sandy soils that orchestrate massive transmission losses during periods of no rainfall across all spatial scales.

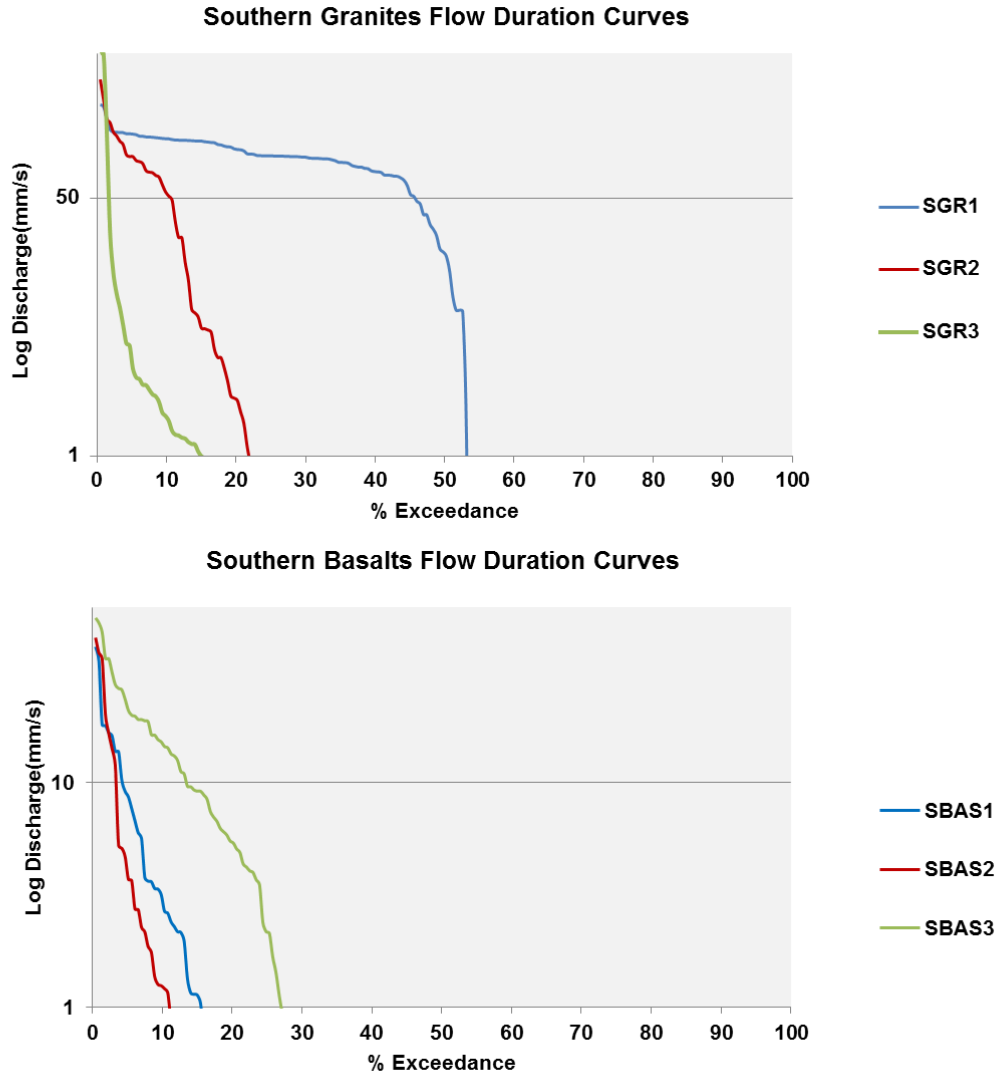


Figure 4.8: Southern Granites (SGR) and Southern Basalts (SBAS) Flow Duration Curves for the period from September 2012 to March 2013.

4.5.2 Southern Basalts FDCs

Streamflow duration is also variable with scale and ephemeral in nature at the Southern Basalts catchment as shown by FDCs which completely cut off at lower tails or during the low flow regime (Figure 4.8). On this basalt geology, the 3rd order catchment (SBAS3) had persistent above-zero mean daily event-driven depths of flow 44% of the time from September 2012 to March 2013. Conversely, at SBAS2 and SBAS1 reaches respectively, such flows were equalled or exceeded for only 32% and 27% of the time. These observations

further support the assertion that SBAS3 reach is gaining from groundwater aquifers. Hillslope contribution is less expected due to very low interfluvial gradients (mean slopes of 1.4% across first to third order subcatchments) and shallow vertically driven soils that promote limited lateral subsurface contribution to streamflow (Le Roux et al., 2011).

4.6 Summary of Hydrometric Findings

The presented surface-subsurface flow characterisations for the catchments enabled the refinement of previously held conceptual models, allowing for clearer formulation of hypotheses as follows:

□ Southern Granites

- SGR1, SGR2 and SGR3 stream reaches are gaining from hillslope riparian zones through near-surface macropore flow and soil interflow at least during rainfall events. However, SGR1 reach has more sustained hillslope inputs which include perched weathered rock interflow contribution during large rainfall events (Refer to Section 4.2.2 page 60).
- SGR2 reach is revealed as an increasingly losing reach with losses also occurring during events of moderate magnitudes.
- SGR3 reach also experiences transmission losses which are however less pronounced than at SGR2.
- Stream network connectivity occurs only during and following large rainfall events or during moderate but sustained rainfall.

□ Southern Basalts

- Stream network connectivity occurs only during and following large rainfall events
- Catchment interfluves play a very limited role in contributing to total stream runoff due to very low gradients.
- The 3rd order reach (SBAS3) was observed to be gaining from deep groundwater possibly through localised fracture flow.

5. RESULTS AND DISCUSSION: TRACERS

5. Introduction

This chapter presents the analyses of environmental tracers which were used to further understand stream-aquifer/hillslope connectivity to augment or refute aforementioned interpretations of hydrometric data. Analysed samples were collected from piezometers installed in streambed aquifers and riparian zones as well as from riparian and crest boreholes in the hillslope. Rainfall samples were collected from bulk rain gauges located 10km and 12km from Southern Granites and Southern Basalts, respectively. Samples were collected during the period, September 2012 to April 2013. Based on the above, tracer analyses in this study led to the testing of hypotheses (conceptual models) that were developed using hydrometric techniques. Results of dissolved silica (SiO_2), electrical conductivity (EC) and stable isotopes ($\delta^{18}\text{O}$) shall be presented and discussed since these are widely used environmental tracers for studies that seek to understand hydrological process behaviour in catchments (e.g. Shanley et al. 2002; Soulsby et al. 2006; Mul et al. 2008; Uhlenbrook et al. 2008;).

Meanings of acronyms and symbols for monitoring and sampling locations referred to in this chapter are given in Figures 5.1A & 5.1B and Tables 5.1A & 5.1B.

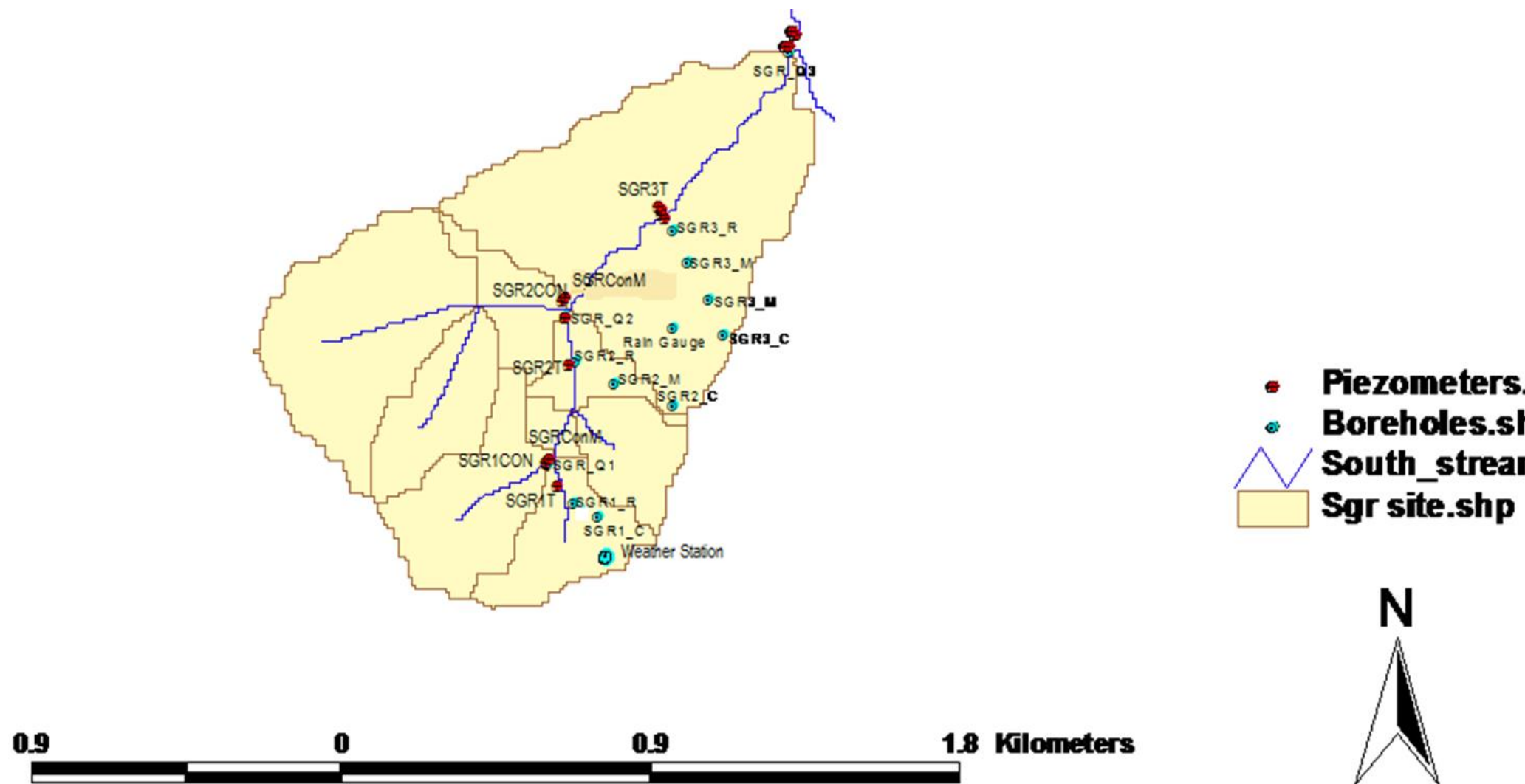


Figure 5.1A Monitoring points for Southern Granites (SGR) study site. (C = Crest; M= Midslope; R= Riparian; Q = flow gauge; T = Transect).

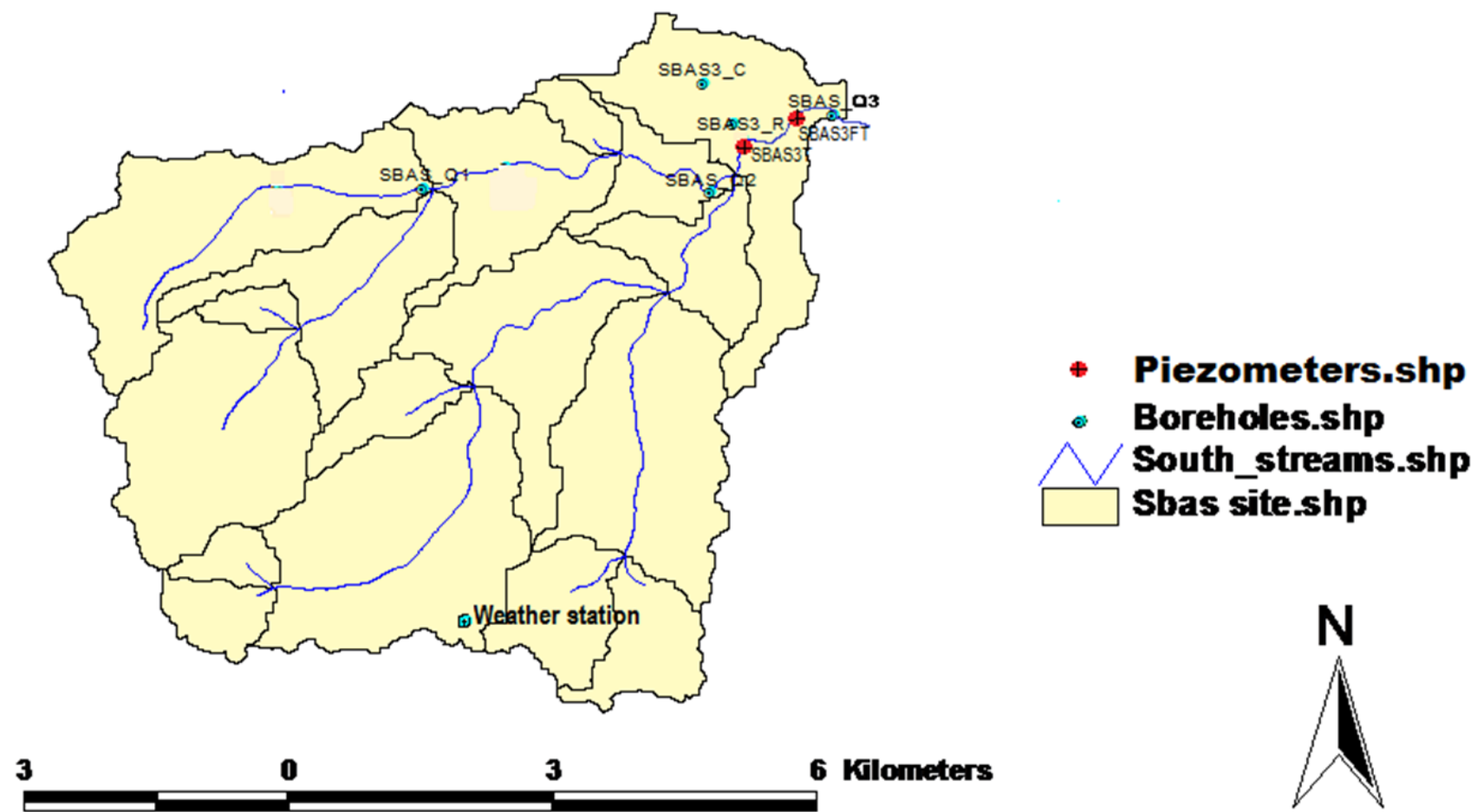


Figure 5.1B Monitoring points for Southern Basalts (SBAS3) study site (T = Transect; Q = Flow gauge; FT = Fever tree)

Table 5.1A Monitoring points acronyms and symbols at Southern Granites study site.

ACRONYM	DESCRIPTION
SW	Surface water
SS	Subsurface water
SGR1T	Southern granite 1 st order water level monitoring transect
SGR1Q	Southern granite 1 st order streamflow gauging station
SGR1Con	Southern granite 1 st order tributary
SGR1Con M	Southern granite 1 st order confluence
SGR2T	Southern granite 2 nd order water level monitoring transect
SGR2Q	Southern granite 2 nd order streamflow gauging station
SGR2Con	Southern granite 2 nd order tributary
SGR2Con M	Southern granite 2 nd order at confluence
SGR3T	Southern granite 3 rd order water level monitoring transect
SGR3Q	Southern granite 3 rd order streamflow gauging station
SGR3Con	Southern granite 3 rd order tributary
SGR3Con M	Southern granite 3 rd order at confluence
SGR1 PR	Southern granite 1 nd order riparian zone piezometer
SGR2 PR	Southern granite 2 st order riparian zone piezometer
SGR3 PR	Southern granite 3 st order riparian zone piezometer
SGR1 Riparian 61m(40m)	Southern granite 1 st order 61m riparian zone borehole sampled at a 40m depth
SGR1 Riparian 61m(50m)	Southern granite 1 st order 61m riparian zone borehole sampled at a 50m depth
SGR1 Riparian 61m(60m)	Southern granite 1 st order 61m riparian zone borehole sampled at a 60m depth
SGR1 Riparian 28m(28m)	Southern granite 2 nd order 28m riparian zone borehole sampled at a 28mm depth
SGR2 Riparian 49m(30m)	Southern granite 2 nd order 49m riparian zone borehole sampled at a depth of 30m
SGR2 Riparian 49m(40m)	Southern granite 2 nd order 49m riparian zone borehole sampled at a depth of 40m
SGR3 Riparian 43m(30m)	Southern granite 3 rd order 43m riparian zone borehole sampled at a depth of 30m
SGR3 Riparian 43m(40m)	Southern granite 3 rd order 43m riparian zone borehole sampled at a depth of 40m
SGR3 Riparian 20m(20m)	Southern granite 3 rd order 20m riparian zone borehole sampled at a depth of 20m

Table 5.1B: Monitoring points' acronyms and symbols at Southern Basalts study site

ACRONYM	DESCRIPTION
SW	Surface water
SBAS3T	Southern basalt 3 rd order water level monitoring transect
SBAS3Q	Southern basalt 3 rd order streamflow gauging station
SBAS3FT	Southern basalt 3 rd order fever tree location
SBAS3 Riparian 80m(20m)	Southern basalt 3 rd order 80m riparian zone borehole sampled at a depth of 20m
SBAS3 Riparian 80m(30m)	Southern basalt 3 rd order 80m riparian zone borehole sampled at a depth of 30m
SBAS3 Riparian 80m(40m)	Southern basalt 3 rd order 80m riparian zone borehole sampled at a depth of 40m
SBAS3 Riparian 80m(50m)	Southern basalt 3 rd order 80m riparian zone borehole sampled at a depth of 50m
SBAS3 Riparian 80m(60m)	Southern basalt 3 rd order 80m riparian zone borehole sampled at a depth of 60m
SBAS3 Riparian 80m(70m)	Southern basalt 3 rd order 80m riparian zone borehole sampled at a depth of 70m
SBAS3 Riparian 80m(80m)	Southern basalt 3 rd order 80m riparian zone borehole sampled at a depth of 80m
SBAS3 Crest 80m(20m)	Southern basalt 3 rd order 80m hillslope crest borehole sampled at a depth of 20m
SBAS3 Crest 80m(30m)	Southern basalt 3 rd order 80m hillslope crest borehole sampled at a depth of 30m
SBAS3 Crest 80m(40m)	Southern basalt 3 rd order 80m hillslope crest borehole sampled at a depth of 40m
SBAS3 Crest 80m(50m)	Southern basalt 3 rd order 80m hillslope crest borehole sampled at a depth of 30m
SBAS3 Crest 80m(60m)	Southern basalt 3 rd order 80m hillslope crest borehole sampled at a depth of 40m
SBAS3 Crest 80m(70m)	Southern basalt 3 rd order 80m hillslope crest borehole sampled at a depth of 20m

5.1 General Isotopic, Physico-chemical and Hydrochemical Trends in Study Sites

▪ Tracer trends at Southern Granites

Rainfall isotopic trends were generally mimicked in most stream samples for the period from September 2012 to March 2013 at Southern Granites study site (Figure 5.2). This is an indication that event water has a significant contribution to runoff in this catchment. For instance, samples collected on the 19th of January and 19 of February 2013 respectively, had -4.71‰; -4.77‰ and -3.47‰; -3.47‰ $\delta^{18}\text{O}$ delta values for the stream and rain respectively. Some subsurface samples across spatial scales also had close concentrations to that of rainfall

indicating rapid responses from the subsurface domain (Table 5.2A). Generally the dominant influence of rainfall to runoff responses is revealed in subsequent depletion of stream samples in the heavier ($\delta^{18}\text{O}$) isotopes following large rainfall events, such as the event on the 19th of January 2013 (Figure 5.2).

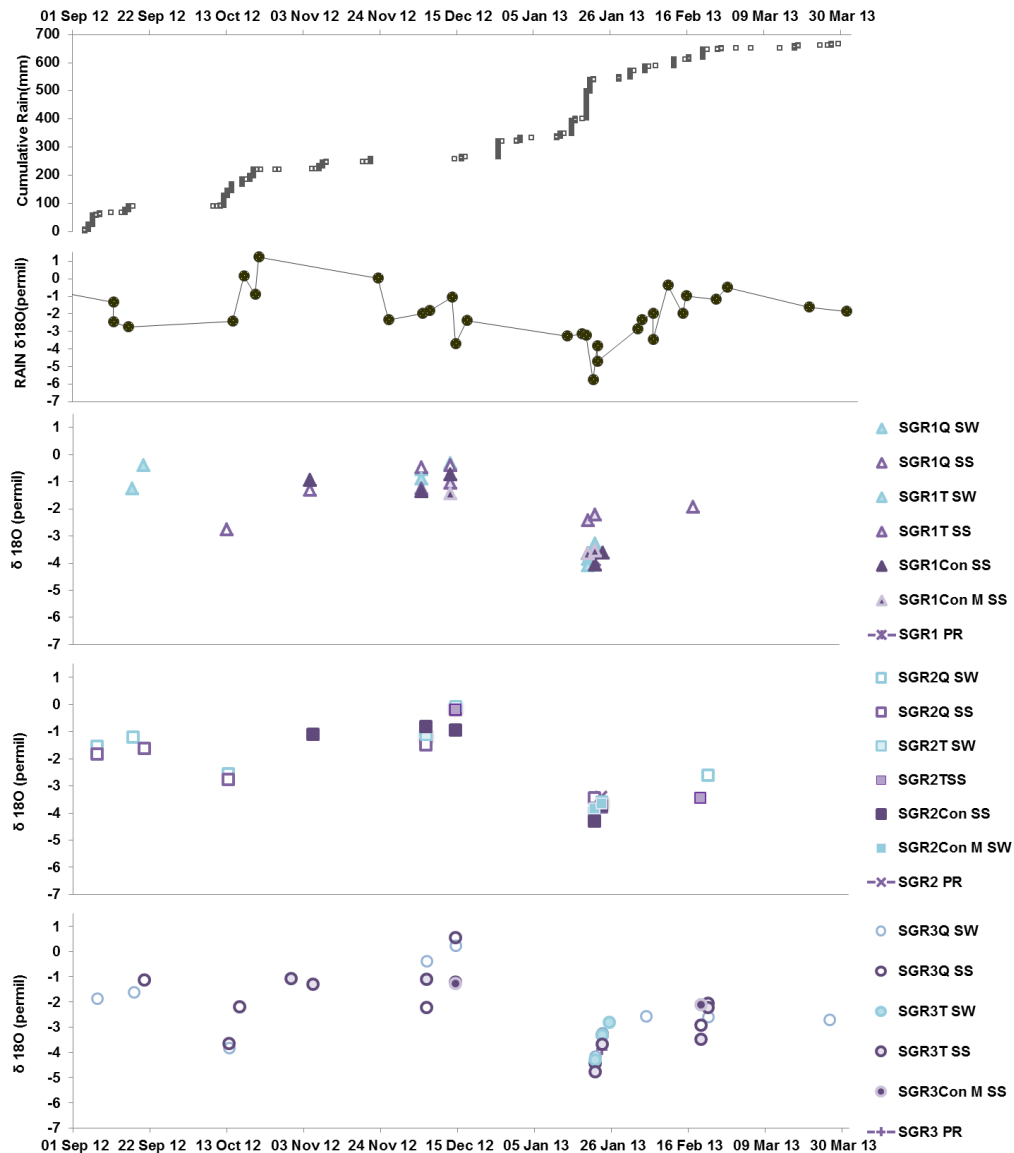


Figure 5.2: Isotopic trends in rainfall and stream samples at Southern Granites from September 2012 to March 2013 (Blue = surface water samples; Purple = subsurface samples; Black = rain samples).

Table 5.2A: Rainfall and stream isotopic signatures at Southern Granites for samples collected between September 2012 and March 2013.

Date	Location	Stream(permil)	Rain(permil)
2012/09/17	SGR2SS	-1.19	-1.35
2012/10/13	SGR2SW	-2.55	-2.44
2012/11/25	SGR3SS	-2.22	-2.36
2012/12/13	SGR1SS	-1.07	-1.27
2013/01/19	SGR3TSW	-4.71	-4.77
2013/01/20	SGR1SW	-3.66	-3.82
2013/02/19	SGR3 SW	-3.47	-3.47

Analytical error for $\delta^{18}\text{O}$ is +/-0.3‰.

EC values for analysed samples ranged between 50.4 $\mu\text{S}/\text{cm}$ to 3640 $\mu\text{S}/\text{cm}$ at the Southern Granites study site (Table 5.2B). Highest values were recorded from groundwater, followed by stream and the lowest were from rainfall samples. Stream EC values dropped momentarily following large rainfall events (e.g. 95.7mm on 19 January, 2013) showing pronounced dilution of solutes in the catchments during such wet conditions. No defined trend was observable for borehole EC values.

Silica (SiO_2) ranged between 0.0mg/L and 63.9mg/L with streams having highest concentrations while rainfall samples had the lowest. Distinct differences in the silica concentrations were observed between boreholes, streams and rain samples. Chloride (Cl) concentrations ranged from 0.9 to 114.5mg/L and these concentrations showed distinct differences between the three domains (groundwater, stream and rain). Since the sample concentrations in the three water sources were very distinct, it was feasible to use silica and chloride for hydrograph separation. On the 6th of December 2012, silica values were lower than they were on the 19th of January and 20th of February 2013. This is possibly due to lower moisture during early December than in the months of January and February where higher soil moisture promoted greater dissolution of silica from silicate compounds (See Table 5.2B).

Table 5.2B: Selected typical EC, silica and chloride concentration ranges at Southern Granites during December 2012 to February 2013.

Date	Location	Borehole			Stream			Rain		
		EC	Silica	Cl	EC	Silica	Cl	EC	Silica	Cl
		($\mu\text{s/cm}$)	(mg/L)	(mg/L)	($\mu\text{s/cm}$)	(mg/L)	(mg/L)	($\mu\text{s/cm}$)	(mg/L)	(mg/L)
2012/02/06	SGR3Q	3640	9.93	--	103	6.98	--	73.8	--	--
2013/01/19	SGR3Q	2850	18.03	114.5	52.5	15.73	5.3	50.4	0	0.9
2013/02/20	SGR3Q	3340	19.47	--	141.4	63.9	--	65	--	--

-- No Data.

▪ Tracer trends at Southern Basalts

At the Southern Basalts study site rainfall isotopic patterns generally aligned with those of stream samples with stream concentrations being depleted at the incidence of large rainfall events (Figure 5.3). Similar stream and rainfall signatures at this site portrayed mixing between these two water sources suggesting the significance of event water contribution to stream runoff (Table 5.3A).

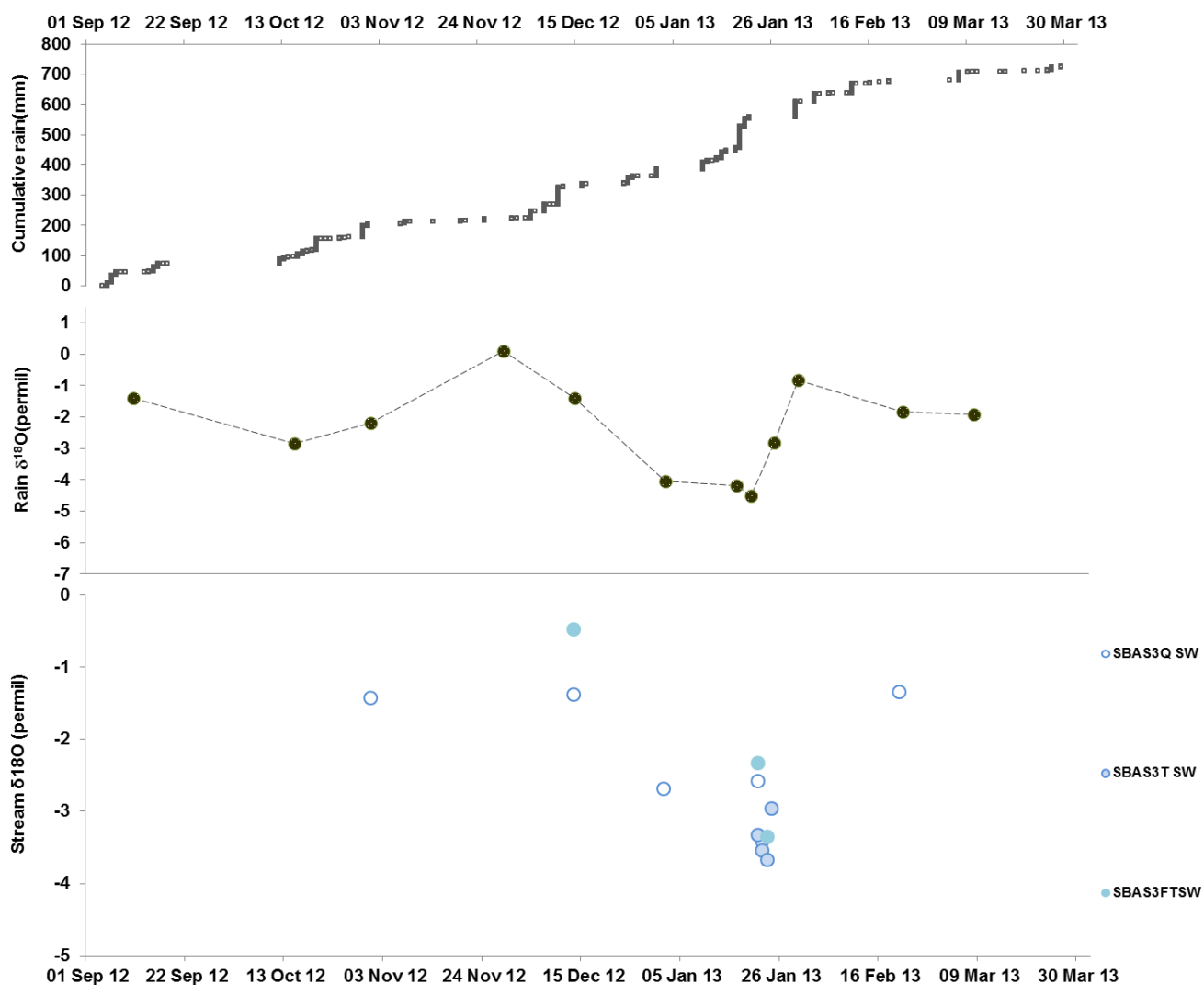


Figure 5.3: Isotopic trends in rainfall and stream samples at Southern Basalts from September 2012 to March 2013.

Table 5.3A: Rainfall and stream isotopic signatures for Southern Basalts site for samples collected between December 2012 and January 2013.

Date	Location	Stream(permil)	Rain(permil)
2012/12/13	SBAS3	-1.38	-1.41
2013/01/21	SBAS3	-2.58	-2.81

Analytical error for $\delta^{18}\text{O}$ is 0.3‰

EC values for analysed samples ranged between 62 μ S/cm to 1491 μ S/cm at Southern Basalts. Highest EC values were recorded for groundwater, lowest for rain and intermediate values for subsurface samples (See Table 5.3B). Stream EC values at this also dropped momentarily following large rainfall events (e.g. 95.7mm on 19 January, 2013) showing pronounced dilution of solutes in the catchments during these very wet conditions. No defined trend was observable for borehole EC values.

Table 5.3B: Selected typical EC, silica and chloride concentration ranges at Southern Basalts during December 2012 to February 2013.

Date	Location	Borehole			Stream			Rain		
		EC	Silica	Cl	EC	Silica	Cl	EC	Silica	Cl
		(μ S/cm)	(mg/L)	(mg/L)	(μ S/cm)	(mg/L)	(mg/L)	(μ S/cm)	(mg/L)	(mg/L)
2012/02/06	SBAS3Q	1442	17.9	--	808	11.05	--	75.6	--	--
2013/01/19	SBAS3Q	1480	24.47	--	367	11.36	--	62	0	--
2013/02/20	SBAS3Q	1491	21.33	--	642	12.2	--	72.6	--	--

At this site silica concentration ranged between 0.0mg/L and 24.47mg/L with groundwater having highest concentrations followed by stream samples while lowest values were recorded in rainfall. Distinct differences in the silica concentrations were also observed between boreholes, streams and rain samples at this site, and this made it possible to use silica for hydrograph separation. Silica concentrations were lower on the 6th of December 2012, than they were on the 19th of January and on the 20th of February 2013 for the same reason given for EC values on these dates (Refer to Table 5.3B).

5.2 Tracer Analysis at Southern Granites

Stable isotopes supported the hypothesis that all 1st to 3rd order reaches gain water from riparian zones at least during or immediately after rainfall events. Similar $\delta^{18}\text{O}$ values for stream and riparian zone piezometers on the 21st of January 2013 attest to this assertion. Considering an analytical error of $\pm 0.3\%$ $\delta^{18}\text{O}$ values in the stream and riparian zone piezometers respectively, at SGR1 (-3.87‰ and -3.89‰), SGR2 (-3.44‰ and -3.41‰) and SGR3 (-3.66‰ and -3.90‰) support that the stream interacts with the shallow subsurface water source in adjacent footslopes (Figure 5.4 and Table 5.5). Silica and chloride

concentrations in the riparian piezometers and the stream provide further support of stream-subsurface connectivity during rainfall events. For instance, on the 21st of January 2013 a sample collected from the riparian zone piezometer at SGR1 had a concentration of 9.12mg/L which was similar (analytical error of +/-0.3mg/L) to the stream concentration of 9.10mg/L (See Table 5.5). On the same date, chloride provided further support of stream-subsurface connectivity at the SGR2 reach where the concentrations were 4.80mg/L and 4.29mg/L for riparian zone piezometer and the stream, respectively (Table 5.5). Near-surface lateral flow is the connecting mechanism as suggested by water levels in shallow piezometers (less than 3m) that never overflowed onto the ground surface. Macropore flow augments soil lateral flow because the rise in water levels in the piezometers was a rapid response to the preceding 90.7mm event.

Interaction between groundwater and streams is isotopically supported by $\delta^{18}\text{O}$ signatures at SGR1 following the large and intense rainfall event on the 19th of January, 2013. Similar $\delta^{18}\text{O}$ signatures (-3.2‰, -3.27‰ and -3.35‰) for the 17m crest borehole, the stream and the 61m riparian borehole respectively, indicate the occurrence of groundwater-surface water interaction (Figure 5.4). Samples collected two days later, also had similar signatures (-3.52‰ and -3.53‰ for stream and borehole, respectively) confirming mixing of riparian borehole water and surface water at downstream sections of the SGR1 reach.

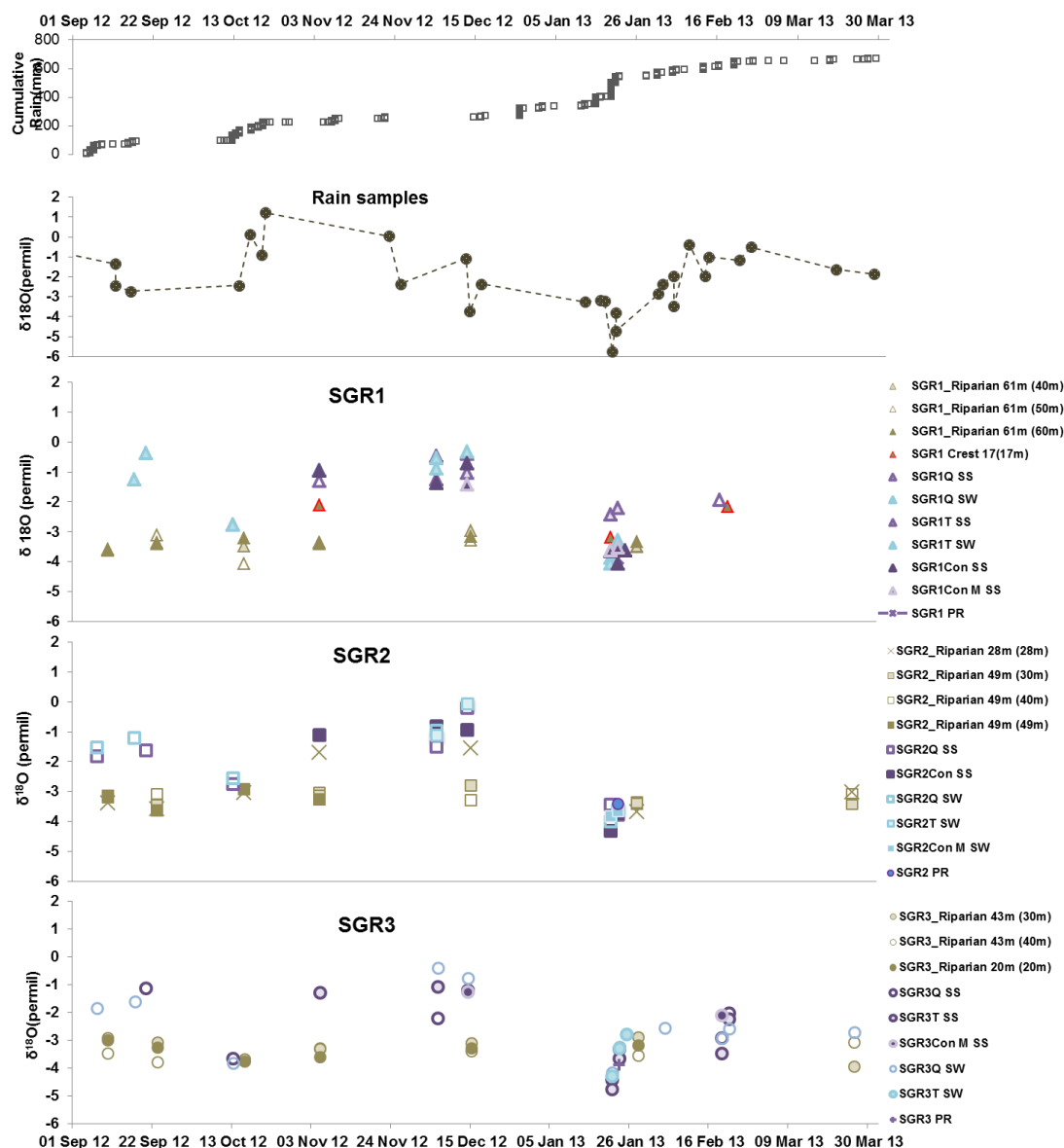


Figure 5.4 Isotopic ($\delta^{18}\text{O}$) delta values for three incremental spatial scales at the Southern Granites study site from September 2012 to March 2013 (Blue = surface water samples; Purple = subsurface samples; Green = groundwater samples).

This observation at SGR1 tallies with the observed 1m positive hydraulic gradient towards the stream from the 17m crest borehole which supports the hypothesis that this headwater reach is gaining during and immediately after rainfall events. This shallow crest borehole does not extend beyond the weathered rock aquifer, which suggests a perched interflow pathway in weathered material overlying a consolidated hard rock of low transmissivity. The deeper 103m crest borehole that extends into the hard rock did not similarly respond to this rainfall event implying that the deeper aquifer might be semi confined. The water being

conveyed by soil/bedrock interflow then seeps onto the ground surface at the footslope as hillslope gradient decreases. Shallow sterkspruit responsive soils characterise this headwater reach (Le Roux et al., 2011) and these become saturated with minimal rainfall input due to low water storage capacity. The hydropedological property of these shallow soils explains the presence of a seasonal headwater wetland flanking the SGR1 reach (Refer to Figure 4.3A in chapter 4 for wetland location). Through saturation overland flow water drains into the stream from this wetland especially during prolonged wet spells such as the one that occurred in the months of January and February of 2013.

Groundwater and stream interaction at the SGR2 reach is evidenced by isotopic delta values (-3.68‰ and -3.66‰) for the 28m riparian borehole and the stream, respectively. The similar isotopic signatures further support the combination of negative hydraulic gradients, unceremoniously rapid recessions and the 30cm riparian zone borehole water level rise (Chapter 4, Figure 4.3A) in affirming the SGR2 reach as increasingly losing to groundwater aquifers. Water levels in boreholes on this reach never exceeded stream water levels during the monitoring period, indicating that the stream's hydraulic head was always above the aquifer water table even during rainfall events. Under such conditions, this reach can be described as having an unsaturated connection to the aquifer (Winter, 2007).

Similar tracer signatures on the 21st of January 2013, for $\delta^{18}\text{O}$ and silica in riparian zone piezometers and the stream at SGR3 support the existence of subsurface and stream water interaction. Isotopic delta values of -3.90‰ and -3.66‰ for riparian and stream samples respectively, indicate mixing of these water sources given an analytical error of +/-0.3‰ (Table 5.5). Silica concentrations for the same samples as above stood at 9.44mg/L and 9.45mg/L providing further support that the subsurface and the stream domains are hydrologically connected at this 3rd order reach (Figure 5.5 and Table 5.5). Time series signatures of silica are presented in Appendix IV.a.

Table 5.4: Isotopic ($\delta^{18}\text{O}$) delta values and hydrochemical (Silica & Chloride) concentrations indicating connectivity points across scales at Southern Granites study site during October 2012 to January 2013.

TRACER	DATE	LOCATION	CONCENTRATION
$\delta^{18}\text{O}$	14/10/2012	SGR2QSS	-2.76‰
		SGR2 Riparian49(49m)	-2.77‰
Silica (SiO ₂)	14/10/2012	SGR1 Crest 17(17m)	19.38mg/L
		SGR1QSS	19.37mg/L
$\delta^{18}\text{O}$	05/11/2012	SGR2 Riparian28(28m)	-1.04‰
		SGR2Con	-1.11‰
	21/01/2013	SGR1PR	-3.89‰
		SGR1QSW	-3.87‰
	21/01/2013	SGR2PR	-3.42‰
		SGR2QSS	-3.44‰
	21/01/2013	SGR3PR	-3.90‰
		SGR3T	-3.66‰
	21/01/2013	SGR1 Crest 17(17m)	-3.2‰
		SGR1QSW	-3.27‰
		SGR1 Riparian 61(40m)	-3.35‰
Silica (SiO ₂)	21/01/2013	SGR1PR	9.12mg/L
		SGR1T	9.10mg/L
		SGR3PR	9.44mg/L
		SGR3T	9.45mg/L
Chloride (Cl)	21/01/2013	SGR2PR	4.80mg/L
		SGR2ConMSW	4.49mg/L
Silica (SiO ₂)	21/02/2013	SGR1	24.93mg/L
		SGR1 Crest 17(17m)	26.23mg/L
$\delta^{18}\text{O}$	23/01/2013	SGR1ConMSS	-3.53‰
		SGR1ConSS	-3.63‰
		SGR1 Riparian61(40m)	-3.52‰
	25/01/2013	SGR2ConMSW	-3.66‰
		SGR2 Riparian 28(28m)	-3.68‰

Analytical error for $\delta^{18}\text{O}$ is +/-0.3‰; for Silica is +/-0.3mg/L and for Chloride is +/-0.3mg/L)

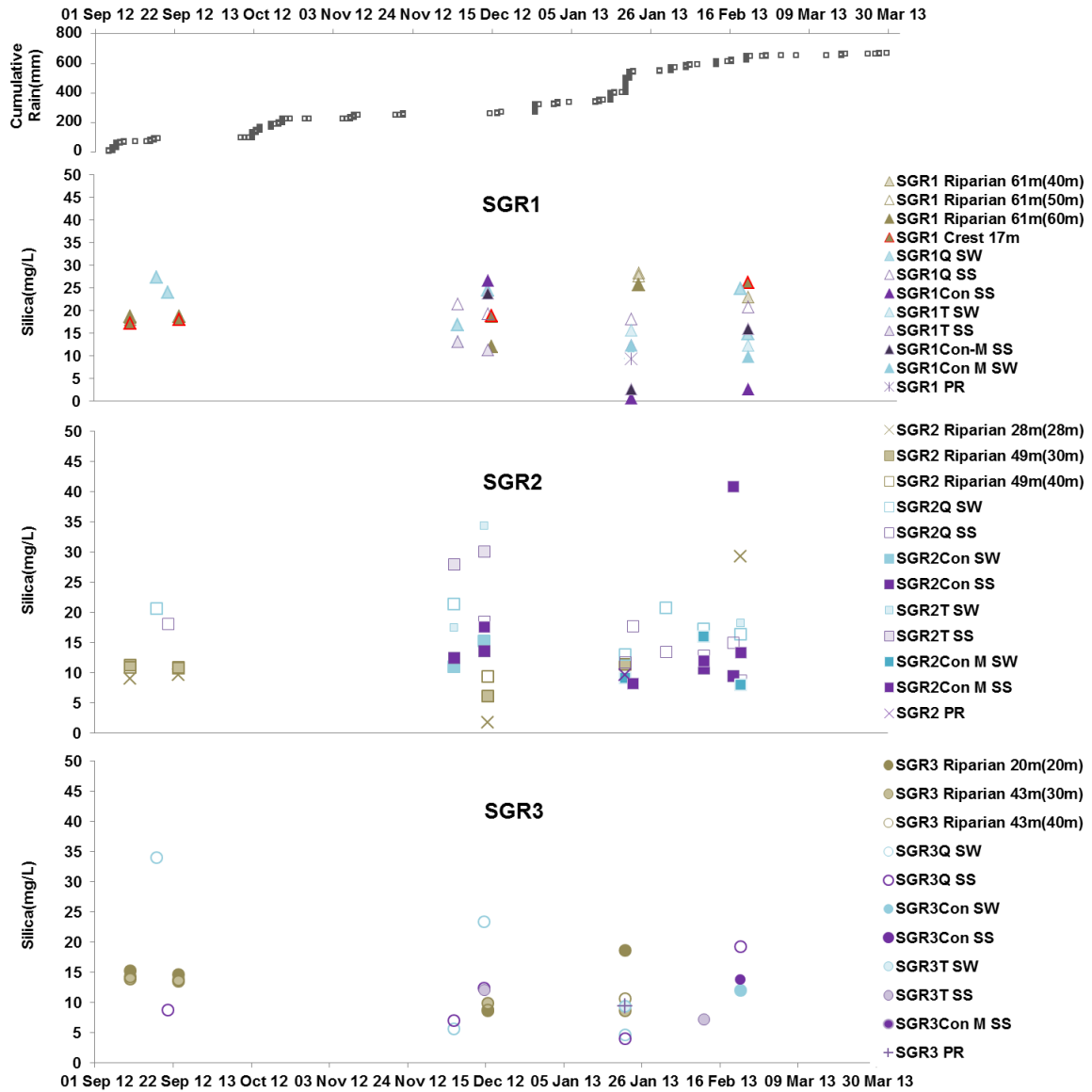


Figure 5.5 Southern Granites time series presentation of silica concentrations for three incremental spatial scales from September 2012 to March 2013 (Blue = surface water samples; Purple = subsurface samples; Green = groundwater samples).

5.3 Tracer Analysis at Southern Basalts

Riparian zone piezometers at this site were mostly dry and whenever they had water, the water levels were too low to allow successful sampling. This observation supports the notion that at Southern Basalts there is less or no subsurface lateral contribution to streamflow due to very low interfluvial gradients. Verification of groundwater and stream interaction at these lower order spatial scales is subject to further research beyond this thesis, upon installation of deep groundwater boreholes. However, at the 3rd order reach (SBAS3) environmental tracers

were used to test the hypothesis that the stream at this order is connected to groundwater through localised fractured rock preferential flow. Similar tracer signatures between selected pools along the stream and groundwater samples were observed at SBAS3 for the sampling period between September 2012 to March 2013 (See Figures 5.6 & 5.7 and Table 5.6). On the 9th of January 2013 samples collected from the stream and riparian zone boreholes respectively, had $\delta^{18}\text{O}$ values of -2.61‰ and -2.68‰, and silica concentrations of 31.94mg/L and 32.25mg/L (Table 5.6). Given the analytical error of ± 0.3 for both $\delta^{18}\text{O}$ and silica the stated values support that there is groundwater contribution to streamflow at SBAS3. Following the large rainfall event on the 19th of January 2013, similar isotopic signatures of -2.20‰ & -2.30‰ for groundwater and the stream respectively, further confirm that the stream is gaining from groundwater aquifers at this scale (Table 5.6).

Table 5.5: Isotopic ($\delta^{18}\text{O}$) delta values and hydrochemical (Silica) concentrations indicating connectivity points at the 3rd order reach of Southern Basalts study site.

TRACER	DATE	LOCATION	CONCENTRATION
$\delta^{18}\text{O}$	09/01/2013	SBAS3Q	-2.68‰
		SBAS3 Riparian 80(40m)	-2.61‰
Silica (SiO ₂)	09/01/2013	SBAS3 Riparian 80(60m)	32.25mg/L
		SBAS3T	31.94mg/L
$\delta^{18}\text{O}$	21/01/2013	SBAS3FT	-2.20‰
		SBAS3 Crest 80(60m)	-2.30‰
	24/01/2013	SBAS3Q	-2.68‰
		SBAS3 Crest 80(80m)	-2.59‰

Analytical error for $\delta^{18}\text{O}$ is ± 0.3 ‰; for Silica is ± 0.3 mg/L)

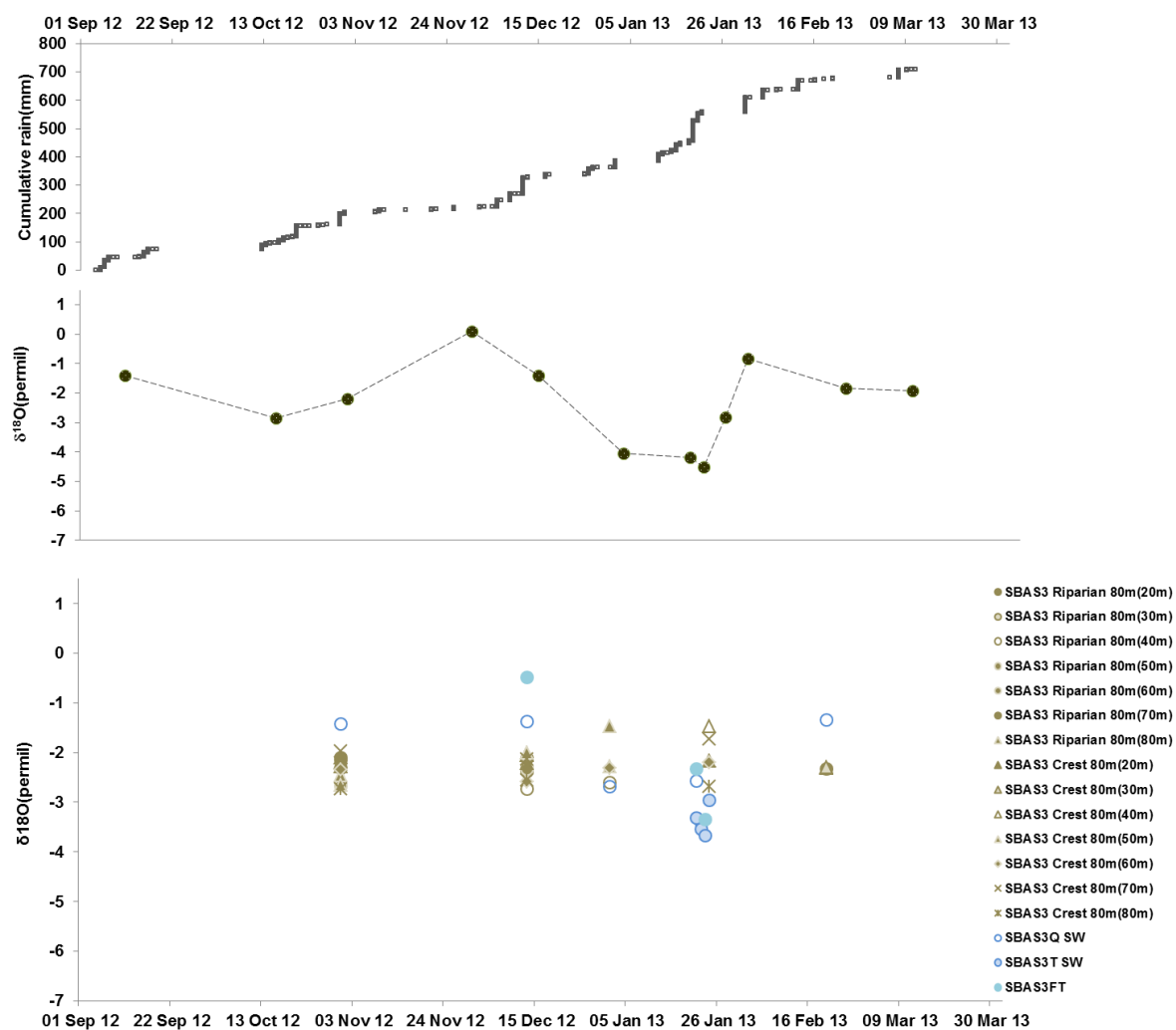


Figure 5.6 Southern Basalts time series presentation of $\delta^{18}\text{O}$ delta values for the 3rd order reach from September 2012 to March 2013. (Blue = surface water; Green = Groundwater).

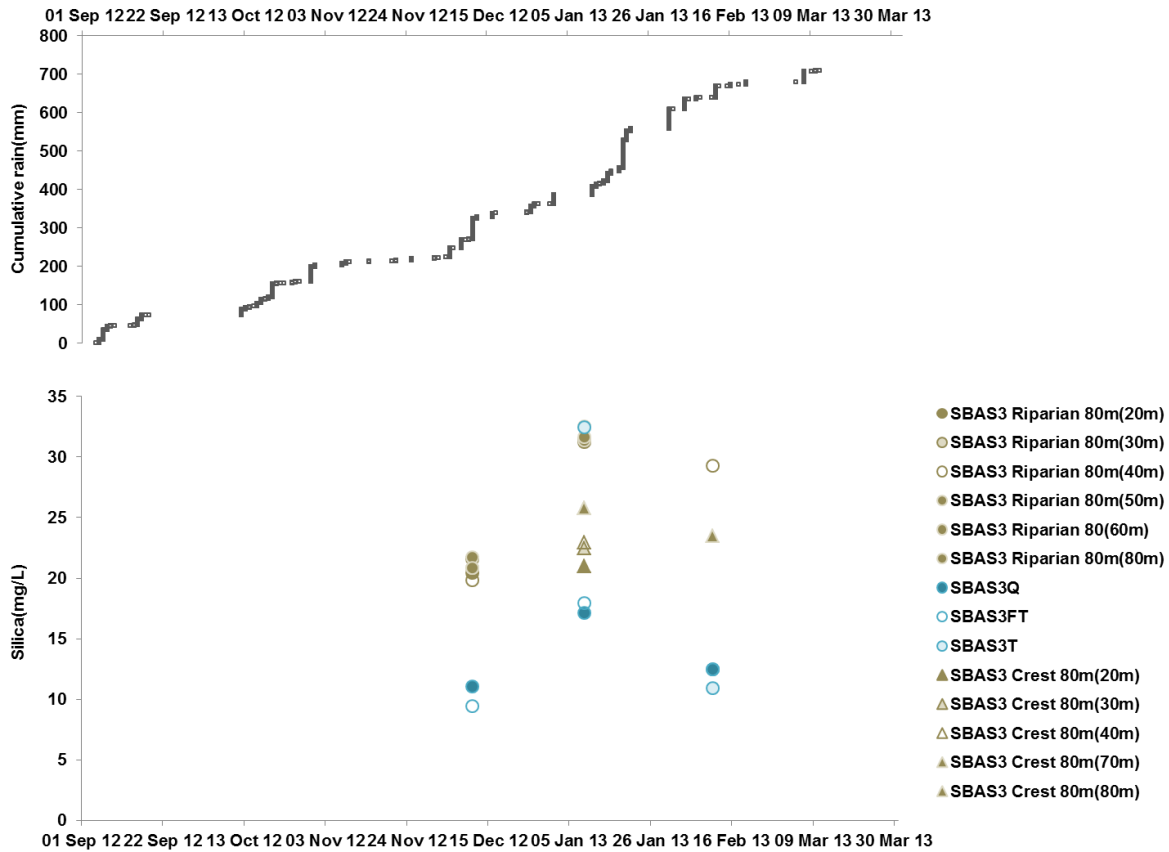


Figure 5.7 Southern Basalts time series presentation of silica concentrations from September 2012 to March 2013.(Blue = surface water; Green = Groundwater)

5.4 Quantifying Contribution of Different Water Sources to Streamflow

Hydrograph separation at Southern Granites relied on automatic sampling at the 3rd order reach and on grab samples for 1st and 2nd order reaches, while at the Southern Basalts only grab samples were used. Two high-intensity rainfall events were selected for hydrograph separation to check whether findings in one event would be similar in the other, thus increasing credibility of results. At Southern Granites, Event 1 which occurred on the 19th of January 2013 had 15-minute peak and mean intensities of 16.3mm and 1.9mm, respectively. Event 2 which occurred on the 20th of February 2013 had 18.6mm and 1.85mm as peak and mean 15-minute intensity values, in that order. Event 1 totalled 95.7mm of rainfall for a period of 10 hours. Almost 60% (56.2mm) of this total was received in two hours. Stream discharge at the third order (SGR3Q) gauging station increased from 0.4m³/s to 6.5m³/s which marked the peakflow for this event. Event 2 with a duration of 4 hours totalled

27.9mm, 84% of which fell in only one hour. It occurred 4 days after the last event which had occurred on the 16th of February 2013. Subsequent discharge at SGR3Q increased from 0.001m³/s at start of event to 0.136m³/s at peakflow.

Similarly at Southern Basalts the aforementioned events (19 January and 20 February 2013) were analysed. Event 1 had 10mm and 0.47mm respectively, as the peak and mean 15-minute intensities while Event 2 had 2.2mm and 0.54mm for peak and mean 15-minute intensities, respectively. Event 1 totalled 70.8mm over 10 hours. Approximately 60% (44.8mm) of the rainfall total fell within two hours. Stream discharge at the third order gauged outlet increased from 0.6m³/s to 2.5m³/s at peakflow. Event 2 lasted for 5 hours and had a total of 5.4mm, 51% (2.8mm) of which fell in two hours. The fact that runoff response in the two geologies (granites and basalts) is controlled by rainfall intensity is in this case further supported. Relatively higher intensities at the granites resulted in higher discharges in stark contrast to smaller responses observed at the basalts.

5.4.1 Event 1 (19 January 2013) at Southern Granites 3rd Order Reach (SGR3)

Component contributions of different sources were first estimated by lumping sample concentrations from each source to give typical end member values (Lorentz et al. 2008). The end members calculated as volume averaged delta values for rainfall, runoff and the groundwater source were set at -5.40‰, -4.96‰ and -3.38‰, respectively. On an $\delta^{18}\text{O}$ and δD plot the runoff end member lies very close to rainfall and further away from the groundwater end member signifying more event water contribution to total runoff (Figure 5.8). A linear interpolation between the end members showed event water contribution of 84% while the pre-event estimate stands at 16%. It is perceived that the SGR3 riparian zone contributes this 16% by soil interflow, being augmented by near-surface macropore flow as connecting mechanisms. For details of linear interpolations please refer to Appendix IV.a.

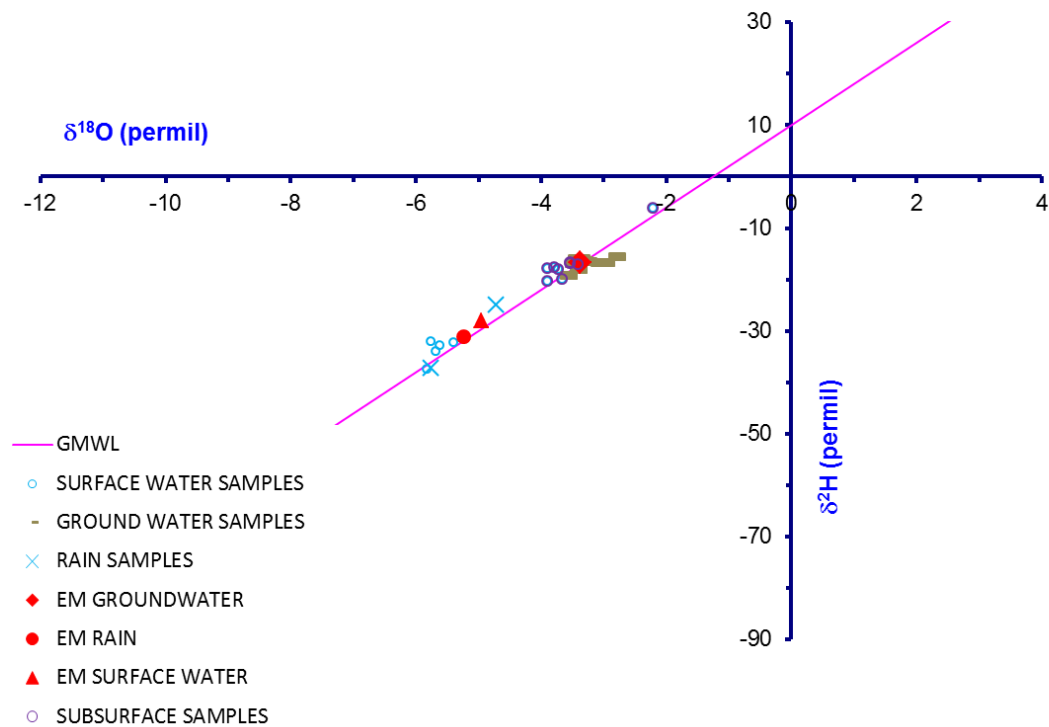


Figure 5.8: Isotope data for samples collected following the January 19, 2013 rainfall event at the 3rd order catchment of Southern Granites study site.

To verify interpolated estimations, two-component hydrograph separations were also done by solving mass balance equations for water and tracers (Sklash and Farvolden, 1979; Uhlenbrook and Hoeg, 2003). The analysis was done using $\delta^{18}\text{O}$, EC and Si as tracers. Isotopic ($\delta^{18}\text{O}$) results for Event 1 showed an overall event water contribution of 84% while pre-event contribution was estimated at 16% (Figure 5.9). The progression of the rising limb of the hydrograph showed domination of event water contribution reaching 93% at peakflow. Thirty minutes into recession the storm runoff comprised 100% event water which thereafter gradually dropped to 75% before flows subsided. Conversely pre-event contribution decreased from 51% to 7% at peakflow and then further dropped to 0% thirty minutes into the recession limb. Thereafter, a gradual increase was noticed until it reached 25% before flow subsidence. The fact that the onset of streamflow was marked by a significant 51% of pre-event water emphasizes the importance of antecedent soil moisture conditions for runoff generation in this catchment. Wet antecedent conditions marked by high soil moisture

exceeding storage thresholds activate subsurface flow on hillslopes resulting in lateral contribution to runoff (Penna et al., 2011). Overall results with silica as a tracer tallied with isotopes at 84% (event water) and 16% (pre-event water), while EC values for the same water sources were 86% and 14%, respectively. Result details for silica and EC are presented in Appendix IV.b.

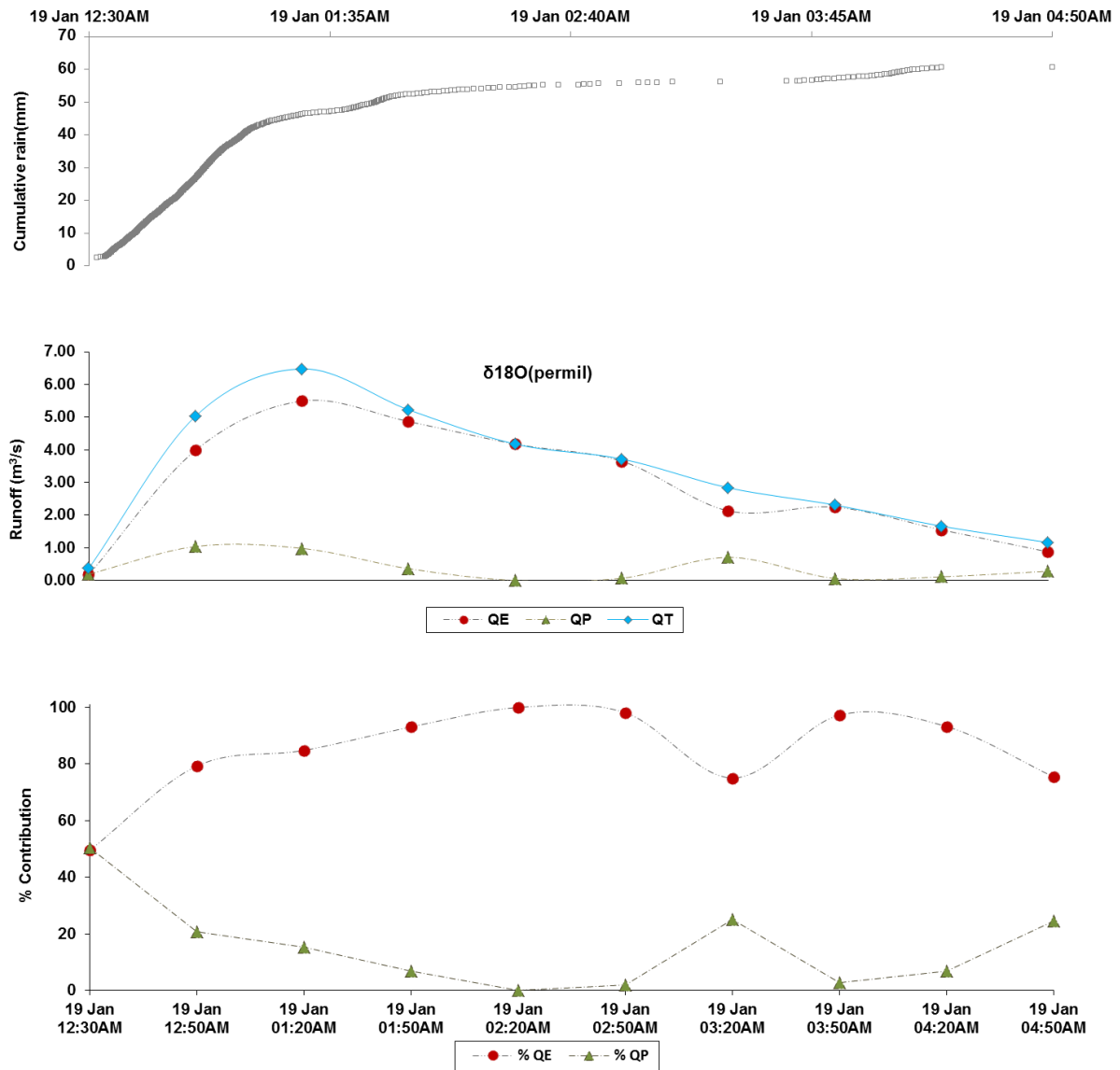


Figure 5.9 Two component hydrograph separation for Event 1 (January 19, 2013) at the 3rd order of Southern Granites showing rainfall, component and total stream runoff, and percentage contributions of event and pre-event water to total runoff. QT = total runoff; QE = Event water contribution; QP = Pre-event water contribution; %QE and %QP = percentage contributions of event and pre-event water, respectively.

5.4.2 Event 1 (19 January 2013) at Southern Granites 1st and 2nd Order Reaches (SGR1 & SGR2)

Mass balance equations for tracers ($\delta^{18}\text{O}$ and EC) and water were solved to determine contributions of different water sources to total runoff. As was observed at the third order catchment, event water also dominated lower order streamflow hydrographs (Figure 5.10). At SGR1 event water contribution was estimated at 71% and 67% using EC and $\delta^{18}\text{O}$, respectively. Respective estimations of the contribution of event water using EC and $\delta^{18}\text{O}$ at SGR2 were 76% and 70%. It is noteworthy that the percentage contribution of event water is incremental with catchment size. The estimated event water contributions are higher across scales thereby supporting and verifying hydrometric findings which showed that streamflows at Southern Granites are purely intermittent and event-driven. On the other hand, an inverse trend exists for pre-event water whose contribution decreases towards higher order reaches (SGR1: EC = 29%, $\delta^{18}\text{O}$ = 33%; SGR2 EC = 24%, $\delta^{18}\text{O}$ = 30%; SGR3 EC= 14, $\delta^{18}\text{O}$ = 16). The highest pre-event water contribution at SGR1 relative to higher order reaches further supports that this reach is gaining from groundwater.

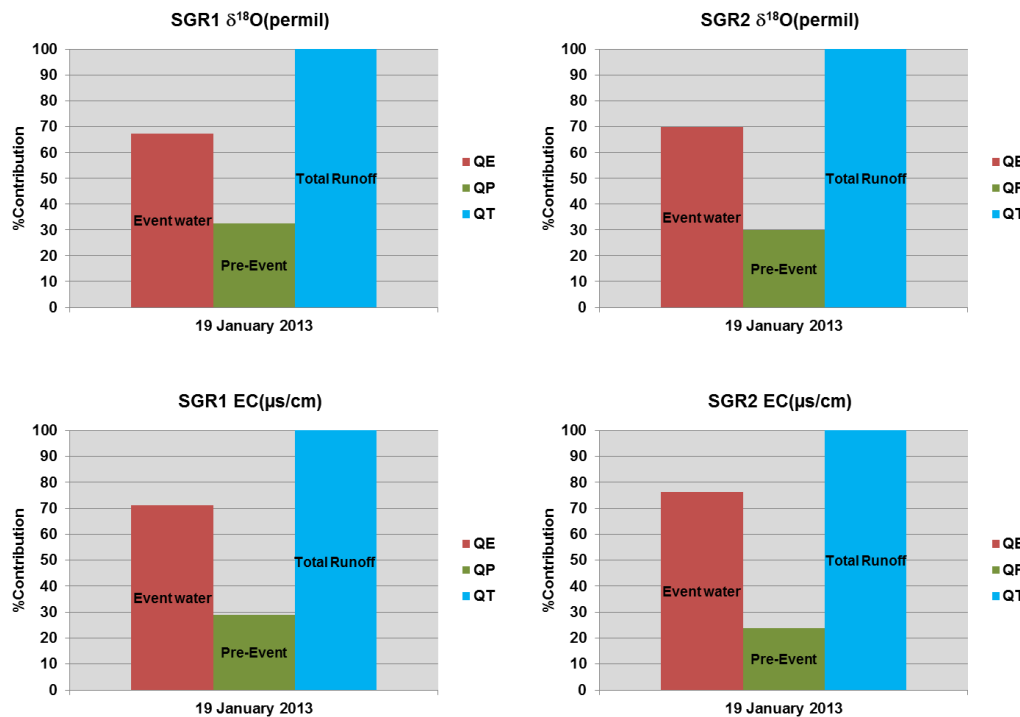


Figure 5.10: Contribution of event and pre-event water to total runoff at SGR1 & SGR2 reaches at Southern Granites using $\delta^{18}\text{O}$ and EC as tracers for the event of 19 January 2013.

5.4.3 Event 2 (20 February 2013) at Southern Granites 3rd Order Reach (SGR3)

The volume averaged end members for Event 2 were set at -1.53, -2.14 and -3.10 for rain, runoff and groundwater samples, respectively (Figure 5.11). Respective interpolated estimates for event water and pre-event water contributions to total runoff were 64% and 36%. The significance of event water contribution to streamflow was further supported.

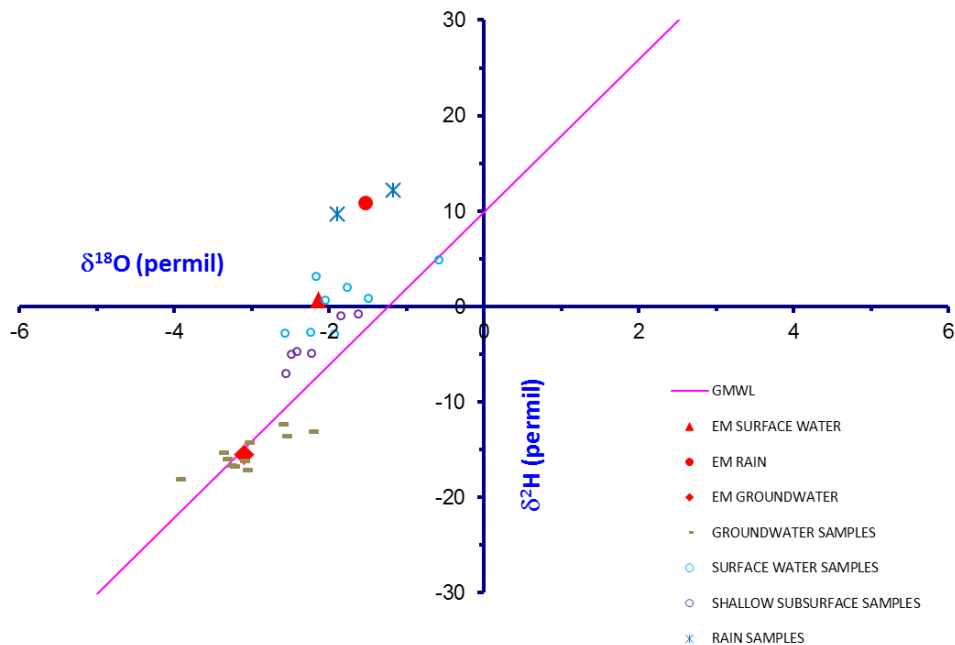


Figure 5.11 Isotope data for samples collected following the February 20, 2013 rainfall event at the 3rd order reach of Southern Granites study site. EM =End Member; GMWL = Global Meteoric Water Line.

To further verify the above observations, a two component hydrograph separation using mass balance calculations for water and $\delta^{18}\text{O}$ as tracer were conducted for Event 2 (Figure 5.12). Overall event water contribution was estimated at 75%, while pre-event contribution constituted 25%.

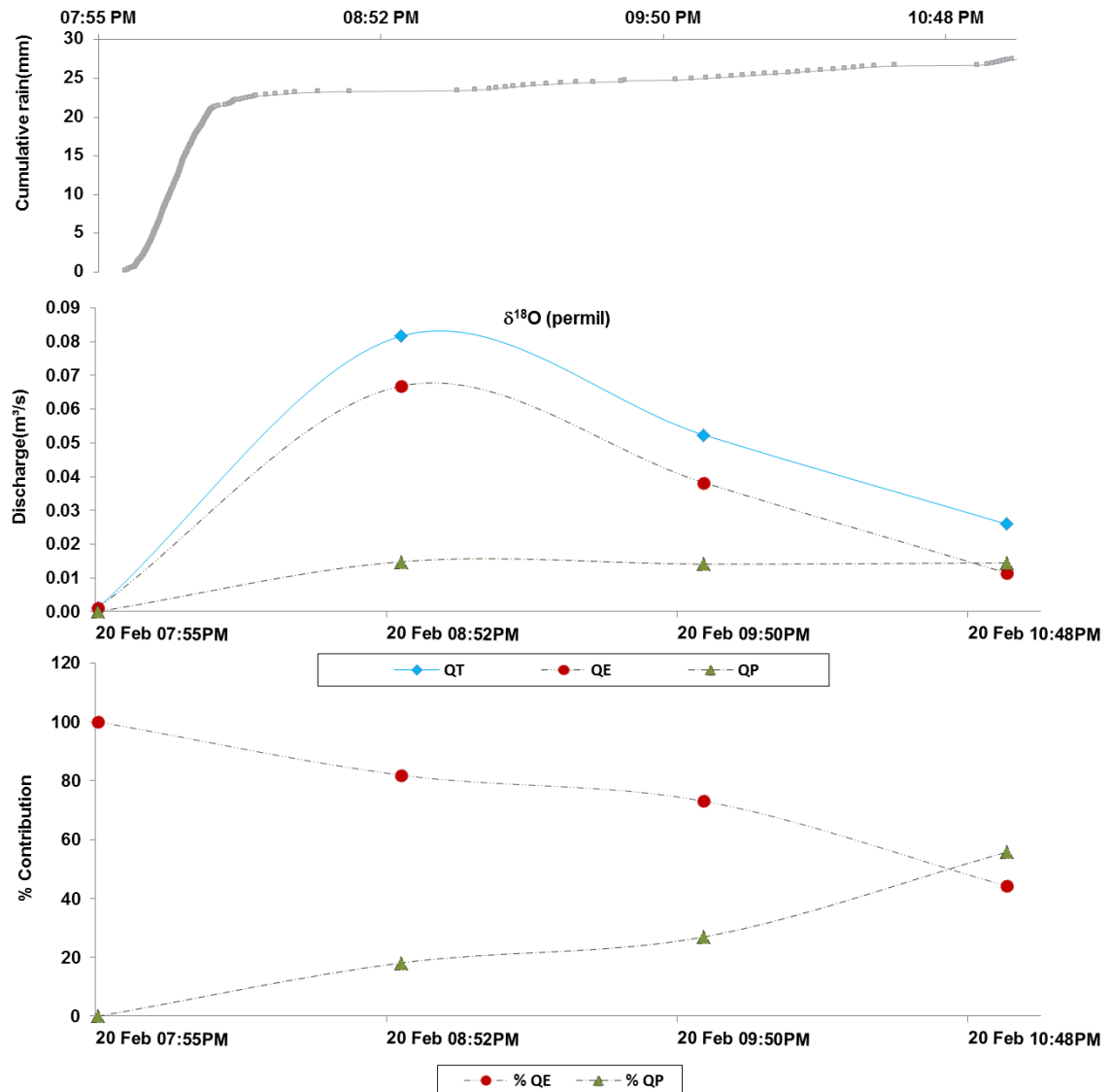


Figure 5.12 Two component hydrograph separation for Event 2 (February 20, 2013) at the 3rd order of Southern Granites showing rainfall, component and total stream discharge, and percentage contributions of event and pre-event water to the stream. QT = Total streamflow; QE = Event discharge; QP = Pre-event discharge; %QE and %QP = percentage contributions of event and pre-event water respectively.

5.4.4 Event 2 (20 February 2013) at Southern Granites 1st and 2nd Order Reaches (SGR1 & SGR2)

Two-component hydrograph separations for this event similarly confirm the dominance of event water in total streamflow at this study site. Using $\delta^{18}\text{O}$ as tracer, event water contributions at SGR1 and SGR2 were estimated at 64% and 60%, respectively, with

corresponding 36% and 40% for pre-event water (Figure 5.13). The increasing trend of event water contributions noted during Event 1 is not repeated in Event 2. The size of the event is a probable explanation to the contrasting observations. In terms of magnitude, Event 1 (95.7mm) was more than three times the size of Event 2 (27.9mm), although the latter was more intense than the former (See section 5.3, this chapter). Looking at these figures suggests that though rainfall intensity is necessary for stream network connectivity, it is the volume of rainfall event that determines the extent of pre-event water contribution to total runoff. Larger and more intense rainfall events result in higher event-water percentage contribution to streamflow than smaller events.

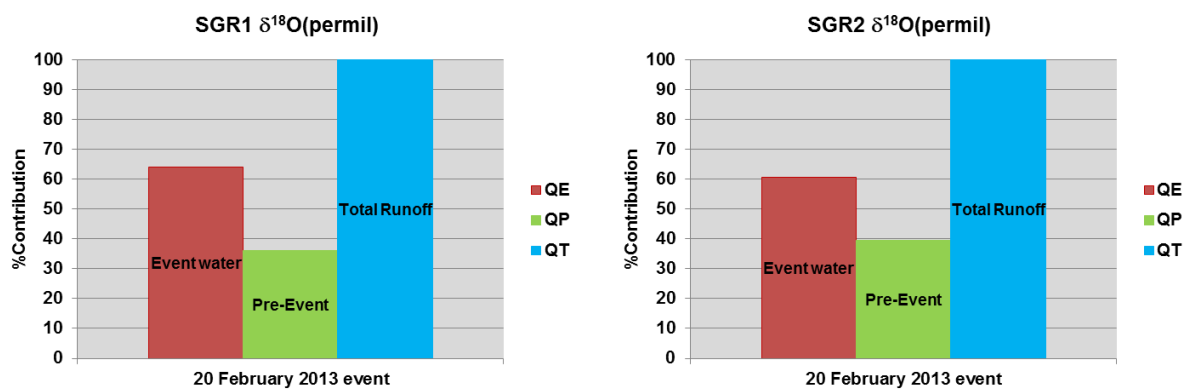


Figure 5.13: Contribution of event and pre-event water to total runoff using $\delta^{18}\text{O}$ as tracer for the event of 20 February 2013 for SGR1 and SGR2 at Southern Granites site.

5.4.5 Three component hydrograph separation at Southern Granites 1st order reach for the 19th of January 2013 rainfall event.

After the contribution of groundwater at SGR1 was tested through hydrometry and tracers (refer to chapter 4 section 4.2.2 and section 5.2 this chapter), the partitioning of stream runoff into three components was conducted. Mass balance equations for two tracers (EC and $\delta^{18}\text{O}$) and water were solved for incident rain, groundwater and subsurface water as components to total runoff (Figure 5.14). Incident rain was estimated at 34% while subsurface and groundwater, were estimated at 40% and 26% respectively. The three component hydrograph separation revealed that the high event water contribution (67% with $\delta^{18}\text{O}$ as tracer) obtained in the two component separation for this reach and event comprised a significant amount of rapid response subsurface flow in addition to the 34% direct channel precipitation. The

connecting mechanism for the rapid response subsurface flow to the stream was clearly through near-surface macropores created for instance, by tree roots and animal burrows in this catchment. These macropores allowed the subsurface water to quickly reach the stream while still retaining similar or very close chemistry to that of the incident rainfall.

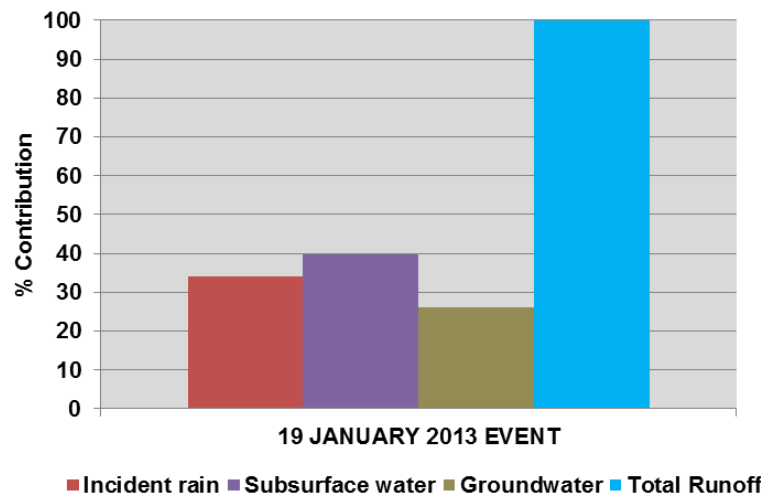


Figure 5.14 Three component hydrograph separation at the 1st order reach (SGR1) of Southern Granites study site for the 19 January 2013 rainfall event.

5.5 Stream Network Connectivity at Southern Granites

The fact that stream network connectivity is event-driven was revealed by time series plots of rainfall and discharge across spatial scales that are based on stream orders (Chapter 4). However, contributions of tributaries draining into the main channel at incremental subcatchments during events were not known. End member mixing analysis (EMMA) using mass balances for water and tracer were calculated to quantify these contributions. The results are presented in Table 5.7 while calculation details are presented in Appendix V.

Table 5.6: Estimated tributary runoff and corresponding percentage contributions to the main channel flows at Southern Granites on the 19th of January and 20th of February 2013. Discharges in brackets were observed at gauging stations.

Subcatchment	Reach	19 JANUARY 2013		20 FEBRUARY 2013	
		Mean Runoff (m ³ /s)	Contribution (%)	Mean Runoff (m ³ /s)	Contribution (%)
SGR1	SGR1Q (main channel)	(0.0218)	10	(0.0126)	11
	SGR1 Tributary	0.1963	90	2.8146	89
	SGR1 Confluence	0.2182	(Total) 100	3.1624	(Total) 100
SGR2	SGR2Q (main channel)	(0.1302)	97	(0.00078)	78
	SGR2 Tributary	0.0040	3	0.00022	22
	SGR2 Confluence	0.1342	(Total) 100	0.00012	(Total) 100
SGR3	SGR3Q (main channel)	(0.6688)	40	(0.0562)	30
	SGR3 Tributary	1.0000	60	0.0856	70
	SGR3 Confluence	1.6700	(Total) 100	0.1223	(Total) 100

The presence of flows at all scales in tributaries and the main channel supports that stream network connectivity occurs during rainfall events. Runoff at gauging stations show incremental change with increasing contributing areas on the 19th of January 2013 (Table 5.7). However, on 20 February 2013, a reduction of runoff (0.6%) is recorded at SGR2 relative to SGR1. This is attributed to transmission losses at SGR2 details of which have already been presented in earlier sections such as Chapter 4, section 4.2). The large size of the 19 January event (95.7mm) initially masked transmission losses at SGR2 at least during

the event itself which however, manifest through rapid recession as already explained. The third order reach (SGR3) shows a 1.39% increase in discharge possibly due to its larger contributing area with more tributary inflows and less transmission losses relative to SGR2.

5.6 Event 1(19 January 2013) at Southern Basalts 3rd Order Reach (SBAS3)

Surface water isotope values were closer to the rain concentration than groundwater, indicating greater event water contribution to stream runoff at the SBAS3 reach (Figure 5.15). Linear interpolation between end members estimated the contribution of event water at 63% with the remaining 37% being pre-event contribution. Mass balance calculations for a two component hydrograph separation estimated this component at 62% and 60% using $\delta^{18}\text{O}$ and EC, respectively (Figure 5.16). These results clearly show that event water is the dominant component in total stream runoff at this reach. Pre-event water contributions estimated at 37% (lumped isotopes technique) as well as 38% and 40% using mass balance calculations for water and tracer ($\delta^{18}\text{O}$ and EC) are evidence of groundwater draining into the stream. Accordingly, the topographic constraints (very low hillslope gradients, approximately 1.4% across all scales) coupled with low aquifer transmissivity, supports that localised fractured rock preferential flow is the dominant groundwater flowpath feeding the stream as originally hypothesized.

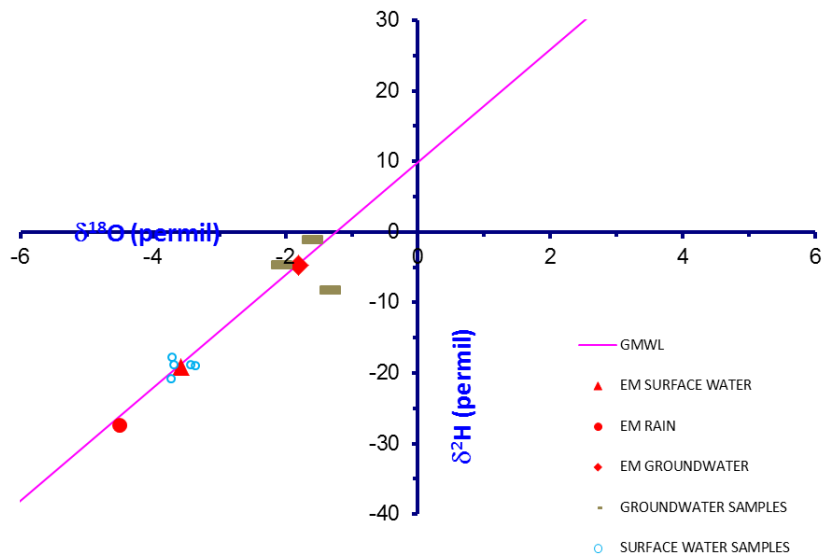


Figure 5.15 Isotope data for samples collected following the January 19, 2013 rainfall event at the 3rd order catchment of Southern Basalts study site. EM =End Member; GMWL = Global Meteoric Water Line.

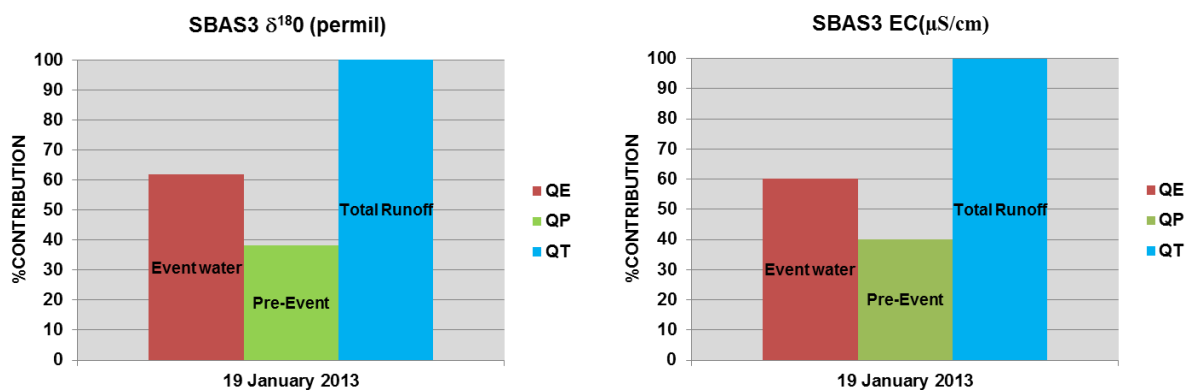


Figure 5.16: Percentage contribution of event and pre-event water to total runoff using $\delta^{18}\text{O}$ and EC as tracers for the event of 19 January 2013 at SBAS3 reach of Southern Basalts site.

5.7 Event 2 (20 February 2013) at Southern Basalts 3rd order reach (SBAS3)

Event water contribution which is the dominant component was estimated at 64% using linear interpolation between end members (Figure 5.17). Mass balance calculations for a two

component hydrograph separation estimated event water contribution at 51% and 60% using $\delta^{18}\text{O}$ and EC, respectively (Figure 5.18).

There is not much difference in event water contribution estimates for both events (Event 1 in January and Event 2 in February 2013) at this catchment. Considerable proportions of pre-event water (49% and 40% for $\delta^{18}\text{O}$ and EC, respectively) further support that significant groundwater drains into the stream through localised fracture flow at this reach.

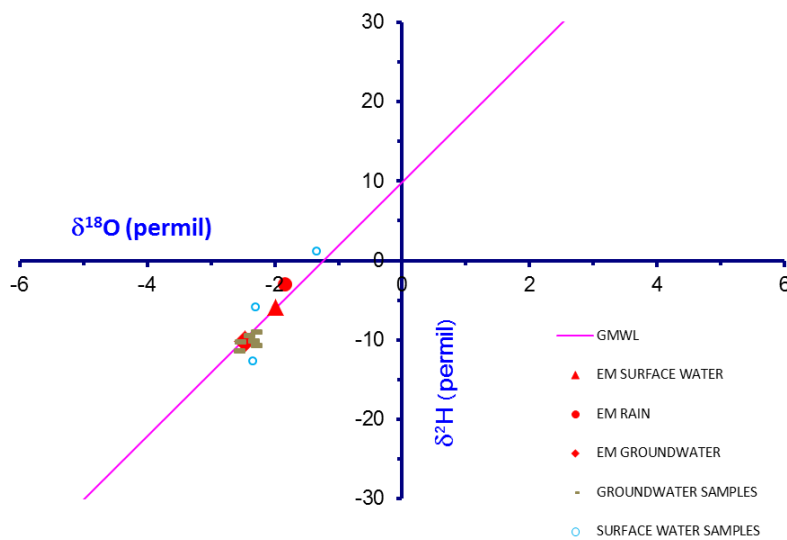


Figure 5.17 Isotope data for samples collected following the February 20, 2013 rainfall event at the 3rd order catchment of Southern Basalts study site. EM =End Member; GMWL = Global Meteoric Water Line.

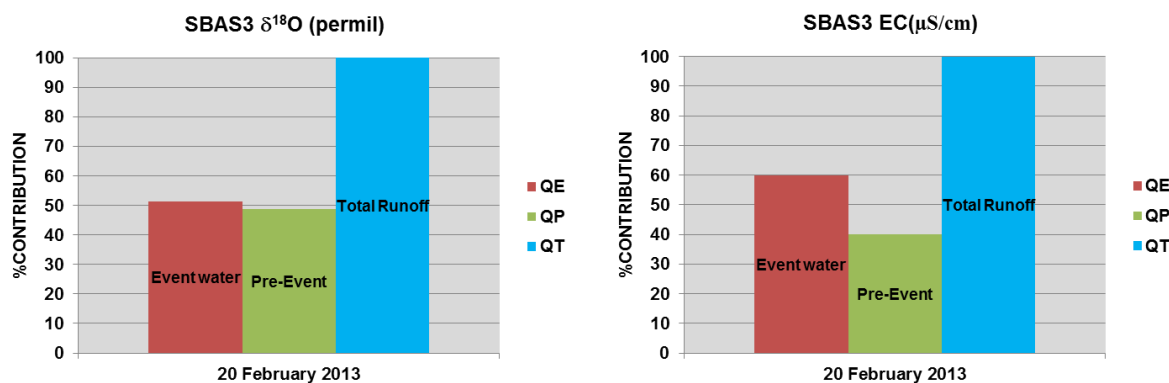


Figure 5.18: Percentage contribution of event and pre-event water to total runoff using $\delta^{18}\text{O}$ and EC as tracers for the event of 20 February 2013 at Southern Basalts study site.

5.8 Results and Discussion of Electrical Resistivity Tomography (ERT) as Supplementary Data for Further Insight into Hydrological Connectivity

A near-surface hard rock intrusion (high electrical resistance material, $>1000 \Omega\cdot\text{m}$) between the 2nd and 3rd order reaches is observed as a likely geological control that retards streamflow velocity, hence, stream power for effective sediment transport downstream (Figure 5.19). This might be the reason for massive sediment deposition physically observed along the 3rd order (SGR3) reach in contrast to predominantly erosive lower order reaches. The base level geomorphic control retards upstream surface water flows, promoting increased infiltration losses at the outlet of SGR2. This occurs with possible groundwater recharge as evidenced by the 2nd order 28m riparian borehole water level responses and similar tracer signatures for stream and borehole samples, as described in Chapter 4 and in section 5.2 of this chapter.

Low near-surface resistivity values (between 3 and 8 $\Omega\cdot\text{m}$) were recorded from ERT surveys conducted during the wetter period of February 2013, at SGR1 reach (Figure 5.19). This was consistent with physical field observations where a seasonal wetland adjacent to the SGR1 reach was visibly waterlogged indicating saturated soil conditions (See Figure 4.3A in Chapter 4). This provides further confirmation of the perched groundwater contribution to the stream that traverses the hillslope as soil bedrock interflow and culminates into saturation overland flow at the break of slope in the riparian zone.

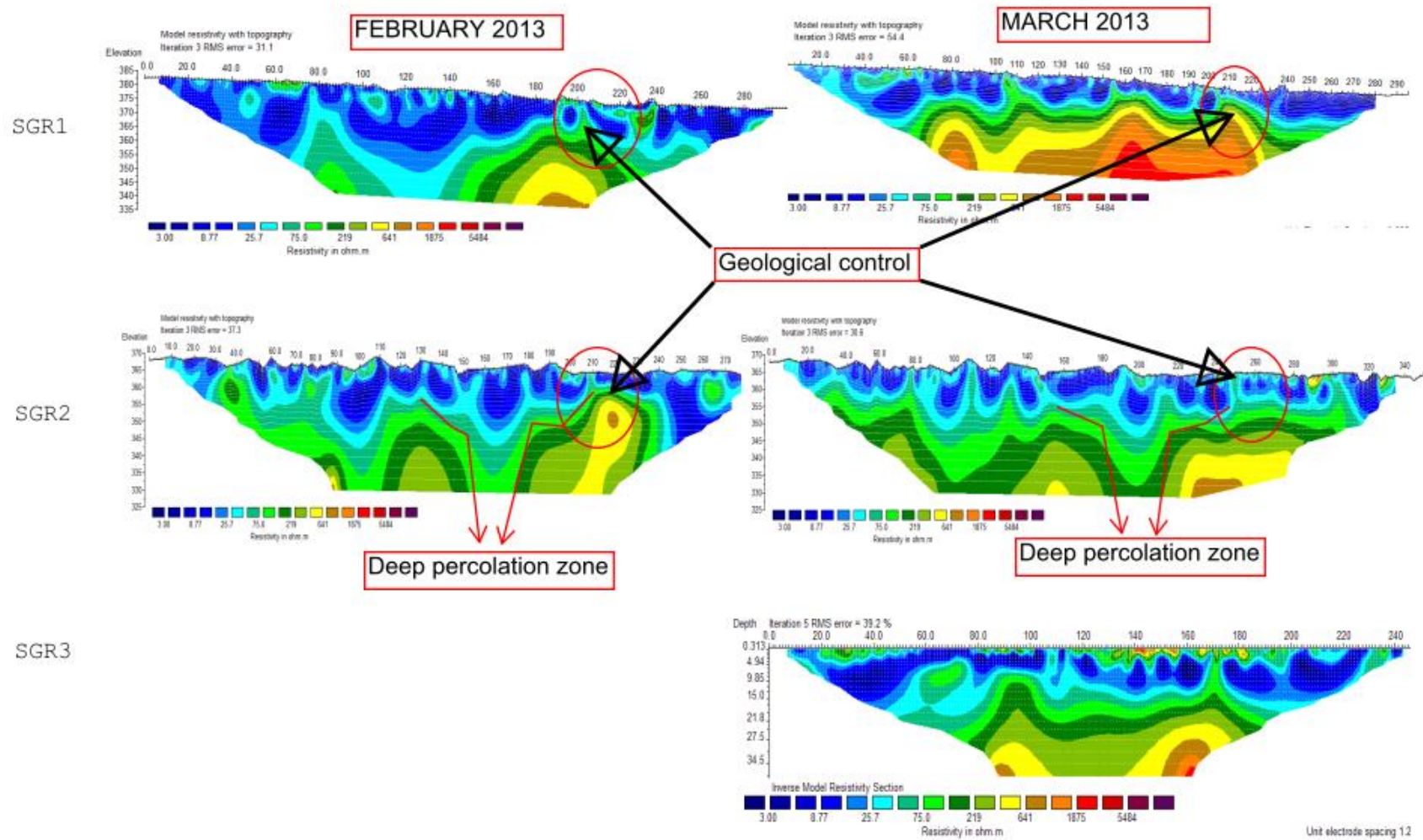


Figure 5.19: ERT for 1st to 3rd order reaches for February and March 2013 at Southern Granites study site

CHAPTER 6: SYNTHESIS

6.1 Introduction

The key objective of this study was to understand and quantify interactions existing between the stream and groundwater sources across spatial and temporal scales in the study sites. The corollary of addressing the aforementioned objective was the definition of connecting mechanisms between groundwater and stream domains and how these are controlled by the geological setting.

6.2 Conceptual understanding of hydrological connectivity at Southern Granites

Borehole and stream data coupled with tracers ($\delta^{18}\text{O}$, EC and silica) demonstrated that the headwater subcatchment (SGR1) is gaining from groundwater. This occurs following the development of a perched water table within the weathered rock aquifer that triggers fluxes downslope as weathered zone interflow towards the stream. Slope decline at the footslope causes interflow water to emerge into an adjacent wetland that drains into the stream through saturation overland flow. Low resistivity values in ERT profiles are evidence of soil saturation at this point (refer to Chapter 5, Figure 5.18). This is consistent with field observations in the months of February and March 2013 when the wetland was fully waterlogged. The 2nd order (SGR2) was clearly portrayed to be a losing reach which was demonstrated by hydrometry and tracers as an indirect groundwater recharge point. Based on the aforementioned findings, the original hypothesis that SGR2 reach is gaining was rejected and a new conceptual understanding that this reach is losing was embraced. This reach experiences minimal subsurface gain during intense rainfall events that raise subsurface riparian hydraulic heads as observed in a riparian piezometer which was always dry but had water after the high intensity event (61.3mm in 15minutes) on the 19th of January 2013. Geophysical surveys revealed a geological base level control at the SGR2/SGR3 transition in the form of a bedrock outcrop. This consistently verifies field observations of massive sediment trapping that has induced localised discontinuity of sediment and surface water transfer to downstream reaches. Trapped sediment barricades surface flows and coupled with high hydraulic conductivities (mean 1054mm/h) at this reach, deep percolation occurs

possibly to recharge groundwater, if the preceding event exceeds a recharge threshold of approximately 95-100mm. Findings have also shown the 3rd order (SGR3) at Southern Granites as a predominantly losing reach between rainfall events with evidence of continuous negative hydraulic gradients between boreholes and stream water levels). Limited interflow occurs at SGR3 due to a low gradient floodplain which is largely decoupled from the hillslope. The conceptual understanding across the three spatial scales is summarised in Figure 6.1.

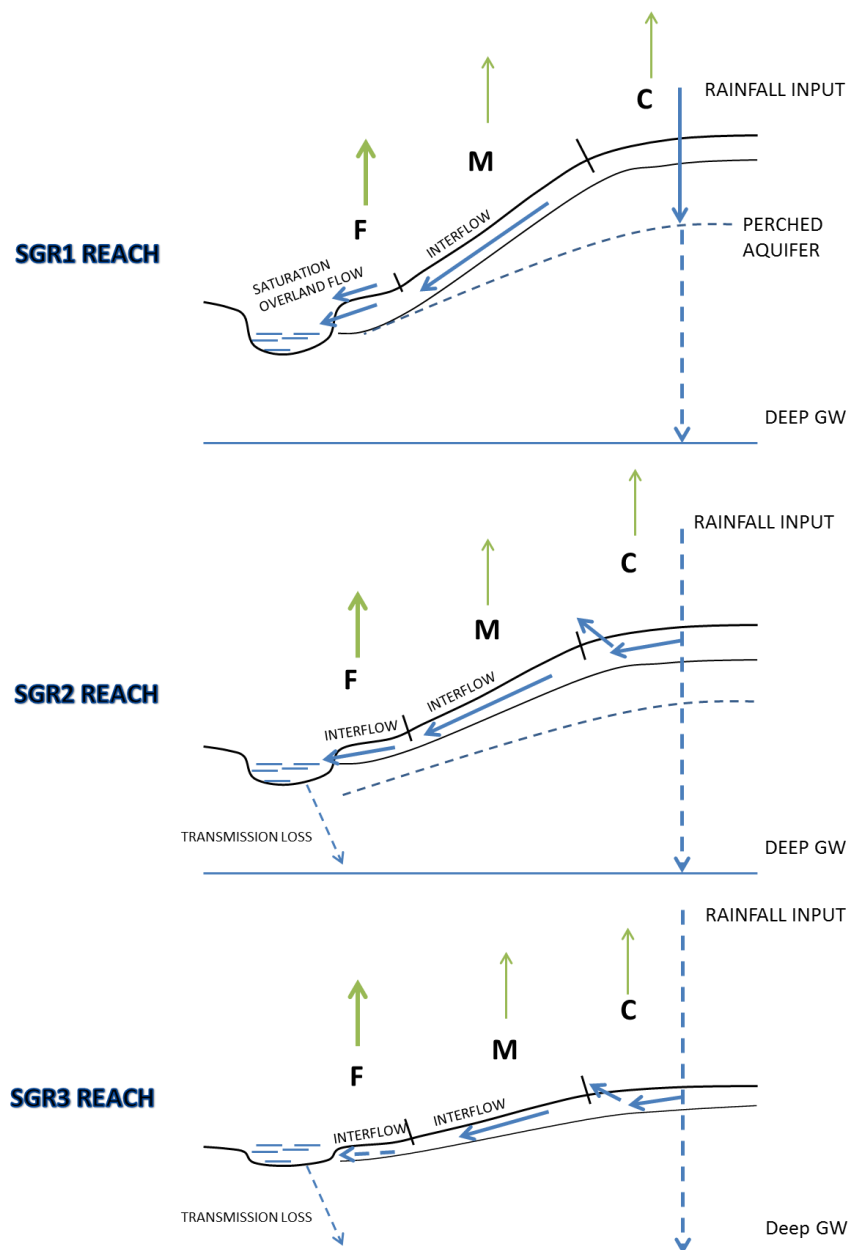


Figure 6.1 Conceptual hydrological connectivity at Southern Granites study site for 1st to 3rd order reaches. (F = footslope; M = Midslope and C = Crest. Dashed arrows show processes of limited extent, green arrows represent evapotranspiration).

6.3 Quantification of Water Sources Contributing to Streamflow at Southern Granites

- **Two component hydrograph separation**

Two component hydrograph separations using $\delta^{18}\text{O}$, EC and silica revealed the dominance of event water contribution to total runoff ranging from 67 to 86% across scales at Stevenson Hamilton site. The proportion of event water contribution increased with increasing catchment size. This is probably explained by increasing proportions of lowly permeable areas towards higher orders that promote greater proportions of quickflow, especially given high intensity events. One significant form of the lowly permeable areas at Southern Granites is sodic sites. Sodium ions (Na^+) in these sites cause a spread out of soil colloids which clog soil pores (McCauley and Jones, 2005), effectively reducing the soil's water permeability. This is consistent with soil surveys in this catchment where 5% of sodium was determined to significantly result in low soil permeability (Le Roux et al., 2013). Clay plugs of various depths ranging from 10 to 20cm in the streambed alluvium were also observed in the 3rd order floodplain during the installation of streambed piezometers. This was also supported by a relatively low mean hydraulic conductivity of 12mm/h at SGR3 reach compared to 2449mm/h and 1054mm/h at the 1st and 2nd order reaches, respectively (Refer to Appendix II.b). Also contributing to increasing event water contribution at Southern Granites are the fairly small catchment areas (0.3km², 0.9km² and 1.5km²) coupled with steeper slopes (3.2%; 2.1% and 1.8%) for 1st to 3rd order, respectively. These smaller catchment areas and steeper slopes reduce times of concentration and event water quickly reaches subcatchment outlets, cumulatively towards the 3rd order.

Higher rainfall event water contributions were observed in other studies conducted around the world which include 80% in Bonell et al. (1998); 70 to 87.5% in McCartney et al. (1998); 62% in Brown et al. (1999); 74% in Shanley et al. (2002) and 73 to 93% of QE, in Riddell et al. (2013). These studies were conducted in catchments that included headwaters and/or wetlands and/or where soils were compacted either naturally or by human activities. Of particular interest is the study by Shanley et al., (2002) in which event water contributions were observed to increase with catchment size, a phenomenon synonymous with the current

study. Shanley et al., (2002) ascribed that trend to topographically controlled increments of surface-saturated areas with increasing catchment size, in addition to increasing agriculturally compacted soils and decreasing soil transmissivity with increasing spatial scale in their study areas. Another study which found increasing proportions of event water with scale was that by McDonnell et al., (1999), even though their findings showed more pre-event contribution than the event water component. They explained their observations in the light of large proportions of valley floor saturated areas with scale which directly partitioned event water inputs into the stream through saturated overland flow as the connecting mechanism. From various research studies the effect of scale on component contributions to total runoff seems to be variable governed by different physiographic settings of study areas. For instance a study by Brown et al., (1999) found that event water contribution was inversely related to catchment size while McGlynn et al., (2004) observed no clear relationship of event water with catchment size.

▪ **Three component hydrograph separation**

The three component hydrograph separation conducted at SGR1 revealed that event water contributing to total runoff included a significant amount of rapid response subsurface flow estimated at 40%. Near-surface macropore flow generated by plant roots and animal burrows was determined as the dominant connecting mechanism contributing 33% of the rapid response subsurface flow in addition to 7% of perceived groundwater return flow. Incident precipitation estimated at 34% represented direct channel precipitation, which when coupled to the macropore flow fraction of the subsurface component would constitute the event water contribution determined by two component hydrograph separation at this SGR1 reach. This finding is consistent with earlier studies elsewhere (e.g. Pilgrim et al., 1979; Leaney et al., 1993; Mulholland, 1993; Klaus et al., 2013) which demonstrated that new water that ends up in streams can be a mixture of direct channel precipitation and rapid response subsurface flow. Mulholland (1993) demonstrated with calcium (Ca) and sulphate (SO₄) as tracers the development of perched water tables in response to large rainfall events which resulted in rapid response subsurface flow via macropores to the stream. This observation is typical of what hydrometry and tracer analysis revealed at Southern Granites 1st order reach in this

study. Using deuterium and chloride, Leaney et al. (1993) found that the signature of these tracers in subsurface flow resembled that of rainfall rather than soil water for all monitored rainfall events and a well-developed network of macropores was determined to be the connecting mechanism. Klaus et al. 2013 assert that subsurface preferential flow can be a direct reflection of new or event water.

6.4 Conceptual Understanding of Hydrological Connectivity at Southern Basalts 3rd Order Reach

Borehole and stream hydrometry, and tracer analysis provided a conceptual understanding that event streamflows at the 3rd order reach reflect localised fractured rock preferential flow contributions. As already explained, very low interfluvial gradients, dry footslope piezometers and close to zero hydraulic conductivities (Le Roux et al., 2011) indicated very limited to no subsurface contributions to streamflow at this reach. However, limited toeslope overland flow possibly occurs since toeslopes are generally defined at this reach. This conceptual understanding is summarised in Figure 6.2.

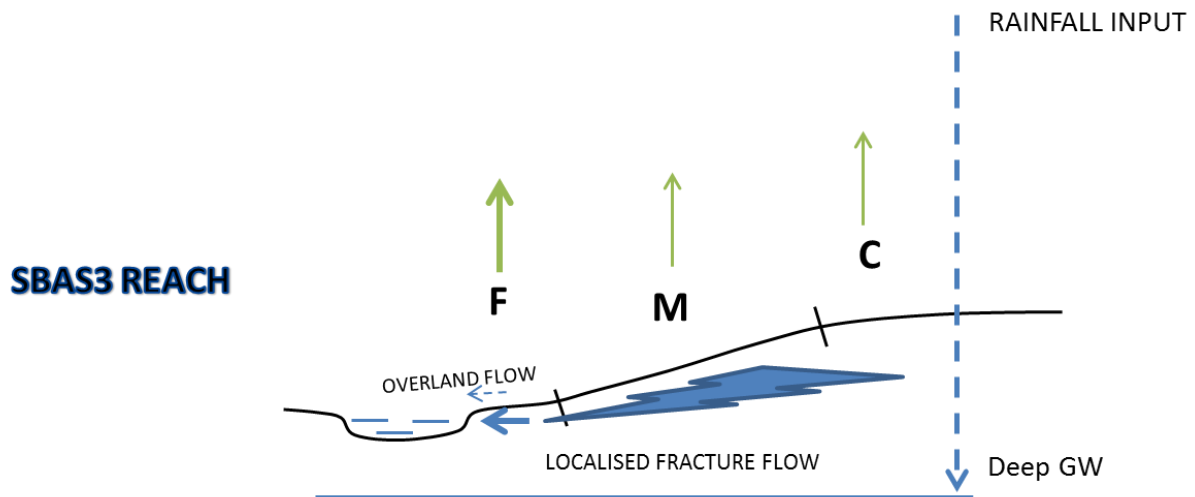


Figure 6.2 Conceptual hydrological connectivity at Southern Basalts study site for the 3rd Order reach. (F = footslope; M = Midslope and C = Crest. Dashed arrows show processes of limited extent, green arrows represent evapotranspiration).

6.5 Quantification of Water Sources Contributing to Streamflow at Southern Basalts 3rd Order Reach

Event water contribution was shown to be dominant at SBAS3 estimated within the range of 51% to 64% using $\delta^{18}\text{O}$ and EC as tracers. High event water contribution is attributed to low soil transmissivities which promote quickflow and inhibit infiltration. Rainfall intensity which is essential for connected runoff generation also influences high event water contribution to total runoff in this catchment. It was however, noted with interest that the proportions of pre-event water is considerable ranging from 36% to 49%. This should be the result of antecedent soil moisture conditions (represented by API-7) which was demonstrated to be important for runoff generation at this reach.

6.6 Limitations of the study

- Rain samples in this study were collected at a place 10km from site for Southern Granites and 12km away from site for the Southern Basalts site due to logistical constraints. However, research (Abiye et al., 2013) has shown that mean rainfall isotopic ($\delta^{18}\text{O}$) distribution is uniform across the KNP region despite possible local rain-out effects.
- Bulk rain samplers were used hence variability of isotopic and hydrochemical signatures over rainstorms were not captured.
- An over reliance on grab samples taken after rainfall events was a source of uncertainty in quantified component contributions.
- No plume tests and digging of trenches could be conducted to get further insight in flow paths and residence times due to the need to preserve the park environment in its natural condition as a fundamental management principle that guides research work in the Kruger National Park.
- Spatial scales were limited to 3rd order catchments while temporal scales were over event based time scales only. Therefore, seasonal and inter-annual variability of hydrological responses were not assessed.

6.7 Conclusions

Within the context of the current study (across 3rd order catchments and event based time scales) determination and quantification of hydrologic connectivity between groundwater and streams were successful. Connecting mechanisms were identified in addition to drivers and controls of hydrologic interactions across specified spatio-temporal scales. The results revealed the importance of headwater catchments as important sources of water for higher order streams at Southern Granites. The fact that considerable transmission losses were noted beginning right from the 2nd order, implies that these lower order catchments contribute to the sustenance of baseflow for higher order and/or perennial rivers. This observation is corroborated by earlier research (Petersen, 2012) which demonstrated that ephemeral streams, Nwaswitsontso for instance, on the granitic geology in KNP are dominant indirect recharge areas whose water emerges at perennial river basin outflows. This has major implications for water resources management within the park and elsewhere with respect to groundwater abstraction policies. Informed management of the groundwater resource in ephemeral catchments is crucial for sustained environmental flows in downstream reaches given the conjunctive nature of surface and groundwater resources upstream and downstream of river channels demonstrated by the current study. Particular reference of unregulated groundwater pumping in areas outside and to the west of KNP could affect environmental flows in the park, especially given the situation that most major rivers flowing through the park originate outside park boundaries from the Drakensburg escarpment. The implication would be reduced downstream flows below prescribed levels for the sustenance of flora and fauna which ensure provision of ecosystem and goods and services. For instance, abstraction of groundwater from Bushbuckridge, Hazyview and further up the Drakensburg escarpment could reduce baseflow in higher order rivers resulting in negative implications for aquatic life and riparian terrestrial ecosystems that are supported by these rivers, especially during low flow periods. Natural abstraction, for instance through extreme temperatures as impacts of global climate change, could severely alter the hydrological function of these ephemeral streams, especially if coupled with the aforementioned anthropogenic activities.

Since water conveys solutes between connected process domains, sustainable water resources management should prioritise quality in addition to quantity considerations. Unregulated human activities that release pollutant substances within losing streams could result in

groundwater contamination through channel leakage to baseflow. Given that groundwater does not recycle readily its contamination could mean prolonged deprivation (Sophocleous, 2002) especially in arid and semi-arid areas where groundwater may be the principal source of drinking water. Similarly, contaminated groundwater inflow to gaining streams can reduce the quality of surface water with disastrous consequences such as death of aquatic life. The reduction of water quantity and quality also occurs if surface water use policies in connected stream networks are not enforced. Unregulated surface water abstraction in upstream reaches, for instance through irrigation, can reduce water quantity supplied to downstream users. In the same way, upstream pollutants are easily conveyed to downstream reaches within connected stream networks.

6.8 Recommendations

Given the limited spatial and temporal scales at which this study was conducted further research is recommended where spatial upscaling (beyond the 3rd order) is recommended. This can provide a holistic understanding at broader scales which could be useful in developing macroscale theories and laws as advocated by Dooge (1986) for prediction in ungauged basins (PUB). Longer-term monitoring involving quantification of ET could be pursued in future research endeavours to capture seasonal and inter-annual signatures of hydrologic connectivity. In addition to the spectrum of disciplines (Hydrology, geohydrology and pedology), that were integrated in the current study incorporating other disciplines such as ecology is recommended for future research where vegetation distribution and structure are used as indicators of hydrologic function to gain further insight into process connectivity (Rodriguez-Iturbe, 2000). This will expand acquired knowledge of process linkages to the ecological functioning of catchments which helps to establish interactive patterns and similarities that could lead to the development of a generic classification framework at broader scales for prediction in ungauged basins (Bloschl and Sivapalan, 2013).

Further research to quantify water transit times using tracer based transit time distributions is also recommended. Transit times are fundamental catchment descriptors that reveal more information about the storage, flow paths and sources of water (McDonnell et al., 2010).

Therefore, this could prove useful to inductively inform hydrological model development and application thus limiting the assumptions of hypothetico-deductive modelling approaches and associated uncertainties that characterise them (Young et al., 2004).

More detailed understanding could possibly be obtained by making use of sequential rain samplers on site as well as automatic incremental streamflow samplers, in order to capture real time signatures of hydrologic responses across spatio-temporal scales in any future research work within these catchments.

REFERENCES

- Abiye, T, Verhagen, B, Freese, C, Harris, C, Orchard, C, Van Wyk, E, Tredoux, G, Pickles, J, Kollongei, J, Xiao, L, Levin, M, Butler, B, Diamond, R, Grellier, S, Talma, S, Lorentz, S, Chaplot, V, Xu, Y. 2013. The Use of Isotope Hydrology to Characterize and Assess Water Resources in Southern Africa. WRC Report No TT 570/13, School of Geosciences, University of the Witwatersrand, Johannesburg, South Africa.
- Aldridge, BN, and Garrett, JM. 1973. Roughness coefficients for stream channels in Arizona. Open-File Report Number 87, USGS,USA.
- Ali, GA, and Roy, AG. 2009. Revisiting Hydrologic Sampling Strategies for an Accurate Assessment of Hydrologic Connectivity in Humid Temperate Systems. *Geography Compass Journal* Volume 3, Issue 1: 350–374.
- Ambroise, B. 2004. Variable “active” versus “contributing” areas or periods: A necessary distinction. *Hydrological Processes Journal* 18: 1149-1155.
- Arcement, G J, and Schneider, VR. 1984. Guide for Selecting Manning's Roughness Coefficients for Natural Channels and Flood Plains. Water Supply Paper 2339,USGS, .USA.
- Baskaran, S, Ransley, T, Brodie, RS and Baker, P. 2009. Investigating groundwater–river interactions using environmental tracers. *Australian Journal of Earth Sciences* 56, 1: 13-19.
- Baxter, C, Hauer, F R, and Woessner, WW. 2003. Measuring Groundwater–Stream Water Exchange: New Techniques for Installing Minipiezometers and Estimating Hydraulic Conductivity. *Transactions of the American Fisheries Society*,132,(3): 493-502.
- Betz, R, Hitt, NP, Dymond, RL and Heatwole, CD. 2010. A Method for Quantifying Stream Network Topology over Large Geographic Extents. *Journal of Spatial Hydrology* Vol.10, No.1 2010.
- Beven, KJ, and Hornberger, GM. 1982. Assessing the effect of spatial pattern of precipitation in modeling stream flow hydrographs. *Journal of the American Water Resources Association* 18: 823–829.
- Beven KJ, and Germann PF. 1982. Macropores and water flow in soils. *Water Resources Research* 18:1311–1325.
- Bloschl, G, Sivapalan, M, Wagener, T, Viglione, A, and Savenije, H. 2013. A synthesis framework for runoff prediction in ungauged basins. In: eds. Bloschl, G, and Sivapalan, M, *Runoff Prediction in Ungauged Basins*. Cambridge University Press. Cambridge, UK.
- Blume, T, Zehe, E and Bronstert, A. 2010. Rainfall-runoff response, event-based runoff coefficients and hydrograph separation. *Hydrological Sciences Journal* 52, (5): 843-862.
- Bohte, R, Mul, ML, Bogaard, TA, Savenije, HHG, Uhlenbrook, S, and Kessler TC. 2010. Hydrograph separation and scale dependency of natural tracers in a semi-arid catchment. *Hydrol. Earth Syst. Sci.* 7: 1343–1372
- Bonell, M, Barnes, CJ, Grant, CR, Howard, A. 1998. High rainfall, response-dominated

- catchments: A comparative study of experiments in tropical northeast Queensland with temperate New Zealand. In: eds. McDonnell JJ, Kendall C. *Isotope Tracers in Catchment Hydrology*. Elsevier Science Publishers, Amsterdam, Netherlands.
- Bouwer, H, and Rice, RC. 1976. A Slug Test for Determining Hydraulic Conductivity of Unconfined Aquifers with Completely or Partially Penetrating Wells. *Water Resources Research* 12, 3.
- Bracken, L. and Croke, J. 2007. The concept of hydrological connectivity and its contribution to understanding runoff-dominated geomorphic systems. *Hydrological Processes* 21: 1749-1763.
- Brown, VA, McDonnell, JJ, Burns, DA, and Kendall, C. 1999. The role of event water, a rapid shallow flow component, and catchment size in summer stormflow. *Journal of Hydrology* 217: 171-190.
- Burns, DA, McDonnell, JJ, Hooper, RP, Peters, NE, Freer, 1, Kendall, C and Beven, K. 2001. Quantifying contributions to storm runoff through end-member mixing analysis and hydrologic measurements at the Panola Mountain Research Watershed. *Hydrological Processes* 15: 1903–1924
- Carter, RW, and Davidian, J. 1989. *Techniques of Water Resources Investigations of the United States Geological Survey. General procedure for gauging streams: Applications of Hydraulics*. USGS, USA.
- Cey, EE, Rudolph, DL, Parkin, GW, and Aravena, R. 1998. Quantifying discharge to a small Perennial stream in southern Ontario, Canada. *Journal of Hydrology* 210: 21-37.
- Chow, VT. 1959. *Open Channel Hydraulics*. McGraw-Hill, New York, USA.
- Costa, AC, Foerster, S, De Araújo, JC, and Bronstert, A. 2012. Analysis of channel transmission losses in a dryland river reach in north-eastern Brazil using streamflow series, groundwater level series and multi-temporal satellite data. *Hydrol. Processes* 10,1002: 9243.
- Cowan, WL. 1956. Estimating hydraulic roughness coefficients: *Agricultural Engineering Journal* 377: 473–475.
- Crook, N, Binley, A, Knight, R, Robinson, DA, Zarnetske, J, and Haggerty, R. 2008. Electrical resistivity imaging of the architecture of substream sediments. *Water Resources Research* 44,10: 1029.
- Cullum, C and Rogers, K. 2011. A framework for the classification of drainage networks in Savanna landscapes. Report No TT 498/11. Water Research Commission, Pretoria, RSA.
- Dent, CL, Grimm, NB and Fisher, SG. 2001. Multi-scale Effects of Surface-subsurface Exchange on Stream Water Nutrient Concentrations. *Journal of the North American Benthological Society* 20, 2: 162-181.
- DHV and DELFT . 1999. How to establish stage-discharge rating curves. Hydrology Project Technical Assistance Module: SWDP-29. New Delhi, India.

- Ehret, U, Gupta, HV, Sivapalan, M, Weijs, SV, Schymanski, SJ, Blöschl, G, Gelfan, AN, Harman, C, Kleidon, A, Bogaard, TA, Wang, D, Wagener, T, Scherer, U, Zehe, E, Bierkens, MFP, Baldassarre, GD, Parajka, J, Van Beek, LPH, Van Griensven, A, Westhoff, MC, and Winsemius, HC. 2014. Advancing catchment hydrology to deal with predictions under Change. *Hydrol. Earth Syst. Sci.* 18: 649–671.
- Fundisi, D, Jumbi, F, Van Niekerk, A, Van Zijl, G, Riddell, ES, Nel, J and Lorentz, SA. 2013. Catchment Monitoring to Understand Surface Water, Groundwater and Vadose Zone Interactions in Selected Pristine Catchments in KNP. Unpublished WRC Progress Report 6. K5/2051.CWRR, University of KwaZulu-Natal, Pietermaritzburg, South Africa.
- Grayson, R and Blöschl, G. 2000. Spatial Modelling of Catchment Dynamics. In: eds. Grayson, R Blöschl, G, *Spatial Patterns in Catchment Hydrology: Observations and Modelling*. Cambridge University Press. Cambridge, UK.
- HACH .2000. DR/2000 Spectrophotometer Instrument Manual, Version 3, Colorado, USA.
- Haria, AH, and Shand, P. 2006. Near-stream soil water–groundwater coupling in the headwaters of the Afon Hafren, Wales: Implications for surface water quality. *Journal of Hydrology* 2006, 331: 567– 579.
- Harrelson, CC, Rawlins, CL, and Potyondy, JP. 1994. Stream Channel Reference Sites: An Illustrated Guide to Field Technique: Gen. Tech. Rep. RM-245. USDA, Fort Collins, USA.
- Harvey, WJ, Wagner, BJ, and Bencala, KE. 1996. Evaluating the reliability of the stream tracer approach to characterise stream-subsurface water exchange. *Water Resources Research* 32, 8: 2441-2451.
- Herron, N, and Wilson, C.2001. A water balance approach to assessing the hydrologic buffering potential of an alluvial fan, *Water Resources Research*, 37(2), 341–351, doi:10.1029/2000WR900253.
- Hersch, RW. 1985. *Streamflow Measurement* (2nd Ed.). Elsevier Applied Science Publishers, Cambridge, UK.
- Hillier, R, Rietkerk, M, van den Bosch, F, Prins, H, and de Kroon, H. 2001. Vegetation pattern formation in semi-arid grazing systems, *Ecology*, 82, 50–61.
- Ivkovic, KM. 2008. A top–down approach to characterise aquifer–river interaction processes *Journal of Hydrology* 365, 2009: 145–155
- Jencso, KG, and McGlynn, BL. 2011. Hierarchical controls on runoff generation: Topographically driven hydrologic connectivity, geology, and vegetation. *Water Resources Research* 47, W11527: 16.
- Jumbi, F, Van Niekerk, A, Fundisi, D, Riddell, ES, Nel, J and Lorentz, SA. 2013. Progress report & summary of first years catchment monitoring. Progress Report 7. Unpublished WRC Report for project K5/2051. CWRR, University of KwaZulu-Natal, Pietermaritzburg. South Africa.
- Kalbus, E, Reinstorf, F, and Schirmer, M. 2006. Measuring methods for groundwater, surface water and their interactions: a review. *Hydrol. Earth Syst. Sci.* 3: 1809–1850.
- Kendall, C and McDonnell, JJ. 1998. eds. *Isotope Tracers in Catchment Hydrology*. Elsevier. New York, USA.

- Kendall, C and Caldwell, EA. 1998. Fundamentals of Isotope Geochemistry. In: eds. Kendall and McDonnell, JJ, Isotope Tracers in Catchment Hydrology, Elsevier. New York, USA.
- Kirchner, WJ, Feng, X, and Neal, C. 2001. Catchment scale advection and dispersion as a mechanism for fractal scaling in stream tracer concentrations. *Journal of Hydrology* 254: 82-101.
- Klaus, J, Zehe, E, Elsner, M, Kulls, C, and McDonnell, JJ. 2013. Macropore flow of old water revisited: experimental insights from a tile-drained hillslope. *Hydrol. Earth Syst. Sci.* 17: 103–118.
- Koning, B. 2006. Definition of Soil Water Dynamics by Combining Hydrometry and Geophysics in a Hillslope Transect in the KNP. Unpublished MSc. Thesis, School of Bioresources Engineering and Environmental Hydrology, University of KwaZulu-Natal, Pietermaritzburg, South Africa.
- Lambs, L. 2003. Interactions between groundwater and surface water at river banks and the confluence of rivers. *Journal of Hydrology* 288, 2004: 312–326.
- Landon, MK, Rus, DL, and Harvey, FE. 2001. Comparison of In-stream methods for Measuring Hydraulic Conductivity in Sandy Streambeds. *Groundwater* 39, 6: 870-885.
- Leaney, FW, Smettem, KRJ, and Chittleborough, DJ. 1993. Estimating the contribution of preferential flow to subsurface runoff from a hillslope using deuterium and chloride, *Journal of Hydrology* 147: 83–103.
- Lee, DR, Cherry, JA, Pickens, JF. 1980. Groundwater transport of a salt tracer through a sandy lakebed. *Limnology and Oceanography Journal* 25, 1: 45-61.
- Leibundgut, C, Maloszewski, P, and Kulls, C. 2009. *Environmental Tracers in Hydrology*. John Wiley & Sons, Chichester, UK.
- Le Roux, PAL, Riddell, E, Lorentz, SA and Nel, JM. 2011. Kruger National Park supersites hydrological response models. Unpublished Report. University of Free State, South Africa.
- Lin, H, Bouma, J, Pachepsky, Y, Western, A, Thompson, J, Van Genuchten, R, Vogel, HJ, and Lilly, A. 2006. *Hydropedology: Synergistic Integration of Pedology and Hydrology*. *Water Resources Research* 42, W05301:4085.
- Loke, MH. 1999. Electrical imaging surveys for environmental and engineering studies. A practical guide to 2D and 3D surveys. www.geometrics.com.
- Lorentz, S, Bursey K, Idowu, O, Pretorius, C, and Ngeleka, K. 2008. Definition and Upscaling of Key hydrological Processes for Application in Models. Report to the Water Research Commission Number 1320/1/08. School of Bioresources Engineering and Environmental Hydrology, University of Kwa-Zulu Natal, South Africa.
- MacKenzie, JA, Jacoby, DL, and Rogers, KH. 2003. Modelling of Terrestrialisation and Technology Transfer to Enable Management of Kruger National Park Rivers. Report To the Water Research Commission Number 1063/1/03. Centre for Water in the Environment, University of Witwatersrand, South Africa.

- MacKinnon, D, and Tetzlaff, D. 2009. Conceptualising Scale in Regional Studies and Catchment Science – Towards an Integrated Characterisation of Spatial Units. *Geography Compass* 3, 2009: 1749-8198.
- Malcolm, IA, Soulsby, C, Youngson, AF, Hannah, DM. 2005. Catchment-scale controls on groundwater–surface water interactions in the hyporheic zone: Implications for salmon embryo survival. *River Research Applications* 21: 977–989.
- Mansell, MG, and Hussey, SW. 2005. An investigation of flows and losses within the alluvial sands of ephemeral rivers in Zimbabwe. *Journal of Hydrology* 314, 2005: 192–203.
- Marimuthu, S, Reynolds, DA. and Le Gal La Salle, C. 2005. A field study of hydraulic, geochemical and stable isotope relationships in a coastal wetlands system. *Journal of Hydrology* 315, 2005: 93–116.
- McCauley, A, and Jones, C. 2005. Salinity and Sodicity Management: Soil and water management module 2, Montana State University, United States of America.
- McDonnell, J, Rowe, L, and Stewart, M. 1999. A combined tracer-hydrometric approach to assess the effect of catchment scale on water flow path, source and age. *Integrated methods in catchment hydrology-tracer, Remote sensing and New Hydrometric Techniques*. IAHS Publication number 258, 99 Symposium HS4, Birmingham, UK.
- McDonnell, JJ, Sivapalan, M, Vache, K, Dunn, S, Grant, G, Haggerty, R, Hinz, C, Hooper, R, Kirchner, J, Roderick, ML, Selker, J, and Weiler, M. 2007. Moving beyond heterogeneity and process complexity: A new vision for watershed hydrology. *Water Resources Research*, 43, W07301: 1029.
- McDonnell, JJ, McGuire, K, Aggarwal, P, Beven, KJ, Biondi, D, Destouni, G, Dunn, S, James, A, Kirchner, J, Kraft, P, Lyon, S, Maloszewski, P, Newman, B, Pfister, L, Rinaldo, A, Rodhe, A, Sayama, T, Seibert, J, Solomon, K, Soulsby, C, Stewart, M, Tetzlaff, D, Tobin, C, Troch, P, Weiler, M, Western, A, Worman, A, and Wrede, S. 2010. How old is stream water? Open questions in catchment transit time conceptualization, modelling and analysis. *Hydrol. Process.* 24: 1745–1754.
- McCartney, MP, Neal, C, and Neal, M. 1998. Use of deuterium to understand runoff generation in a headwater catchment containing a dambo. *Hydrological and Earth System Sciences* 2,1: 65-76.
- McGlynn, BL, and McDonnell, JJ. 2003. Quantifying the relative contributions of riparian and hillslope zones to catchment runoff. *Water Resources Research* 39, 11: 1310.
- McGlynn, BL, McDonnell, JJ, Seibert, J, and Kendall, C. 2004. Scale effects on headwater catchment runoff timing, flow sources and groundwater-streamflow relations. *Water Resources Research*, 40, W07504: 2494.
- Michaelides, K, and Chappell, A. 2009. Connectivity as a concept for characterising hydrological behaviour. *Hydrological Processes* 23: 517–522.
- Mul, ML, Mutiibwa, RK, Uhlenbrook, S, Savenije, HHG. 2008. Hydrograph separation using hydrochemical tracers in the Makanya catchment, Tanzania. *Physics and Chemistry of the Earth*, 33: 151–156.
- Mulholland, PJ. 1993. Hydrometric and stream chemistry evidence of three storm flowpaths in Walker Branch Watershed. *Journal of Hydrology* 151: 291-316.

- Nadeau, TL, and Rains, MC. 2007. Hydrological Connectivity Between Headwater Streams and Downstream Waters: How Science Can Inform Policy. *Journal of the American Water Resources Association* 43(1):118-133.
- Neil, LI. 1998. Isotopic Variations in Precipitation. In: eds. Kendall and McDonnell, JJ, *Isotope Tracers in Catchment Hydrology*, Elsevier, New York, USA.
- Noguchi, S, Tsuboyama, Y, Sidle, RC and Hosoda, I. 1999. Morphological Characteristics of Macropores and the Distribution of Preferential Flow Pathways in a Forested Slope Segment. *Soil Sci. Soc. Am. Journal* 63: 1413–1423.
- Nuttle, WK. 2002. Is ecohydrology one idea or many? *Hydrological Sciences Journal* 47,5: 805.
- Ogunkoya, OO. and Jenkins, A. 1993. Analysis of storm hydrograph and flow pathways using a three component hydrograph separation model. *Journal of hydrology* 142: 71-88.
- O’Keeffe, J and Rogers, KH. 2003. Heterogeneity and Management of the Lowveld Rivers. In: eds. Du Toit, JT, Rogers, KH, and Biggs, HC, *The Kruger Experience: Ecology and Management of Savanna Heterogeneity*. Island Press. Washington DC, USA.
- Pen, L, Till, B, Janicke, S, and Muirden, P. 2001. Stream Channel Analysis. Water and Rivers Commission Report number RR 9. East Perth, Australia.
- Penna, D, Tromp-van Meerveld, HJ, Gobbi, A, Borga, M, and Dalla Fontana, G. 2011. The influence of soil moisture on threshold runoff generation processes in an alpine headwater catchment. *Hydrol. Earth Syst. Sci.* 15: 689–702
- Petersen, RM. 2012. A Conceptual Understanding of Groundwater Recharge Processes and Surface water-Groundwater Interactions in the Kruger National Park. Unpublished Master’s Thesis, Department of Environment and Water Sciences, University of Western Cape, South Africa.
- Pilgrim, DH, Huff, DD, Steele, TD. 1979. Use of Specific Conductance and Contact Time Relations for Separating Flow Components in Storm Runoff. *Water Resources Research* 15, 2.
- Plummer, LN. 2003. Environmental tracers and how they are used to understand the aquifer. In: eds. Bartolino, JR and Cole, JC, *U.S. Geological Survey Circular 1222*. USA
- Praamsma, T, Novakowski, K, Kyser, K, Hall, K. 2009. Using stable isotopes and hydraulic head data to investigate groundwater recharge and discharge in a fractured rock aquifer. *Journal of Hydrology* 366: 35–45.
- Pringle, C. 2003. What is hydrologic connectivity and why is it ecologically important? *Hydrological Processes Journal* 17: 2685-2689.
- Renshaw, C. 2010. HydroToolBox Excel Add-in, version 1.4
www.dartmouth.edu/reshaw/hydrotoolbox/
- Rice, KC and Hornberger, GM. 1988. Comparison of hydrochemical tracers to estimate source contributions to peakflow in a small, forested, headwater catchment. *Water Resources Research* 34, 7: 1755-1766.
- Riddell, ES. 2011. Characterisation of the hydrological processes and responses to Rehabilitation of a headwater wetland of the Sand River, South Africa. Unpublished PhD Thesis in the School of Bioresources Engineering and Environmental Hydrology,

- University of KwaZulu-Natal, Pietermaritzburg, South Africa.
- Riddell, ES, Everson, C, Clulow, A, and Mengistu, M. 2013. The hydrological characterisation and water budget of a South African rehabilitated headwater wetland system. *Water SA* 39, 1: 0378-4738.
- Riddell, ES, Peterson, R, Van Niekerk, A, Fundisi, D, Neil, J, Thibela, D, Lorentz, SA. 2012. Progress Report 3 – Report on conceptual model development for southern and Northern supersites in KNP. Unpublished WRC Report for project K5/2051. CWRR, University of KwaZulu-Natal, Pietermaritzburg. South Africa.
- Rodriguez-Iturbe, I. 2000. Ecohydrology: A hydrologic perspective of climate-soil-vegetation dynamics. *Water Resources Research* 36, 1: 3–9.
- Sawicz, K, Wagener, T, Sivapalan, M, Troch, PA, and Carrillo, G. 2011. Catchment classification: empirical analysis of hydrologic similarity based on catchment function in the eastern USA, *Hydrol. Earth Syst. Sci.* 8: 4495-4534.
- Scanlon, BR., Healy, RW. and Cook, PG. 2002. Choosing appropriate techniques for quantifying groundwater recharge. *Hydrogeology Journal* 10: 18–39.
- Scientific Services. 2013. Kruger National Park Rainfall Summary.
www.sanparks.org/docs/parks_kruger/rainfall_stats/jan13
- Shanley, JB, Kendall, C, Smith, TE, Wolock, DM, and McDonnell, JJ. 2002. Controls on old and new water contribution to streamflow at some nested catchments in Vermont, USA. *Hydrological Processes Journal*. 16: 589-609.
- Schroder, B. 2006. Pattern, process, and function in landscape ecology and catchment hydrology – how can quantitative landscape ecology support predictions in ungauged basins? *Hydrol. Earth Syst. Sci.* 10: 967–979.
- Simons, FW, and Sinclair, AK. 2001. Surface water-groundwater interactions Lower Dungeness River and vertical hydraulic conductivity of streambed along the sediments, USGS Water-Resources Investigations Report 02-4161. Washington. USA.
- Sivapalan, M. 2005. Process, Pattern and Function: Elements of a Unified Theory of Hydrology at Catchment Scale. In: ed. Anderson, MG, *Encyclopaedia of Hydrological Sciences*, John Wiley and Sons. Crawley, Australia.
- Sklash, MG, and Farvolden, RN. 1979. The Role of Groundwater in Storm Runoff. *Journal of Hydrology* 43: 45-65.
- Smit, IPJ, Riddell, ES, Cullum, C and Petersen, R. 2013. Kruger National Park Research Supersites: Establishing long-term research sites for cross-disciplinary, multi-scaled Learning. *Koedoe* 55,1: 1107.
- Solinst Levelogger Model 3001, Software version 4. User Guide.
<http://www.solinst.com/Downloads/>
- Sophocleous, M. 2002. Interactions between groundwater and surface water: the state of the science. *Hydrogeology Journal* 10:52–67.
- Soulsby, C, Neal, C, Laudon, H, Burns, DA, Merot, P, Bonell, M, Dunn, SM, and Tetzlaff, D. 2008. Catchment data for process conceptualization: simply not enough? *Hydrological Processes Journal* 22: 2057–2061.
- Soulsby, C, Tetzlaff, D, Van den Bedem, N, Malcolm, IA, Bacon, PJ, Youngson, AF. 2006. Inferring groundwater influences on surface water in montane catchments from

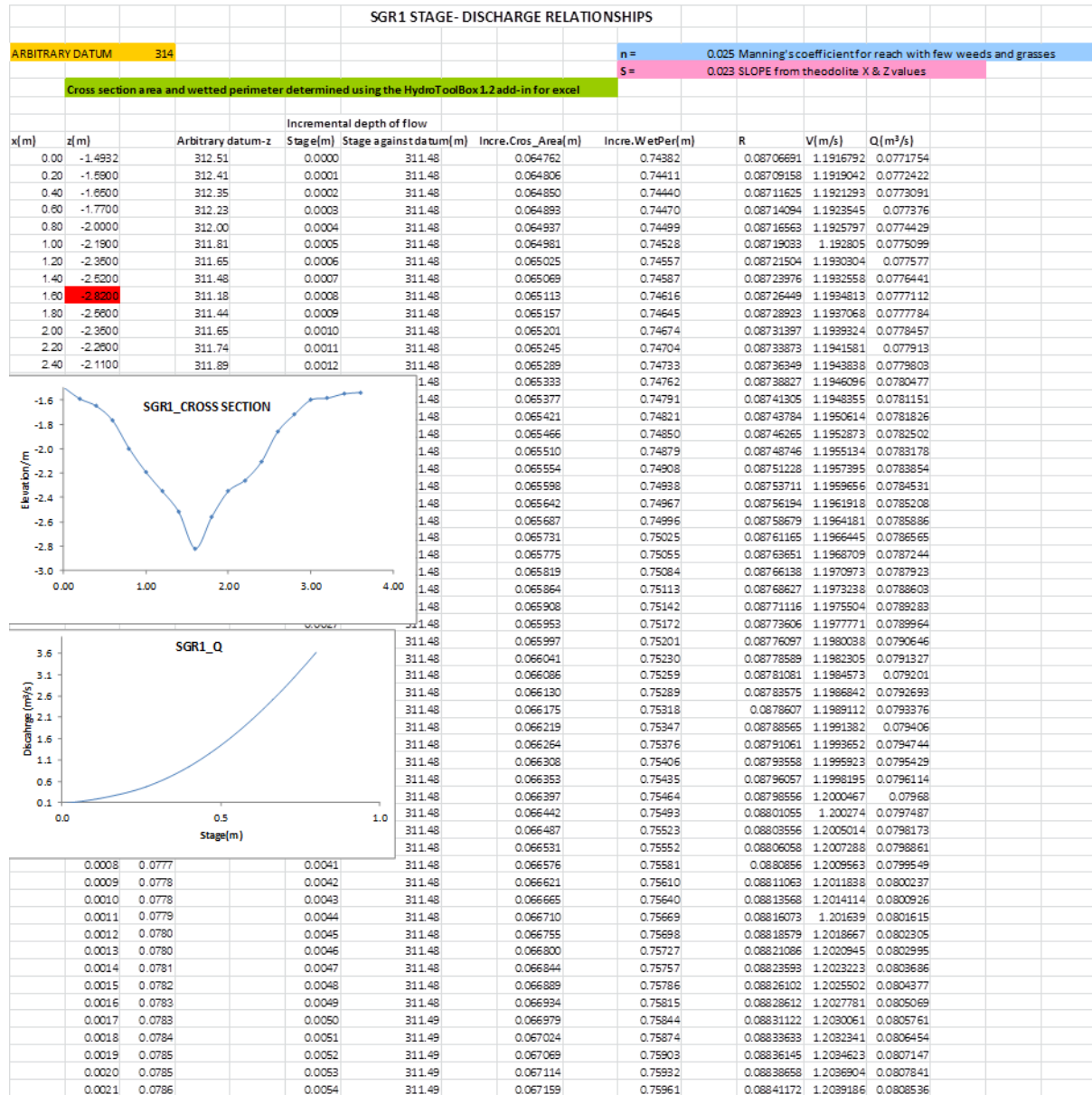
- hydrochemical surveys of springs and stream waters. *Journal of Hydrology* 333: 199–213.
- Stromberg, JC, Lite, SJ, and Dixon, MD. 2010. Effects of stream flow patterns on riparian vegetation of a semiarid river: implications for a changing climate. *River Research Applications* 26: 712–729.
- Sturm, TW. 2001. *Open Channel Hydraulics*. McGraw-Hill. New York, USA.
- Sundaram, B, Feitz, AJ, Caritat, P, De Plazinska, A, Brodie, RS, Coram, J, and Ransley, T. 2009. *Groundwater Sampling and Analysis: A Field Guide Record 2009* (27): 95. Geoscience Australia, Australia.
- Sundaram, B, Ransley, T, Brodie, RS. and Baker, P. 2009. Investigating groundwater–river interactions using environmental tracers. *Australian Journal of Earth Sciences International Geoscience Journal of the Geological Society of Australia* 56 (1): 13-19.
- Tetzlaff, D, Waldron, S, Brewer, MJ, and Soulsby, C. 2007. Assessing nested hydrological and hydrochemical behaviour of a mesoscale catchment using continuous tracer data. *Journal of Hydrology* 336: 430– 443.
- Tetzlaff, D, Carey, SK, Laudon, H, McGuire, K. 2010. Catchment processes and heterogeneity at multiple scales—benchmarking observations, conceptualization and prediction. *Hydrological Processes* 24: 2203–2208.
- Thompson, SE, Harman, CJ, Troch, PA, Brooks, PD and Sivapalan, M. 2011. Spatial scale dependence of ecohydrologically mediated water balance partitioning: A synthesis framework for catchment ecohydrology. *Water Resources Research*, 47, W00J03.
- Uchida, T, Van Meerveld, IT, McDonnell, JJ. 2005. The role of lateral pipe flow in hillslope runoff response: An inter-comparison of non-linear hillslope response. *Journal of Hydrology* 311: 117–133.
- Uhlenbrook, S, Wenninger, J, and Lorentz, S. 2005. What happens after the catchment caught the storm? Hydrological processes at the small, semi-arid Weatherley catchment, South-Africa. *Advances in Geosciences* 2: 237–241.
- Uhlenbrook, S, Didszun, J, Wenninger, J. 2008. Source areas and mixing of runoff components at the hillslope scale: a multi-technical approach. *Hydrological Sciences Journal* 53,4.
- Uhlenbrook, S, and Hoeg, S. 2003. Quantifying uncertainties in tracer-based hydrograph separations: a case study for two-, three- and five-component hydrograph separations in a mountainous catchment. *Hydrological Processes* 17: 431–453.
- USGS. 2008. Standard operating procedure for continuous measurement of discharge. NPDES CM 1000. USGS Publication.
- Van Beek, E, Hellmuth, M, Schulze, R, Stakhiv, E, Dorland, K, Kwadjik, J, Rasmussen, J, Rockstrom, J, and Veraart, J. 2003. Coping with Climate Variability and Climate Change in Water Resources. In: eds. Kabat, P, Schules, RE, Hellmuth, ME, and Veraart, JA, *Coping with Impacts of Climate Variability and Climate Change in Water Management: A Scoping Paper*. Dialogue on Water and Climate, Wageningen, Netherlands.
- Van Tol, JJ, Le Roux, PAL, Hensley, M, and Lorentz, SA. 2010. *Water SA* 36,(5).

- Van Tol, JJ, Le Roux, PAL, Lorentz, SA, and Hensley, M. 2013. Hydropedological Classification of South African Hillslopes. *Vadose Zone Journal* 2136(7).
- Venter, FJ, and Bristow, JW. 1986. An account of the geomorphology and drainage of the Kruger National Park. *Koedoe* 29: 117-129.
- Venter, FJ, and Gertenbach, WPD. 1986. A Cursory Review of Climate and Vegetation of the Kruger National Park. *Koedoe* 29: 139-148.
- Vidon, PGF, and Hill, AR. 2004. Landscape controls on the hydrology of stream riparian Zones. *Journal of Hydrology* 292(1-4): 210-228.
- Vivoni, ER, Istanbulluoglu, E, and Bras, RL. 2003. Coupling catchment hydrology and landscape evolution: Interactive effects on hydrograph and basin shape. *American Geophysical Union, H42C*: 1094.
- Wagener, T, Sivapalan, M, and McGlynn, B. 2008. Catchment Classification and Services—Toward a New Paradigm for Catchment Hydrology Driven by Societal Needs. In: Anderson, MG, *Encyclopaedia of Hydrological Sciences*. John Wiley & Sons. New York, USA.
- Wenninger, J, Uhlenbrook, S, Lorentz, S, and Leibundgut, C. 2008. Identification of runoff generation processes using combined hydrometric, tracer and geophysical methods in a headwater catchment in South Africa *Hydrological Sciences Journal* 53(1).
- Winter, TC. 1998. Relation of streams, lakes and wetlands to groundwater flow systems. *Hydrogeology Journal* 7: 28-45.
- Winter, TC. 2007. The role of groundwater in generating streamflow in headwater areas and in maintaining base flow. *Journal of the American Water Resources Association* 43, 1: 102-115.
- Yochum, S and Bledsoe, B. 2010. Flow resistance estimation in high-gradient streams Report prepared for the 4th Federal Inter-agency Hydrologic Modeling Conference June 27 - July 1, 2010, Las Vegas, Nevada, USA.
- Yokoo, Y, and Sivapalan, M. 2011. Towards reconstruction of the flow duration curve: development of a conceptual framework with a physical basis. *Hydrol. Earth Syst. Sci.* 15: 2805–2819.
- Young, PC, Chotai, A, and Beven, K. 2004. Data-Based Mechanistic Modelling and the Simplification of Environmental Systems. In: eds. Wainwright, J, and Mulligan, M, *Environmental Modelling: Finding Simplicity in Complexity*. John Wiley and Sons, London, UK.
- Younger, PL. 2006. *Groundwater in the Environment: An Introduction*. Blackwell. Newcastle Upon Tyne, UK.

APPENDICES

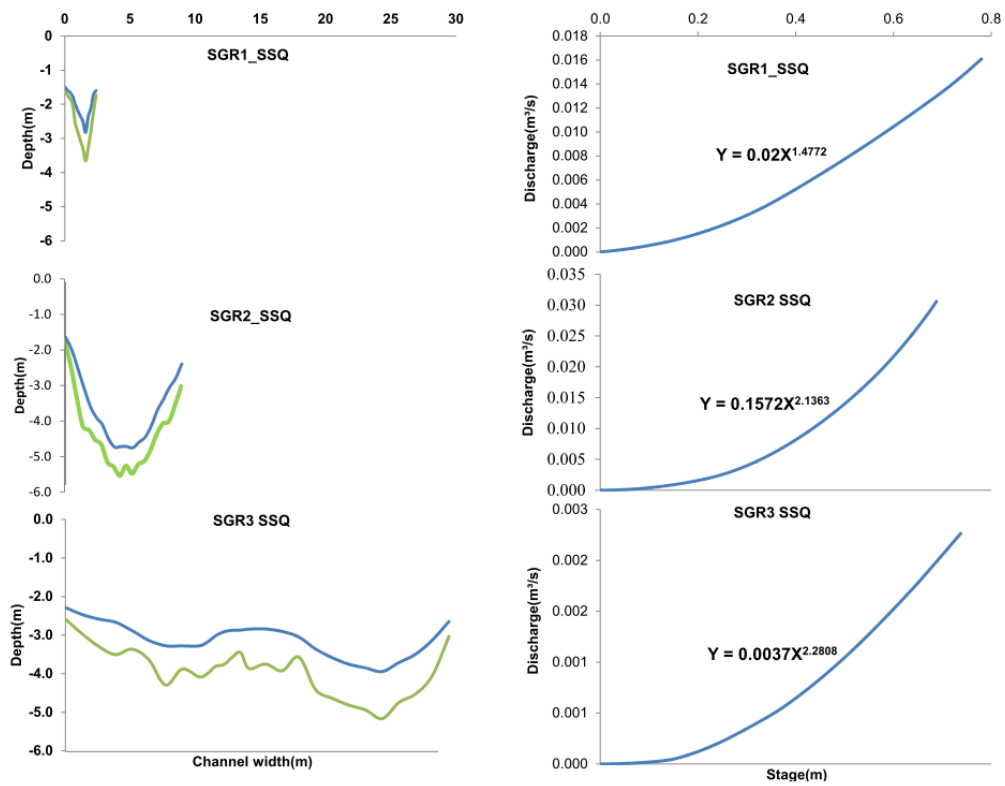
APPENDIX I:

a. Example, stream channel ratings conducted at the 3rd order of Southern Granites



b. Southern Granites subsurface ratings

c



APPENDIX II:

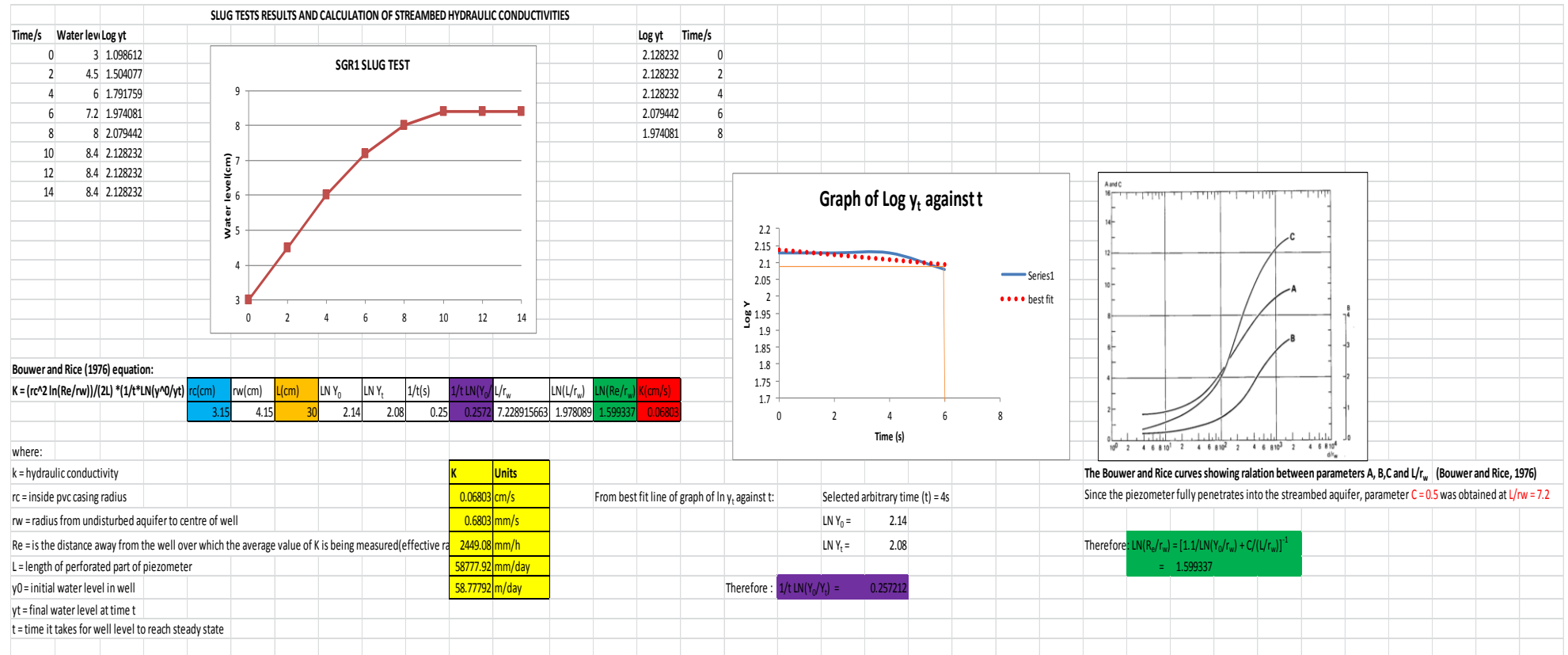
a. Determination of manning's roughness coefficients

Manning's roughness coefficients determined using Cowan (1956) procedure:		
$n = (n_b + n_1 + n_2 + n_3 + n_4)m$		
where n_b is a base value of n for a straight, uniform natural channel		
n_1 is a correction factor for the effect of surface irregularities		
n_2 is a value for the variations in shape and size of channel cross section		
n_3 is a value for obstructions		
n_4 is a value for vegetation and flow conditions		
m is a correction factor for the meandering of the channel		
SGR1-Q		
ROUGHNESS FACTOR	ASSIGNED VALUE	COMMENT
n_b	0.012	Sandy channel with 0.2 median size of bed material
n_1	0.006	considerable roughness, eroded side slopes
n_2	0.001	gradual change in shape and size of channel
n_3	0.2	few scattered obstructions including exposed roots, isolated boulders and logs
n_4	0	few vegetation on banks and bed
m	1	minor meandering
Manning's roughness coefficient		0.219
SGR2Q		
ROUGHNESS FACTOR	ASSIGNED VALUE	COMMENT
n_b	0.012	Sandy channel with 0.2 median size of bed material
n_1	0.006	considerable roughness, eroded side slopes

n ₂	0.001	gradual change in shape and size of channel
n ₃	0.004	few scattered obstructions including exposed roots, isolated boulders and logs
n ₄	0.002	few vegetation on banks and bed
m	1	minor meandering
Manning's roughness coefficient		0.025
SGR3Q		
ROUGHNESS FACTOR	ASSIGNED VALUE	COMMENT
n _b	0.017	Sandy channel with 0.2 median size of bed material
n ₁	0.006	flood plain with high width to depth ratio and considerable roughness
n ₂	0.011	marked change in shape and size of channel
n ₃	0.014	presence of scattered obstructions including exposed roots, isolated boulders and logs
n ₄	0.012	large trees, brushes and grass on banks and bed
m	1	minor meandering
Manning's roughness coefficient		0.06
SBAS1Q		
ROUGHNESS FACTOR	ASSIGNED VALUE	COMMENT
n _b	0.05	Stable channel with firm soil as bed material
n ₁	0.02	flood plain with high width to depth ratio and considerable roughness
n ₂	0.021	marked change in shape and size of channel
n ₃	0.011	presence of scattered obstructions including exposed roots and logs
n ₄	0.018	large trees, brushes and grass on floodplain and bed
m	1	minor meandering

Manning's roughness coefficient		0.120
SBAS2Q		
ROUGHNESS FACTOR	ASSIGNED VALUE	COMMENT
n _b	0.032	Stable channel with firm soil as bed material
n ₁	0.015	high width to depth ratio and considerable channel irregularities
n ₂	0.021	marked change in shape and size of channel
n ₃	0.014	presence of scattered obstructions including exposed roots, isolated boulders and logs
n ₄	0.018	large trees, brushes and grass on bed and banks
m	1	minor meandering
Manning's roughness coefficient		0.100
SBAS3Q		
ROUGHNESS FACTOR	ASSIGNED VALUE	COMMENT
n _b	0.012	Sandy channel with 0.2 median size of bed material
n ₁	0.001	flood plain with high width to depth ratio and considerable roughness
n ₂	0.001	gradual change in shape and size of channel
n ₃	0.004	presence of scattered obstructions including cobbles and isolated boulders
n ₄	0.002	brush and grass on banks and bed
m	1	minor meandering
Manning's roughness coefficient		0.02

b. Example determination of hydraulic conductivity from slug tests



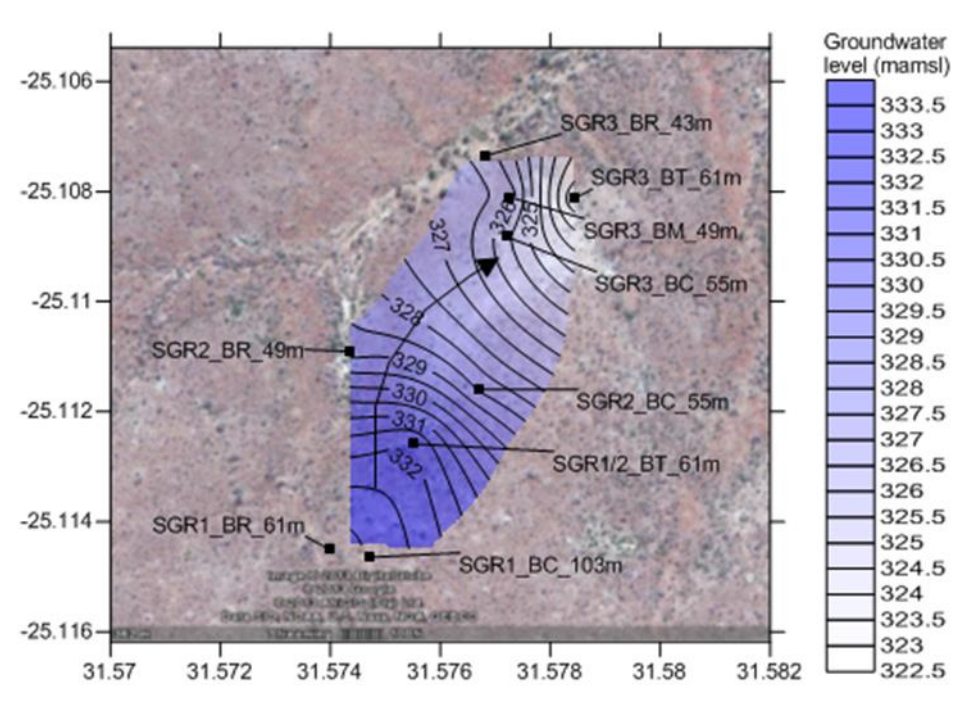
c. Vertical component of fluxes in the hyporheic zone at Southern Granites

VERTICAL HYDRAULIC GRADIENT CALCULATION FOR SGR1 REACH ON 18-01-2013 using Baxter et al (2003) method									
VHG = water surface elevation - piezometer water level/ Depth of piezometer screen									
DATUM	378.4								
				Water level in piezometer at SGR1Q					
				378.29					
				Water surface elevation at SGR1Q					
				379.69					
				Depth of piezometer screen					
				0.60					
Dimensionless Vertical Hydraulic Gradient (VHG) is:				2.34083333	(Upwelling)				

VERTICAL HYRAULIC GRADIENT CALCULATION FOR SGR2 REACH ON 18-01-2013 using Baxter et al (2003) method				
	VHG = water surface elevation - piezometer water level/ Depth of piezometer screen			
DATUM	363.4			
			Water level in piezometer at SGR2Q	
			364.28	
			Water surface elevation at SGR2Q	
			364.04	
			Depth of piezometer screen	
			0.32	
Dimensionless Vertical Hydraulic Gradient (VHG) is:			-0.7575	(Downwelling)

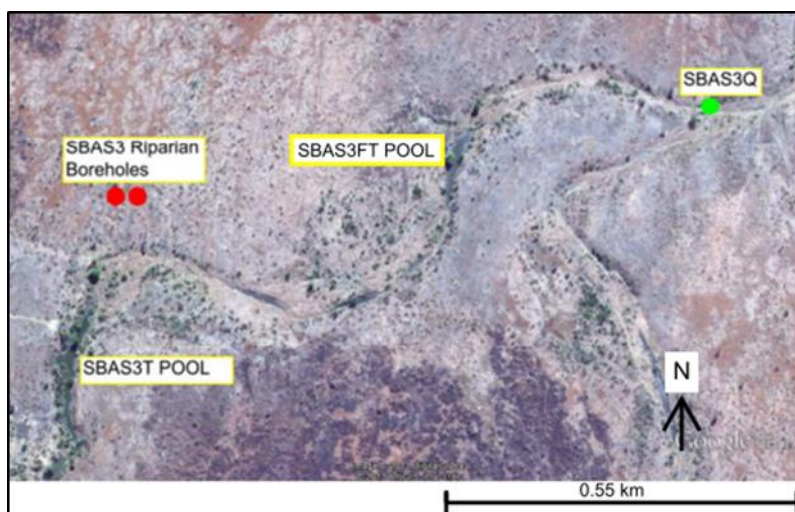
VERTICAL HYRAULIC GRADIENT CALCULATION FOR SGR3 REACH ON 18-01-2013 using Baxter et al (2003) method					
VHG = water surface elevation - piezometer water level/ Depth of piezometer screen					
DATUM	348.4				
			Water level in piezometer P115 at SGR3Q		
			348.9		
			Water surface elevation at SGR3Q		
			348.81		
			Depth of piezometer screen		
			0.32		
Dimensionless Vertical Hydraulic Gradient (VHG) is:			-0.2834375	(Downwelling)	

- d. General groundwater flow direction of deeper boreholes at Southern Gradients (adapted from Jumbi et al., 2013).



BR = Riparian borehole; BM = Midslope borehole and BC = Crest borehole.

- e. Google Earth image showing location of persistent pools at the 3rd order reach of Southern Basalts (SBAS3T = pool adjacent borehole transect; SBAS3FT = pool close to a fever tree).



APPENDIX III: Rainfall-Runoff Analysis

a. Statistical analysis (Pearson Product Moment Correlation Coefficient)

						Runoff Coefficients(%)			P_Int _{max}	P_DUR	API _i	Pint _{mean}	Runoff Peak Discharge			Runoff Delay Time		
DATE	Event Number	SGR_Q1(mm)	SGR_Q2(mm)	SGR_Q3(mm)	Rain Total(mm)	SGR1Q	SGR2Q	SGR3Q					SGR1Q	SGR2Q	SGR3Q	SGR1Q	SGR2Q	SGR3Q
2012/12/26	1	3.68508338	1.490819003	0.031664031	55.3	6.66380358	2.695875	0.057258646	8	23	52.3	0.42	0.026	0.027	0.003	2.4	2.6	2.3
2013/01/19	2	17.40587245	26.33725067	38.98992874	95.7	18.1879545	27.52064	40.74182732	16.3	23	130.96	1.9	1.089	2.192	6.958	0.22	0.47	0.77
2013/02/20	4	0.665969861	0.048788219	0.289734679	27.9	2.38698875	0.174868	1.038475551	18.6	5	50.44	1.85	0.025778	0.03913883	0.089428	0.27	0.32	0.67
												Runoff Rising Time			Catchment Area			
A	Rc & P tot Pearson's Product Moment Correlation Coefficients					0.98897701	0.946093	0.907087111					SGR1Q	SGR2Q	SGR3Q	SGR1Q	SGR2Q	SGR3Q
B	RVol & P Int max Pearson's Product Moment Correlation Coefficients					0.05110792	0.230273	0.330656598					1.17	0.92	1.08	108000	427000	1482000
C	RVol & P DUR Pearson's Product Moment Correlation Coefficients					0.70917651	0.570489	0.481583351					0.50	0.60	0.80			
D	RVol & P Amt Pearson's Product Moment Correlation Coefficients					0.97054074	0.934288	0.913454697					0.5	0.62	0.83			
E	Rc & API Pearson's Product Moment Correlation Coefficients					0.97025977	0.997999	0.999144203										
F	RVol & Pint mean Pearson's Product Moment Correlation Coefficients					0.28462919	0.452751	0.543405576										
G	RDT & Pint mean Pearson's Product Moment Correlation Coefficients					-0.9999533	-0.99608	-0.17437796										
H	RRT & Pint mean Pearson's Product Moment Correlation Coefficients					-0.9995575	-0.99966	-0.99769047										
I	RDT & P API Pearson's Product Moment Correlation Coefficients					-0.4998741	-0.43002	-0.43370969										
J	RRT & P API Pearson's Product Moment Correlation Coefficients					-0.4823739	-0.53049	-0.56554259										
K	RPQ & RVol Pearson's Product Moment Correlation Coefficients					0.98556690	0.99855	0.999987										
L	RRT & Pint max Pearson's Product Moment Correlation Coefficients					-0.97850	-0.96547	-0.95370687										
M	RPQ & P Amt Pearson's Product Moment Correlation Coefficients					0.91575	0.913743	0.911367832										
N	RPQ & PDUR Pearson's Product Moment Correlation Coefficients					0.49992	0.495623	0.490570175										
O	RPQ & P Imean Pearson's Product Moment Correlation Coefficients					0.52562	0.529827	0.534744318										
P	RPQ & P Imax Pearson's Product Moment Correlation Coefficients					0.31072	0.315428	0.320934239										
Q	RPQ & P API Pearson's Product Moment Correlation Coefficients					0.99979	0.99968	0.999516718										
R	RDT & P Amt Pearson's Product Moment Correlation Coefficients					-0.12997	-0.05138	-0.05546704										
S	RDT & P DUR Pearson's Product Moment Correlation Coefficients					0.48250121	0.550067	0.546647816										
T	RDT & P Intmax Pearson's Product Moment Correlation Coefficients					-0.9741591	-0.98894	-0.98832122										
U	RRT & P DUR Pearson's Product Moment Correlation Coefficients					0.5	0.45091	0.413113671										
V	RRT & P Amt Pearson's Product Moment Correlation Coefficients					-0.1100292	-0.1653	-0.20648459										
W	RVol & API Pearson's Product Moment Correlation Coefficients					0.98880408	0.999592	0.99962231										
X	Rc & P DUR Pearson's Product Moment Correlation Coefficients					0.63932018	0.541655	0.495007076										
Y	Rc & P Intmean Pearson's Product Moment Correlation Coefficients					0.37401573	0.483409	0.530428639										
Z	Rc & P Intmax Pearson's Product Moment Correlation Coefficients					0.14532935	0.263892	0.316100794										
AA	RDT & RVol Pearson's Product Moment Correlation Coefficients					-0.3650387	-0.40406	-0.45698059										
BB	RRT & RVol Pearson's Product Moment Correlation Coefficients					-0.346262	-0.50606	-0.58678513										
CC	P Amt & PDUR Pearson's Product Moment Correlation Coefficients							0.805752582										
DD	P Amt & P API Pearson's Product Moment Correlation Coefficients							0.923722105										
EE	P DUR & P API Pearson's Product Moment Correlation Coefficients							0.517421368										
FF	P DUR & P Intmean Pearson's Product Moment Correlation Coefficients							-0.47401694										
GG	P DUR & P Intmax Pearson's Product Moment Correlation Coefficients							-0.66786506										
HH	P amt & P Intmean Pearson's Product Moment Correlation Coefficients							0.139547085										
II	P Amt & P Intmax Pearson's Product Moment Correlation Coefficients							-0.09733106										
JJ	P API & P Intmean Pearson's Product Moment Correlation Coefficients							0.508217896										
KK	P API & P Intmax Pearson's Product Moment Correlation Coefficients							0.291337666										
LL	CA & RPD Pearson's Product Moment Correlation Coefficients					-0.9672388	0.998946	0.999728925										
						Dec 26 2012	19-Jan-13	20-Feb-13										

b. Significance Test For Identified Dependences (*t*-test)

Pearson's correlation coefficients were tested for significance using the t-test as follows:														
$t = \frac{r - \rho}{Sr}$	where r is the correlation coefficient; ρ is rho which is equal to zero under the null hypothesis; S_r is the standard error, which was calculated as follows:													
$Sr = \sqrt{\frac{1 - r^2}{N - 2}}$	A	B	C	D	E	F	G	H	I	J	K	L		
	SGR1Q	0.148069121	0.998	0.705	0.241	0.242	0.959	0.009661	0.029747153	0.866098	0.875965	0.169286	0.20624692	
	SGR2Q	0.32389546	0.973	0.821	0.357	0.063	0.892	0.088481	0.026060083	0.902818	0.847692	0.053827	0.26051196	
	SGR3Q	0.420942956	0.944	0.876	0.407	0.041	0.839	0.984679	0.067924409	0.901053	0.824719	0.005099	0.30073778	
$Sr = \sqrt{\frac{1 - r^2}{N - 2}}$	M	N	O	P	Q	R	S	T	U	V	W	X		
	SGR1Q	0.401758962	0.866070665	0.850720993	0.95050117	0.020325	0.99151735	0.875895	0.225862721	0.866025	0.993928	0.14922	0.76894064	
	SGR2Q	0.406292685	0.868537761	0.848105455	0.94894949	0.02528	0.998678941	0.835121	0.148343058	0.89257	0.986243	0.028566	0.84060088	
	SGR3Q	0.41159285	0.871401689	0.845013914	0.94710148	0.031086	0.998460518	0.837363	0.152384907	0.910679	0.97845	0.025989	0.86888894	
$Sr = \sqrt{\frac{1 - r^2}{N - 2}}$	Y	Z	AA	BB	CC	DD	EE	FF	GG	HH	II	JJ	KK	LL
	0.92742236	0.989383333	0.930992334	0.938137837										0.253868
	0.875394822	0.964552249	0.914733867	0.86249985										0.045905
	0.847729591	0.948725613	0.889476668	0.809742682	0.59225229	0.383063	0.855730757	0.880516	0.744282377	0.990215	0.995252	0.861229	0.95662028	0.023283
t = :	A	B	C	D	E	F	G	H	I	J	K	L		
	SGR1Q	6.679157736	0.051210341	1.005924123	4.02714001	4.009338	0.296797903	-103.507	-33.6017857	-0.57716	-0.55068	5.82189	-4.7443131	
	SGR2Q	2.920982211	0.236663314	0.694870828	2.61705247	15.84126	0.507568147	-11.2575	-38.3598311	-0.47631	-0.6258	18.5512	-3.7060511	
	SGR3Q	2.154893192	0.35027182	0.549752684	2.24436044	24.36937	0.64768245	-0.17709	-14.6882467	-0.48134	-0.68574	196.1143	-3.171224	
t = :	M	N	O	P	Q	R	S	T	U	V	W	X		
	SGR1Q	0.691530935	-1.154586312	-1.174953321	-0.5259058	-23.7328	0.993998639	-1.11714	4.054433814	0.57726	0.528828	2.082306	1.30022185	
	SGR2Q	1.11434639	-1.146844632	-1.178698206	-0.4531561	-20.9844	0.99987118	-1.15609	6.159661277	0.555277	0.537218	11.04208	1.18924502	
	SGR3Q	0.623599406	-0.200112029	-1.180679341	-0.4579337	-18.1929	1.001528835	-1.13894	5.980696171	0.538686	0.546522	12.34888	1.15033886	
t = :	Y	Z	AA	BB	CC	DD	EE	FF	GG	HH	II	JJ	KK	LL
	0.403285219	0.146888822	-0.392096385	-0.369095055										-3.81
	0.552217833	0.273590101	-0.441720681	-0.586733224										21.76095
	0.625704995	0.333184632	-0.513763435	-0.724656292	1.36048875	2.411409	0.604654401	-0.53834	-0.89732753	0.140926	-0.0978	0.590108	0.30454891	42.93899
p values = :	A	B	C	D	E	F	G	H	I	J	K	L		
	SGR1Q	0.010844654	0.481906269	0.21018814	0.01375835	0.028474	0.397303338	4.67E-05	0.000442251	0.311071	0.318574	0.014129	0.02083521	
	SGR2Q	0.04997083	0.417474458	0.27950475	0.03960108	0.001981	0.331096589	0.003899	0.000339449	0.340408	0.297671	0.001447	0.03285622	
	SGR3Q	0.08198182	0.379792413	0.318839631	0.05525694	0.000084	0.291805147	0.437874	0.322177801	0.338896	0.000776	1.3E-05	0.40893231	
p values = :	M	N	O	P	Q	R	S	T	U	V	W	X		
	SGR1Q	0.280359652	0.187714917	0.175876056	0.32366411	0.007178	0.212483298	0.19009	0.027895426	0.311043	0.324874	0.086375	0.16159222	
	SGR2Q	0.190543751	0.1845465	0.180471669	0.34777966	0.000753	0.211349658	0.183559	0.01267909	0.317261	0.322444	0.004051	0.17819686	
	SGR3Q	0.298266105	0.42964284	0.180632633	0.34625422	0.000765	0.211030866	0.186373	0.013418523	0.32202	0.319766	0.003247	0.18449056	
p values = :	Y	Z	AA	BB	CC	DD	EE	FF	GG	HH	II	JJ	KK	LL
	0.362883317	0.448344844	0.373765118	0.373765118										0.03125
	0.318134554	0.405032092	0.350844592	0.30832009										0.001053
	0.297696302	0.385340613	0.329204622	0.271900897	0.15335721	0.0687	0.303435118	0.322218	0.232190311	0.450421	0.465435	0.307455	0.39473879	0.162628

APPENDIX IV: Hydrograph Separation

a. Linear interpolations between end members

Hydrograph separation using lumped end member mixing analysis for total runoff following the 19 January 2013 rainfall event at Stevenson Hamilton site.

END MEMBER	VOLUME AVERAGED VALUE
Event water (Rain)	-1.97; -0.44
Pre-event water (GW)	-3.15; -16.16

Streamflow (Total Runoff) volume averaged delta values = -2.36; -16.16

Delta value distance between GW and rain (100%):

$$B^2 = (1.9)^2 + (14.73)^2$$

$$\text{Therefore } B = \sqrt{(1.9)^2 + (14.73)^2}$$

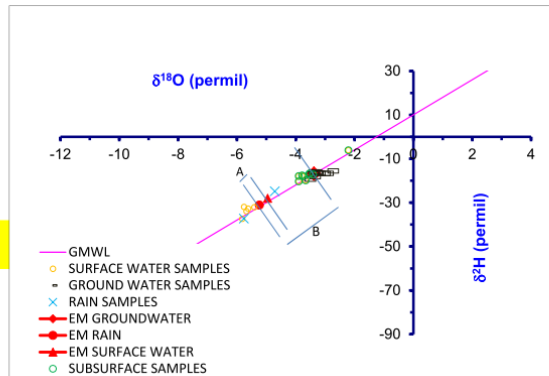
$$= 14.85$$

Delta value distance between surface water and rain:

$$A^2 = (0.28)^2 + (3.04)^2$$

$$\text{Therefore } A = \sqrt{(0.28)^2 + (3.04)^2}$$

$$= 3.05$$



GMWL = Global Meteoric Water Line; SGR = Southern Granite; EM = End Member.

% Pre-event contribution: $(a/b) \times 100$

$$\% \text{ Pre-event contribution} = \left(\frac{3.05}{14.85} \right) \times 100$$

$$= 20.4\% \approx 20\%$$

$$\% \text{ Event contribution} = 100 - 20.5 = 79.5\% \approx 80\%$$

Hydrograph separation using lumped end member mixing analysis for total runoff following the 20 February 2013 rainfall event at Stevenson Hamilton site

END MEMBER	VOLUME AVERAGED VALUE
Event water (Rain)	-1.53; 10.86
Pre-event water (GW)	-3.10; -15.48

Streamflow (Total Runoff) volume averaged delta values = -2.14; 0.73

Delta value distance between end members = 100% :

$$B^2 = (1.57)^2 + (26.34)^2$$

$$\text{Therefore } B = \sqrt{(1.57)^2 + (26.34)^2}$$

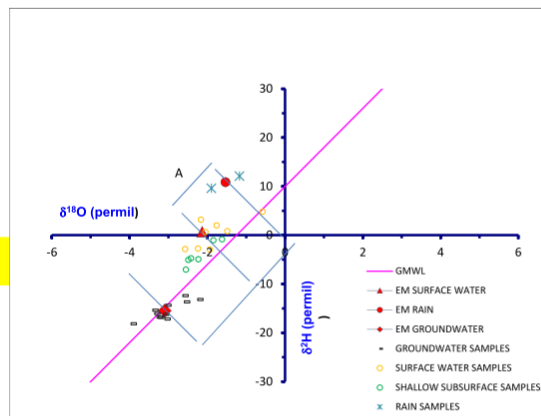
$$= 27.91$$

Delta value distance between surface water and rain:

$$A^2 = (0.61)^2 + (10.13)^2$$

$$\text{Therefore } A = \sqrt{(0.61)^2 + (10.13)^2}$$

$$= 10.15$$



GMWL = Global Meteoric Water Line; SGR = Southern Granite; EM = End Member.

% Pre-event contribution: $(a/b) \times 100$

$$\% \text{ Pre-event contribution} = \left(\frac{10.15}{27.91} \right) \times 100$$

$$= 36.4\% \approx 36\%$$

$$\% \text{ Event contribution} = 100 - 36.4 = 63.6\% \approx 64\%$$

Hydrograph separation using lumped end member mixing analysis for total runoff following the 19 JAN 2013 rainfall event at Nhlowa site.

END MEMBER	VOLUME AVERAGED VALUE
Event water (Rain)	-4.51; -27.29
Pre-event water (GW)	-1.8; -4.75

Streamflow (Total Runoff) volume averaged delta values = -3.57; -18.93

Delta value distance between end members = 100% :

$$B^2 = (-2.71)^2 + (-22.54)^2$$

$$\text{Therefore } B = \sqrt{(-2.71)^2 + (-22.54)^2}$$

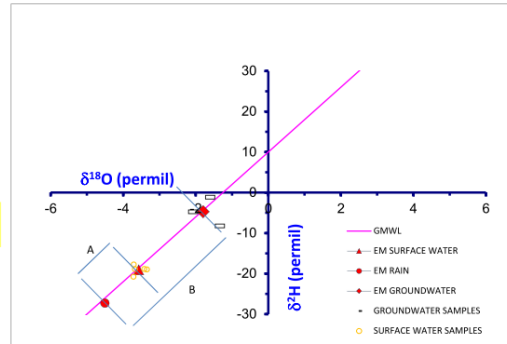
$$= 22.7$$

Delta value distance between surface water & rain:

$$A^2 = (-0.94)^2 + (-8.36)^2$$

$$\text{Therefore } A = \sqrt{(-0.94)^2 + (-8.36)^2}$$

$$= 8.4$$



GMWL = Global Meteoric Water Line; SGR =Southern Granite; EM = End Member.

% Pre-event contribution: (a/b)*100

$$\% \text{ Pre-event contribution} = \left(\frac{8.4}{22.7} \right) * 100 = 37\%$$

$$\% \text{ Event contribution} = 100 - 37 = 63\%$$

Hydrograph separation using lumped end member mixing analysis for total runoff following the 20 February 2013 rainfall event at Nhlowa site

END MEMBER	VOLUME AVERAGED VALUE
Event water (Rain)	-1.84; -2.92
Pre-event water (GW)	-2.46; -10.23

Streamflow (Total Runoff) volume averaged delta values = -1.99; -5.84

Delta value distance between end members = 100% :

$$B^2 = (0.62)^2 + (7.31)^2$$

$$\text{Therefore } B = \sqrt{(0.62)^2 + (7.31)^2}$$

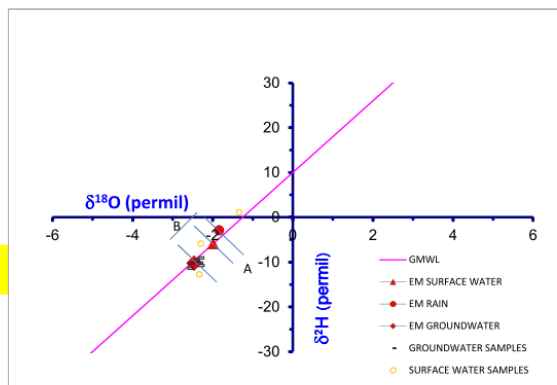
$$= 7.34$$

Delta value distance between surface water and rain:

$$A^2 = (0.15)^2 + (2.92)^2$$

$$\text{Therefore } A = \sqrt{(0.15)^2 + (2.92)^2}$$

$$= 2.92$$



GMWL = Global Meteoric Water Line; SGR =Southern Granite; EM = End Member.

% Pre-event contribution: (a/b)*100

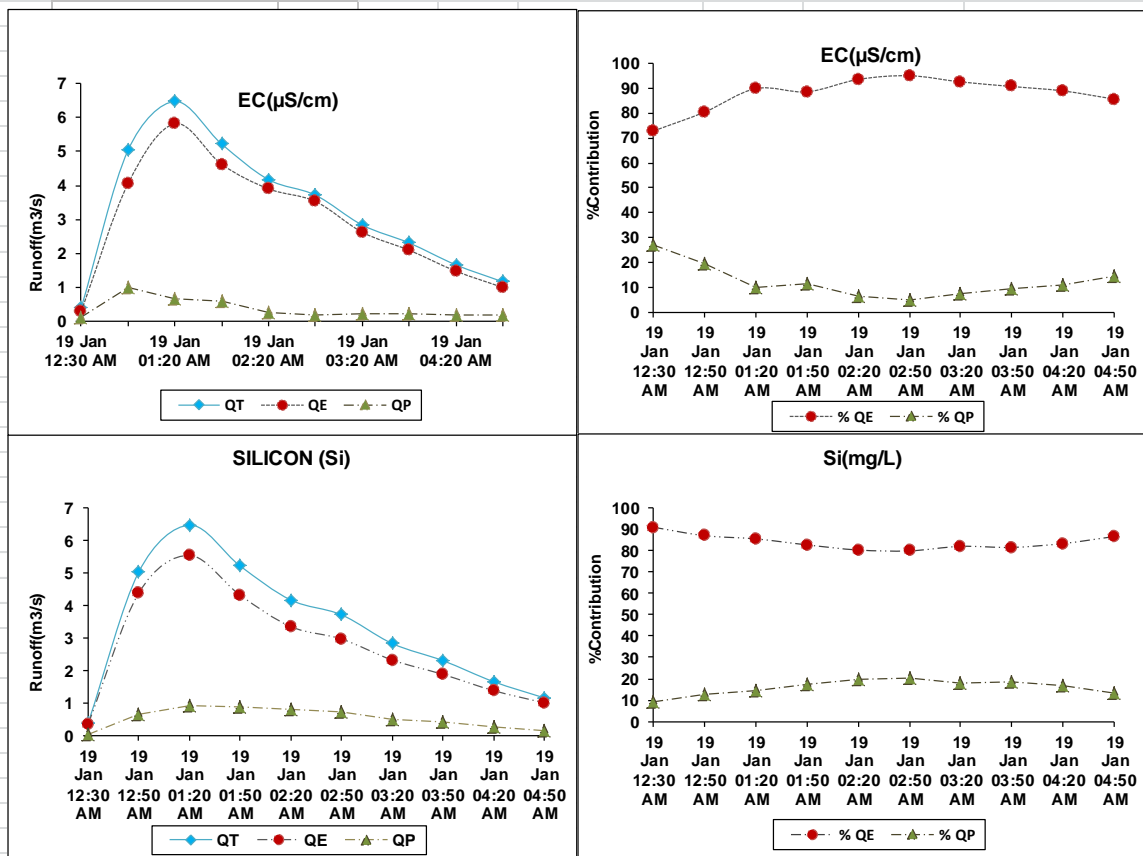
$$\% \text{ Pre-event contribution} = \left(\frac{2.92}{7.34} \right) * 100$$

$$= 39.7\% \approx 40\%$$

$$\% \text{ Event contribution} = 100 - 39.7 = 60.3\% \approx 60\%$$

b. Mass balance calculations for water and tracers (Silica and EC)

Hydrograph separation method based on 2 component mixing model described in Uhlenbrook & Hoeg (2003) in Hydrological Processes 17 p431-453						
For event of 19-JAN-2013						
SKUKUZA RAIN SAMPLE _19-01-2013 is our event water						
C _E	Si	-1.00				
	EC	50.40				
SGR3Q SS Sample 18-01.2013 is pre event water						
C _p	Si	23.60				
	EC	252.00				
C _T	From 19 JAN 2013 event		max	min		
	Si		0.00	0.00		
	EC		105.20	60.50		
	Si	EC	Q _T (m ³ /s)			
		1.20	105.2	2013/01/19 12:30:00 AM	0.39	
		2.17	89.9	2013/01/19 12:50:00 AM	5.04	
		2.55	70.9	2013/01/19 01:20:00 AM	6.48	
		3.24	73.5	2013/01/19 01:50:00 AM	5.22	
		3.83	63.5	2013/01/19 02:20:00 AM	4.17	
		3.93	60.5	2013/01/19 02:50:00 AM	3.72	
		3.41	65.5	2013/01/19 03:20:00 AM	2.83	
		3.53	69.2	2013/01/19 03:50:00 AM	2.31	
		3.08	72.8	2013/01/19 04:20:00 AM	1.66	
		2.28	79.4	2013/01/19 04:50:00 AM	1.16	
	Si	EC				
	Q _E	Q _P	Q _E	Q _P		
	0.35	0.03	0.28	0.105336971		
	4.39	0.65	4.05	0.986792138		
	5.54	0.93	5.82	0.65858218		
	4.32	0.90	4.62	0.598068751		
	3.35	0.82	3.90	0.271053681		
	2.97	0.74	3.53	0.186127653		
	2.33	0.51	2.62	0.21221271		
	1.88	0.42	2.09	0.215055956		
	1.38	0.28	1.47	0.184240114		
	1.00	0.15	0.99	0.166738424		
	%	%	%	%		
	2013/01/19 12:30:00 AM	91.04	8.96	72.82	27.18	
	2013/01/19 12:50:00 AM	87.09	12.91	80.41	19.59	
	2013/01/19 01:20:00 AM	85.58	14.42	89.83	10.17	
	2013/01/19 01:50:00 AM	82.77	17.23	88.54	11.46	
	2013/01/19 02:20:00 AM	80.37	19.63	93.50	6.50	
	2013/01/19 02:50:00 AM	79.96	20.04	94.99	5.01	
	2013/01/19 03:20:00 AM	82.08	17.92	92.51	7.49	
	2013/01/19 03:50:00 AM	81.59	18.41	90.67	9.33	
	2013/01/19 04:20:00 AM	83.40	16.60	88.89	11.11	
	2013/01/19 04:50:00 AM	86.68	13.32	85.62	14.38	
	MEAN % CONTRIBUTION	84.47	15.53	86.68	13.32	



APPENDIX V:

- Estimation of tributary flows through water & tracer mixing analysis

END MEMBER MIXING ANALYSIS ON 19 JANUARY 2013 TO DETERMINE TRIBUTARY CONTRIBUTION TO MAIN STREAM CHANNEL AFTER UHLENBROOK & HOEG (2003)

$$Q_T = Q_1 + Q_2 = f_1 + f_2 = 1$$

Equation (1)

where f1 and f2 are fractions of the combined discharge (QT) after the confluence in the main channel

$$C_T(Q_T) = C_1 f_1(Q_T) + C_2 f_2(Q_T)$$

Equation (2)

$$C_T = C_1 f_1 + C_2 f_2$$

Equation (3)

$$C_T = C_1 f_1 + C_2(1-f_1)$$

Equation (4)

From equation (4) $f_1 =$ 0.1

Therefore $f_2 = 1 - 0.1 =$ 0.9

Concentra	Tributary 1 (SGR1Q)	Tributary 2(SGR1Con)	Main channel (SGR1Con M)	Discharge(m³/s)			% Contribution of tributaries	
				SGR1Q	SGR1Con	SGR1Con	SGR1Q	SGR1Con
$\delta^{18}O$ (permil)	-3.87	-3.92	-3.85	0.021816	0.196344	0.21816	10	90

The diagram illustrates a stream confluence. A tributary, labeled "SGR1Con (f₂)", joins a main stream, labeled "Main channel (SGR1Con M)". A red dot marks the confluence point, labeled "Sampling point". Another red dot is located further downstream on the main channel, labeled "SGR1Q (f₁)". A blue line represents the "Stream".

